NUREG/CR-5769
EGG-2653

Natural Circulation Cooling in U.S. Pressurized Water Reactors

Prepared by
P. R. McHugh, R. D. Hentzen

Idaho National Engineering Laboratory
EG&G Idaho, Inc.

Prepared for
U.S. Nuclear Regulatory Commission

AVAILABILITY NOTICE

Availability of Reference Materials Cited in NRC Publications

Most documents cited in NRC publications will be available from one of the following sources:

1. The NRC Public Document Room, 2120 L Street, NW., Lower Level, Washington, DC 20555
2. The Superintendent of Documents, U.S. Government Printing Office, P.O. Box 37082, Washington, DC 20013-7082
3. The National Technical Information Service, Springfield, VA 22161

Although the listing that follows represents the majority of documents cited in NRC publications, it is not intended to be exhaustive.

Referenced documents available for inspection and copying for a fee from the NRC Public Document Room include NRC correspondence and internal NRC memoranda; NRC bulletins, circulars, information notices, inspection and investigation notices; licensee event reports; vendor reports and correspondence; Commission papers; and applicant and licensee documents and correspondence.

The following documents in the NUREG series are available for purchase from the GPO Sales Program: formal NRC staff and contractor reports, NRC-sponsored conference proceedings, international agreement reports, grant publications, and NRC booklets and brochures. Also available are regulatory guides, NRC regulations in the *Code of Federal Regulations*, and *Nuclear Regulatory Commission Issuances*.

Documents available from the National Technical Information Service include NUREG-series reports and technical reports prepared by other Federal agencies and reports prepared by the Atomic Energy Commission, forerunner agency to the Nuclear Regulatory Commission.

Documents available from public and special technical libraries include all open literature items, such as books, journal articles, and transactions. *Federal Register* notices, Federal and State legislation, and congressional reports can usually be obtained from these libraries.

Documents such as theses, dissertations, foreign reports and translations, and non-NRC conference proceedings are available for purchase from the organization sponsoring the publication cited.

Single copies of NRC draft reports are available free, to the extent of supply, upon written request to the Office of Administration, Distribution and Mail Services Section, U.S. Nuclear Regulatory Commission, Washington, DC 20555.

Copies of industry codes and standards used in a substantive manner in the NRC regulatory process are maintained at the NRC Library, 7920 Norfolk Avenue, Bethesda, Maryland, for use by the public. Codes and standards are usually copyrighted and may be purchased from the originating organization or, if they are American National Standards, from the American National Standards Institute, 1430 Broadway, New York, NY 10018.

DISCLAIMER NOTICE

This report was prepared as an account of work sponsored by an agency of the United States Government. Neither the United States Government nor any agency thereof, or any of their employees, makes any warranty, expressed or implied, or assumes any legal liability of responsibility for any third party's use, or the results of such use, of any information, apparatus, product or process disclosed in this report, or represents that its use by such third party would not infringe privately owned rights.

NUREG/CR-5769
EGG-2653
R4

Natural Circulation Cooling in U.S. Pressurized Water Reactors

Manuscript Completed: November 1991
Date Published: January 1992

Prepared by
P. R. McHugh, R. D. Hentzen

Idaho National Engineering Laboratory
Managed by the U.S. Department of Energy

EG&G Idaho, Inc.
Idaho Falls, ID 83415

Prepared for
Division of Systems Research
Office of Nuclear Regulatory Research
U.S. Nuclear Regulatory Commission
Washington, DC 29555
NRC FIN A6328
Under DOE Contract No. DE-AC07-76ID01570

ABSTRACT

This document is a synthesis of data and analysis concerning natural circulation cooling in U.S. Pressurized Water Reactors during off-normal operation and accident transients. Its objective is the integration of important research findings concerning PWR natural circulation phenomena into a single reference document. Sources of information include the Nuclear Regulatory Commission, reactor vendors, utility sponsored research groups, utilities, national laboratories, research reports, meeting papers, archival literature, and foreign sources.

Three modes of natural circulation are discussed: single-phase, two-phase, and reflux/boiling condensation. General characteristics, analytical expressions, noncondensible gas effects, secondary effects, and nonuniform flow are described with regard to each of the natural circulation modes. Plant operational data, tests in scaled experimental facilities, and analysis with thermal hydraulic system codes have demonstrated the effectiveness of single-phase natural circulation as a cooling mechanism. Evidence suggests that two-phase natural circulation and reflux/boiling condensation can also be effective methods of alternate core cooling. Experimental test facility data and analysis are the primary components of the two-phase and reflux/boiling condensation natural circulation knowledge base.

FIN No. A6328–Thermal-Hydraulic Research Center.

ACKNOWLEDGMENTS

The authors would like to acknowledge the contributions made by the many researchers whose work is cited in this document. Thanks are due to V. T. Berta of INEL and Dr. B. E. Boyack of LANL who provided the groundwork for this document. Suggestions by S. A. Naff, G. E. Wilson, G. W. Johnsen, and D. N. Chien of INEL were very helpful and are greatly appreciated. The authors would also like to thank Professor Peter Griffith of MIT; Professor Raymond Viskanta of Purdue University; and Professor Virgil Schrock of the University of California, Berkeley for reviewing this document.

CONTENTS

FIGURES

TABLES

ACRONYMS AND ABBREVIATIONS

AFW	Auxiliary Feedwater
ANL	Argonne National Lab
ATOG	Abnormal Transient Operating Guidelines
ATWS	Anticipated Transient Without Scram
B&W	Babcock and Wilcox
BCM	Boiler Condenser Mode
BETHSY	Boucle d'Etudes ThermoHydrauliques SYstème (French facility)
BWR	Boiling Water Reactor
CCFL	Counter Current Flow Limiting
CE	Combustion Engineering
ECCS	Emergency Core Cooling System
EFW	Emergency Feedwater
EPRI	Electric Power Research Institute
FLECHT-SEASET	Full-Length Emergency-Cooling Heat Transfer-Separate Effects and Systems Effects Test (joint program by NRC, EPRI, and W)
FRG	Federal Republic of Germany
HPI	High-Pressure Injection
HPIS	High-Pressure Injection System
HPSI	High-Pressure Safety Injection
INEL	Idaho National Engineering Laboratory
JAERI	Japan Atomic Energy Research Institute
KAERI	Korean Atomic Energy Research Institute
KWU	Kraftwerk Union
LBLOCA	Large Break Loss of Coolant Accident
LER	Licensee Event Report

LOBI	Loop Blowdown Investigation (Italian facility)
LOCA	Loss-of-Coolant Accident
LOFT	Loss-of-Fluid Test (facility)
LOFW	Loss-of-Feedwater Transient
LOSP	Loss of Offsite Power
LPIS	Low-Pressure Injection System
LPSI	Low-Pressure Safety Injection
LSTF	Large Scale Test Facility
MIST	Multiloop Integral System Test (B&W facility)
NRC	Nuclear Regulatory Commission
NSPS	Near Single-Phase Stable
NSPO	Near Single-Phase Oscillatory
NSSS	Nuclear Steam Supply System
OTIS	Once-Through Integral System
OTSG	Once-Through Steam Generator
PKL	Primärkreisläufe facility (FRG)
PORV	Power Operated Relief Valve
PWR	Pressurized Water Reactor
RCP	Reactor Coolant Pump
RCS	Reactor Coolant System
RV	Reactor Vessel
SBLOCA	Small Break Loss-of-Coolant Accident
SG	Steam Generator
SRI	Stanford Research Institute
SRV	Safety Relief Valve
TMI-2	Three Mile Island Unit 2
TSP	Tube Support Plate

UCSB	University of California at Santa Barbara
UMCP	University of Maryland College Park
UPTF	Upper Plenum Test Facility
UTSG	U-tube Steam Generator
VLPF	Very Large Peak Flow
W	Westinghouse

NATURAL CIRCULATION COOLING IN U.S. PRESSURIZED WATER REACTORS

EXECUTIVE SUMMARY

Natural circulation in pressurized water reactors (PWRs) refers to primary coolant flow within the loops of a closed primary system. Natural circulation flow is driven by differences in the average coolant density within the primary system. These density differences result from the heating of the reactor coolant in the core and the subsequent cooling of the reactor coolant in the steam generators, which are elevated relative to the core, resulting in a loop gravitational driving force. Natural circulation cooling is an essential means of removing shutdown decay-heat in U.S. pressurized water reactors (PWRs) when forced circulation by the reactor coolant pumps (RCPs) is not possible. The loss of forced circulation may result from the loss of offsite power, pump failure, or operator action based on operating procedures for abnormal conditions.

The U.S. Nuclear Regulatory Commission (NRC) declared shutdown decay-heat removal an unresolved safety issue (USI A-45) in December 1980. A U.S. NRC task action plan was formed to resolved this safety issue, resulting in considerable study and analysis of the behavior and phenomena that control the effectiveness of natural circulation cooling in PWRs. Information from integral test facilities, separate effects experiments, operating plant data, and analysis have made significant contributions to the natural circulation knowledge base and many important phenomena have been identified through this research. The purpose of this report is to integrate and synthesize the important results from this extensive research effort.

Three modes of natural circulation cooling are normally recognized: the single-phase mode, the two-phase mode, and either the reflux condensation mode [U-tube steam generators (UTSGs)] or the boiling condenser mode [once-through steam generators (OTSGs)] depending on the type of steam generator. General characteristics, analytical expressions, noncondensable gas effects, secondary side effects, and nonuniform flow are described with regard to each mode. Additionally, the role of thermal hydraulic system codes in predicting natural circulation behavior, and the detection of natural circulation in operating plants, are also discussed.

Single-phase natural circulation is the flow of an essentially subcooled liquid driven by temperature induced density differences within the primary loop. The dominant heat transfer mechanism is convection, making the loop mass flow rate the dominant heat removal parameter. Plant operational data, tests in scaled experiments, and analysis with thermal hydraulic system codes have demonstrated the effectiveness of single-phase natural circulation. However, the presence of noncondensable gases or low secondary liquid levels may compromise the heat removal efficiency of this mode. The location, amount, type, rate of accumulation, and migration of the noncondensable gas determine the extent of the noncondensable gas influence. However, the combined effects of these parameters are not completely understood.

Flow stall and reversal has been observed in the U-tubes of UTSGs during scaled single-phase natural circulation experiments. The net mass flow rate may be reduced slightly as a result of these tube-to-tube instabilities, but adequate single-phase natural circulation cooling will not cease. Although this problem may not be a significant safety concern, simulating this phenomena may serve as a useful test case for thermal hydraulic system codes. Note, it is important to identify and understand nonuniform flow behavior because there is a strong coupling between primary flow and heat transfer, and because flow instabilities may cause operator confusion.

Two-phase natural circulation is generally defined as the continuous flow of liquid and

vapor through the loops of the primary system. Vapor is generated in the core and flows along with the saturated liquid to the steam generators where at least some of the vapor is condensed. Density gradients and hence, the mass flow rate, are affected by not only the loop temperature distribution but also by the loop void distribution. Because of the additional heat transfer from condensation, the required primary-to-secondary temperature difference is smaller than that required during single-phase natural circulation.

The two-phase flow behavior for plants with UTSGs and OTSGs are similar if voids are entrained in the flow and pass into the steam generator tubes. However, in plants with OTSGs, flow interruption may occur because of voids accumulating in the hot leg upper bend. Depending on the primary and secondary side conditions, flow interruption may last for an extended period of time and/or lead to an intermittent type circulation. In plants with UTSGs, the peak two-phase mass flow rate occurs when voids occupy most of the volume in the upflow sides of the U-tubes, but little volume in the downflow sides.

The efficiency of two-phase natural circulation cooling may be reduced by degraded secondary side conditions and/or the presence of noncondensable gases. However, lost heat transfer during two-phase natural circulation causes increases in the primary pressure, which compresses the noncondensable gas volumes. In this manner, the primary pressure acts as a correcting mechanism to compensate for lost heat transfer. This process makes two-phase natural circulation more tolerant of noncondensable gases than single-phase natural circulation.

Nonuniform flow may also affect the heat removal efficiency of two-phase natural circulation. Types of nonuniform flow in UTSG plants include: U-tube flow stall/reversal phenomena; cyclic fill and dump behavior in steam generator U-tubes; oscillatory U-tube flow resulting from low secondary liquid levels; nonuniform flow caused by the transition from single-phase natural circulation, and unbalanced loop secondary side conditions. Causes of nonuniform flow in OTSG plants include: the intermittent circulation mentioned previously, multi-channel instability, flow geometry effects, and nonuniform emergency feedwater (EFW) behavior.

During reflux/boiling condensation, single-phase vapor is generated in the core and flows to the steam generators where it is condensed. Condensation is the primary heat removal mechanism. Consequently this flow mode is characterized by small mass flow rates and small primary-to-secondary temperature differences. During reflux condensation in plants with UTSGs, vapor from the core flows through the hot leg to the steam generator U-tubes, where condensation occurs. Condensate in the upflow sides of the steam generator U-tubes drains back to the vessel along the bottom of the hot leg. Thus, a countercurrent flow of liquid exists in the steam generator U-tubes and hot leg. Condensate in the downflow sides of the U-tubes flows concurrently with any uncondensed steam into the steam generator outlet plenum and cold leg pump suction piping. Two types of boiling condensation have been observed in test facilities with OTSGs. Pool boiling condensation occurs when the primary side vapor is adjacent to the secondary side liquid, or pool. EFW boiling condensation occurs when a condensing surface exists below the secondary EFW sparger spray elevation located near the top of the steam generator.

It is well established that noncondensable gases impede the condensation process. Effective heat transfer areas are reduced and higher primary-to-secondary temperature differences are required to remove the decay heat. As for two-phase natural circulation, primary system pressure acts as a correcting mechanism to compress noncondensable gas volumes in order to compensate for these adverse effects. A secondary effect of noncondensable gases in UTSG plants is the enhancement of flooding tendencies at the steam generator U-tube inlet. Noncondensable gases tend to force additional condensation to occur in the upflow sides of the steam generator U-tubes resulting in an increased amount of condensate that must drain against a vapor upflow.

In OTSGs, there is a potential for lost heat sink behavior when EFW is not available,

because the steam generator primary side condensing surface may be driven above the secondary pool level by reductions in the secondary liquid level and/or by the presence of noncondensable gases in the steam generator tubes.

In UTSG plants, the flow of vapor to the steam generators may be impeded by flooding, both at the hot leg bend and at the steam generator U-tube inlet. For typical reflux conditions, flooding at the hot leg bend is unlikely; but flooding at the steam generator U-tube inlet has been observed in numerous scaled experiments. Flooding at this location may also initiate an oscillatory U-tube flow pattern, characterized by liquid holdup in the steam generator U-tubes, which may aggravate loop seal, core level depression effects.

Thermal-hydraulic system codes must be used in order to apply the results from scaled experiments to large-scale operating reactors. This is especially true in the case of the two-phase and reflux/boiling natural circulation modes. Many comparisons of code calculations to experimental data for natural circulation have shown good agreement for a wide range of geometrical scales. However, certain types of transients provide unique modeling problems for the thermal-hydraulic system codes. Although, considerable progress has been made in simulating most of the important natural circulation phenomena, additional code and model development is needed to ensure that simulation of the more complex phenomena can be performed with confidence.

An important issue to reactor safety is the ability to detect natural circulation. In some instances, operator action may be necessary to initiate natural circulation, and plant operators cannot reliably depend on flow rate readings at natural circulation levels. Therefore, trends in temperature measurements must be used to detect natural circulation flow.

This report shows the effectiveness of single-phase natural circulation, two-phase natural circulation, and reflux/boiling condensation as heat removal mechanisms. However, the heat removal efficiency of of all three modes depends, to a certain degree, on the effects of noncondensable gases, secondary side conditions, and nonuniform flow behavior.

1. INTRODUCTION

Natural circulation cooling is an essential means of removing shutdown decay heat in U.S. pressurized water reactors (PWRs) following the loss of forced circulation by the reactor coolant pumps (RCPs) during operational transients or following accidents. Following the TMI-2 accident in March of 1979, the Nuclear Regulatory Commission (NRC) declared shutdown decay-heat removal an Unresolved Safety Issue (USI) in December of 1980 (USI A-45, Shutdown Decay-Heat Removal.)[1,2] A task action plan was formed to resolve the concerns about the reliability and effectiveness of shutdown decay-heat removal in nuclear power plants. The formation of the task action plan resulted in a considerable devotion of resources and effort towards the behavior and phenomena that control the effectiveness of natural circulation as a mechanism for shutdown decay-heat removal.[3] This effort resulted in the generation of a vast amount of data from many sources including the NRC, reactor vendors, universities, utilities and utility-sponsored research, national laboratories, and foreign sources. In addition to the experimental work, a complementary effort was devoted to the development and assessment of thermal hydraulic system codes that could simulate and predict the natural circulation cooling phenomena. The purpose of this report is to integrate and synthesize the important findings from this research into a single document.

This report will concentrate on PWRs having plant designs utilizing U-tube type steam generators (UTSGs) or once through type steam generators (OTSGs). The report does not address phenomena associated with severe accident natural circulation. The goal is to combine quantitative results of experiments and/or analyses to enable the prediction of limitations, operating boundaries, and uncertainties of system response under various abnormal transient or accident conditions.

The majority of the information presented in this report has been gleaned from the results of scaled experiments and/or analysis; not from full-scale plants. Therefore, the establishment and use of appropriate scaling parameters in these studies was necessary in order to ensure that the results were applicable to full-scale PWRs. See References 4 through 16 for detailed discussions of scaling analyses for natural circulation driven flow. The scaling criteria used by the experimental test facilities are shown in Appendix A.

Natural circulation refers to coolant flow within a closed loop (or reactor coolant system piping) in which heating and cooling effects result in different average densities in the heated and cooled sides of the loop. In the case of a PWR, these differing densities are created by the heat up of the reactor coolant in the core (heat source) and the subsequent cooling in the steam generators (heat sink), which are located at an elevation above that of the heat source to enhance the buoyancy effect. A net gravitational force is thereby available to drive the natural circulation flow. Periods of natural circulation cooling in PWRs are initiated by failure of the reactor coolant pumps, which causes the loss of forced circulation. This can be caused by events such as a loss of offsite power (LOSP), pump failure, and operator termination of forced circulation based on operating procedures for abnormal operational conditions. Lanning and Wunderlicks[17] estimate that approximately eight such events occur per year in U.S. PWRs, so these events are not uncommon. A compilation of actual nuclear plant tests/incidents, between 1973 and 1990, is presented in Table 1-1. Tests/incidents between 1973 and 1980 were taken from a list presented by Zvirin,[18] and updates have been included from more recent [illegible]s by searching through Licensee Event Reports (LERs) and selecting those pertaining to natural circulation cooling.

The report provides a concise summary of natural circulation (Section 2) as well as a detailed review of natural circulation phenomena (Sections 3, 4, and 5). An entire section is devoted to each mode of natural circulation (single-phase, two-phase, and reflux/boiling condensation). Sufficient repetition of key points in each of these sections provides an understanding of the relationships between the different modes. In addition, there are two sections that address the

issues associated with the role of thermal hydraulic system codes in predicting natural circulation cooling behavior and also the detection of natural circulation. The final Sections include a Summary and Conclusions (Section 8), a list of References, the Appendices, and an Index. Appendix A serves as a quick reference for information regarding the integral test facilities cited in this document. Appendix B provides a quick reference for information pertinent to thermal-hydraulic system codes.

Table 1-1. Summary of natural circulation plant data[18]

Plant	Type/Power (MW)	Test/Incident	Remarks
ANO-1	B&W 860	• Loss of electrical power • 2/22/75	• Transient of only 5 min. • Far from steady state
Calvert Cliffs	CE 845	• Test--natural circulation	--
Crystal River 3	B&W 858	• Test--loss of electrical power • 4/23/77	• Transient of 20 min. • Non-symmetrical loops operational • SG level changing • Quasi-steady state not fully established
Davis Besse 1	B&W 906	• Test--loss of offsite power • 12/3/78	• Transient of 14 min. • Secondary pressure changing • Quasi-steady state not reached
Davis Besse 1	B&W 906	• Test--loss of offsite power • 1/15/79	• Transient of 9 min. • Apparent quasi-steady state
Davis Besse 1	B&W 906	• Test--natural circulation • 12/3/78	• Constant power • Steady state temperatures • Oscillations in SG levels
Ft. Calhoun	CE 457	• Test--natural circulation	• Typically, 40 min. transient transition from forced to natural circulation
Haddam Neck	W (4 loop) 527	• Test--natural circulation	• Test initiated by pumps trip 1 hr after reactor shutdown, following 1 month operation at 70% power
Kewaunee	W (2 loop) 535	• Backdown and shutdown due to hot reserve aux. bus, RCPs tripped • 4/26/75	• Natural circulation transient of 2 days until RHR activated • Steady state
Kewaunee	W (2 loop) 535	• Shutdown due to turbine blade burst • 1/17/77	• Natural circulation transient of 2 days until RHR activated • Steady state

Table 1-1. (continued)

Plant	Type/Power (MW)	Test/Incident	Remarks
Kewaunee	W (2 loop) 535	• Loss of offsite power • 1/17/80	• Transient of 9 hours until RHR activated • Steady state
North Ana 2	W (3 loop) 939	• Test--natural circulation	---
Oconee-1	B&W 860	• Natural circulation imposed by pressure decrease in SG. • 5/1/73	• No input power. • Transient (30 min.) towards new steady state at lower temp.
Oconee-1	B&W 860	• Test--loss of offsite power • 11/4/73	• Transient of 22 min., quasi steady state.
Oconee-2	B&W 860	• Reactor trip following separation from grid. • 5/2/74	• Long transient. • HPSI kept constant.
Palisades	CE 798	• Test--natural circulation • 4/20/72	• Transient of 45 min. • Nearly steady state
Point Beach	W (2 loop) 497	• Test--natural circulation	---
Prairie Island	W (2 loop) 520	• Tube break in SG • 10/2/79	• Pumps stopped after 13 min. • Transient of 16 hours until RHR on • Injection of water to make up for leaks
Sequoyah	W (4 loop) 1148	• Test--natural circulation • 6/80	• Pre-test RETRAN calculations
St. Lucie	CE 810	• Test--natural circulation	---
St. Lucie	CE 810	• Loss of offsite power • 6/11/80	• Pressurizer level controlled by spraying to fill void in the reactor dome caused by depressurization
St. Lucie	CE 810	• Loss of offsite power • 4/15/80	• Behavior similar to above incident. • Depressurization and pressure control were slower
TMI-2	B&W 880	• Accident • 3/28/79	• Switch to natural circulation 4/27/79
TMI-2	B&W 880	• Test--loss of offsite power • 4/22/78	• Transient of 40 min. • Oscillations in temperatures

Table 1-1. (continued)

Plant	Type/Power (MW)	Test/Incident	Remarks
Trojan	W (4 loop) 1130	• Test--natural circulation • 2/14/76	• Transient of 100 min. (from startup)
Yankee Rowe	W (4 loop) 1175	• Test--loss of offsite power	• Transient of 3 hours • Steady state
Zion-1	W (4 loop) 1040	• Test--natural circulation	• Results in agreement with theoretical calculations
Diablo Canyon Unit-1	W (4 loop) 1073	• Reactor trip due to power range high positive rate • 6/14/90 • LER #2759000S	• Reactor placed in natural circulation following reactor trip
Salem Station Unit-1	W (4 loop) 1100	• Loss of offsite power • 8/26/86 • LER #31186007	• Reactor core cooled using safety injection and natural circulation
Beaver Valley Unit-2	W (3 loop) 833	• Turbine trip/reactor trip due to personnel error • 11/17/87 • LER #31787003	--
St. Lucie Unit-2	CE (2X4 loop) 839	• Reactor trip • 9/9/85 • LER #31787003	• Unit stabilized using natural circulation
Diablo Canyon Unit-1	W (4 loop) 1087	• Reactor trip following an electrical ground on a connector to RCP 2-2 • 7/17/88 • LER #32388008	• Cooldown to cold shutdown initiated using natural circulation and RHR system (28 hours)
Indian Point Unit-2	W (4 loop) 900	• Loss of power during hot shutdown • 10/4/83 • LER #24783035	• Reactor cooled with natural circulation for approximately 14 min
Byron Unit-2	W (4 loop) 1105	• Reactor trip and subsequent loss of offsite power due to a personnel error • 10/2/87 • LER #45587019	• Natural circulation was used to cool the primary loop following loss of offsite power
Rancho Seco	B&W 963	• Reactor trip • 10/14/88 • LER #31288015	• Natural circulation was maintained for approximately 1.5 hours

Table 1-1. (continued)

Plant	Type/Power (MW)	Test/Incident	Remarks
Prairie Island Unit-2	W (2 loop) 500	• Reactor trip and loss of power to RCPs • 12/21/89 • LER #30689004	• Reactor cooled by natural circulation for approximately 3 hours
Crystal River Unit-3	B&W (2 loop, lowered) 666	• Degraded offsite power & reactor trip • 7/17/89 • LER #30289023	• RCS cooled by natural circulation in 'B' loop • Thermal decoupling occurred in 'A' loop
Turkey Point Unit-4	W (3 loop) 666	• Reactor trip • 6/17/85 • LER #25185011	• Natural circulation established, verified, and maintained
Virgil C. Summer	W (3 loop) 885	• Reactor trip • 3/5/90 • LER #39584010	• Natural circulation was effectively established
Joseph M. Farley Unit-2	W (3 loop) 830	• Reactor trip • 8/14/85 • LER #36485010	• Natural circulation verified and maintained for approx. 25 min
Catawba Unit-1	W (4 loop) 1129	• Test--natural circulation • 11/19/85 • LER #31787003	--
Calvert Cliffs Unit-1	CE (2X4 loop) 845	• Loss of non-emergency ac power • 8/20/87 • LER #31787012	• Natural circulation observed
Palisades	CE (2X4 loop) 768	• Loss of offsite power • 7/14/87 • LER #25587024	• Plant maintained in hot standby with natural circulation for 9 hours
Indian Point Unit-2	W (4 loop) 900	• Reactor trip • 12/12/85 • LER #24785016	• Natural circulation established for approximately 2 hours
Wolf Creek	W (4 loop) 1135	• Reactor trip • 9/10/87 • LER #48287037	• Natural circulation established for 5 min.
Beaver Valley Unit 1	W (3 loop) 665	• Reactor trip • 8/25/87 • LER #41287019	• Plant stabilized following turbine trip using natural circulation

Table 1-1. (continued)

Plant	Type/Power (MW)	Test/Incident	Remarks
Palo Verde Unit-1	CE (2X4 loop) 1221	• Reactor trip • 9/12/85 • LER #52885063	• Natural circulation established and verified following trip
Millstone Point Unit-2	CE (2X4 loop) 863	• Shutdown due to hurricane "Gloria" • 9/27/85 • LER #33685014	• Natural circulation maintained for approximately 24 hours
Point Beach	W (2 loop) 485	• Loss of load reactor trip due to lightning strike • 8/16/87 • LER #30187002	• Adequate natural circulation indicated by differential temperatures between the hot and cold legs
H. B. Robinson Unit-2	W (3 loop) 665	• Loss of offsite AC event • 1/28/86 • LER #26186005	• Plant cooled by natural circulation and by using SG PORVs
Turkey Point Unit-3	W (3 loop) 666	• Reactor trip • 3/19/84 • LER #25084007	• Natural circulation verified
Palo Verde Unit-1	CE (2X4 loop) 1221	• Loss of offsite power • 10/7/85 • LER #52885076	• Reactor coolant system cooled via natural circulation after loss of forced circulation

B&W – Babcock and Wilcox

CE – Combustion Engineering

W – Westinghouse

2. NATURAL CIRCULATION PHENOMENA

The purpose of this section is to address the general phenomena associated with each natural circulation mode in sufficient detail to allow effective discussions of specific issues in later sections. In addition, distinctions in natural circulation behavior between plants with UTSGs and OTSGs are made.

Three modes of natural circulation are normally recognized. Single-phase natural circulation and two-phase natural circulation are two of these modes. The third mode is called either reflux condensation or boiling condensation, depending on the type of steam generator. As mentioned in the introduction, natural circulation flow in PWRs is driven by temperature induced density gradients, enhanced by a thermal center elevation difference between the hot (core) and cold (steam generator) regions in the primary loop.[19,20] This density gradient produces a buoyancy effect that drives the natural circulation flow. Thus, single-phase natural circulation is the flow of an essentially subcooled primary liquid driven by liquid density differences within the primary loop. Two-phase natural circulation is normally defined as the continuous flow of liquid and vapor. In this mode of natural circulation, vapor generated in the core enters the hot leg and flows along with the saturated liquid to the steam generator, where at least some of the vapor is condensed. Hence, density gradients are affected in the two-phase mode not only by temperature differences, but also mainly by the presence of voids in the primary loop. In both single-phase and two-phase natural circulation, the mass flow rate is the most important heat removal parameter.[21] Conversely, during reflux/boiling condensation, the loop mass flow rate has a negligible effect because the primary mechanism of heat removal is vapor condensation. In the reflux/boiling condensation mode, single-phase vapor generated in the core flows through the hot leg piping, is condensed in the steam generator, and flows back to the core as a liquid. In summary, the three modes of natural circulation are distinguishable based upon characteristic mass flow rates, loop temperature difference behavior, and basic phenomenological differences.[19] These distinguishing features are discussed below.

In order to provide a more accurate discussion of the three modes of natural circulation, it is necessary to differentiate between plants with UTSGs and plants with OTSGs. The major geometric differences between the two designs are the shape of the tubes within each steam generator, and the geometry of the hot leg. These geometric differences have little effect on the response of single-phase natural circulation or even the early stages of two-phase natural circulation; but as the amount of voids in the primary system increases, the natural circulation behavior of the two designs may diverge. Figure 2-1 (see Reference 21) presents a simple schematic design of a PWR system with a UTSG, while Figure 2-2 (see Reference 22) presents a schematic of a PWR system with a OTSG. In the UTSG design, multiple tubes of different lengths are shaped in the form of an inverted U, and the hot leg has a short vertical section that enters the bottom of the steam generator. In the OTSG design, the multiple, equal length tubes are vertical. The hot leg has a long vertical section leading to an inverted U-bend, sometimes called the "candy cane" region, which connects to the top of the steam generator.

Figure 2-3 (see Reference 23) is a representative natural circulation flow map for a UTSG design [specifically, the Primärkreisläufe (PKL) facility in West Germany]. The primary side mass flow rate (measured at the downcomer) and the temperature difference between the primary side coolant at the steam generator inlet to the secondary side fluid (the rectangular zones indicate measurement uncertainty) are plotted versus the primary mass inventory for two-phase natural circulation and reflux condensation, and the level of subcooling for single-phase natural circulation. Note that for single-phase natural circulation the loop mass flow rates and primary-to-secondary temperature differences are nearly independent of subcooling. As the primary inventory is reduced, the primary pressure and the amount of

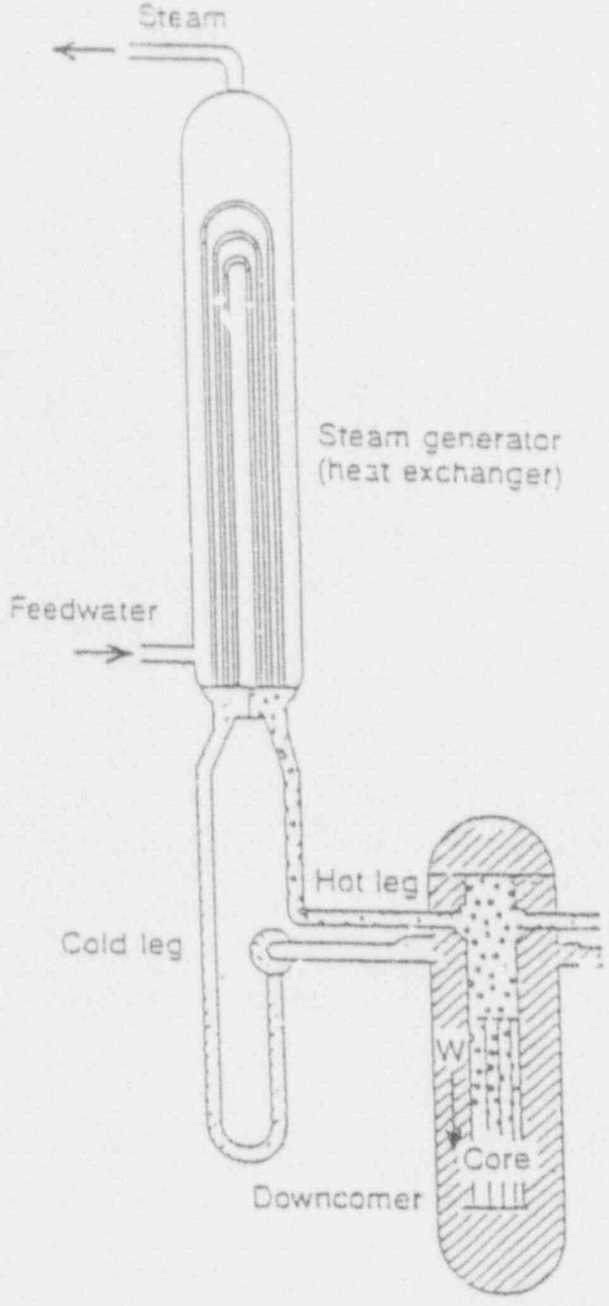

Figure 2-1. Schematic of typical PWR system with U-tube type steam generator,[21] W = Mass flow rate.

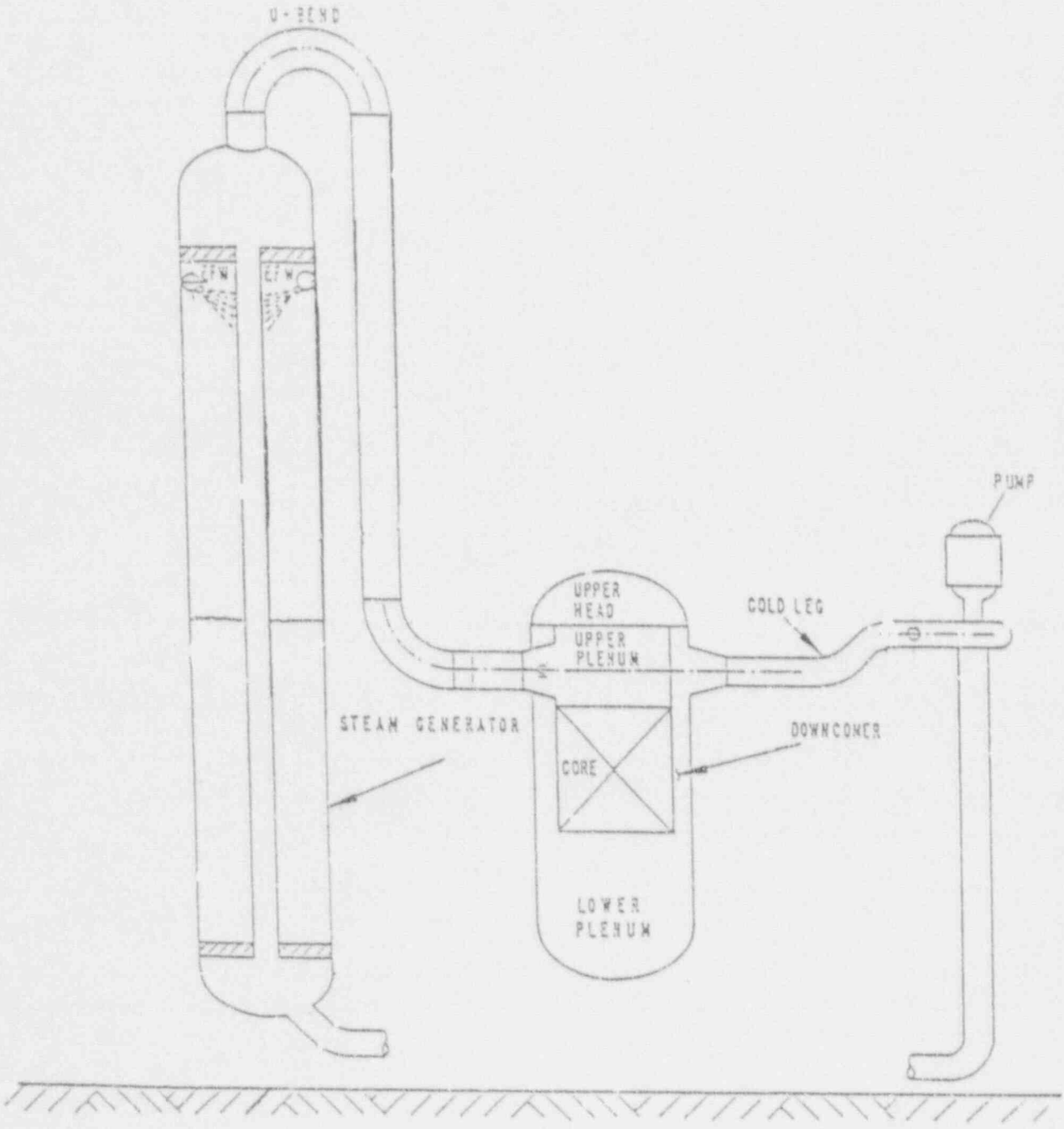

Figure 2-2. Schematic of typical PWR system with a once through steam generator.[22]

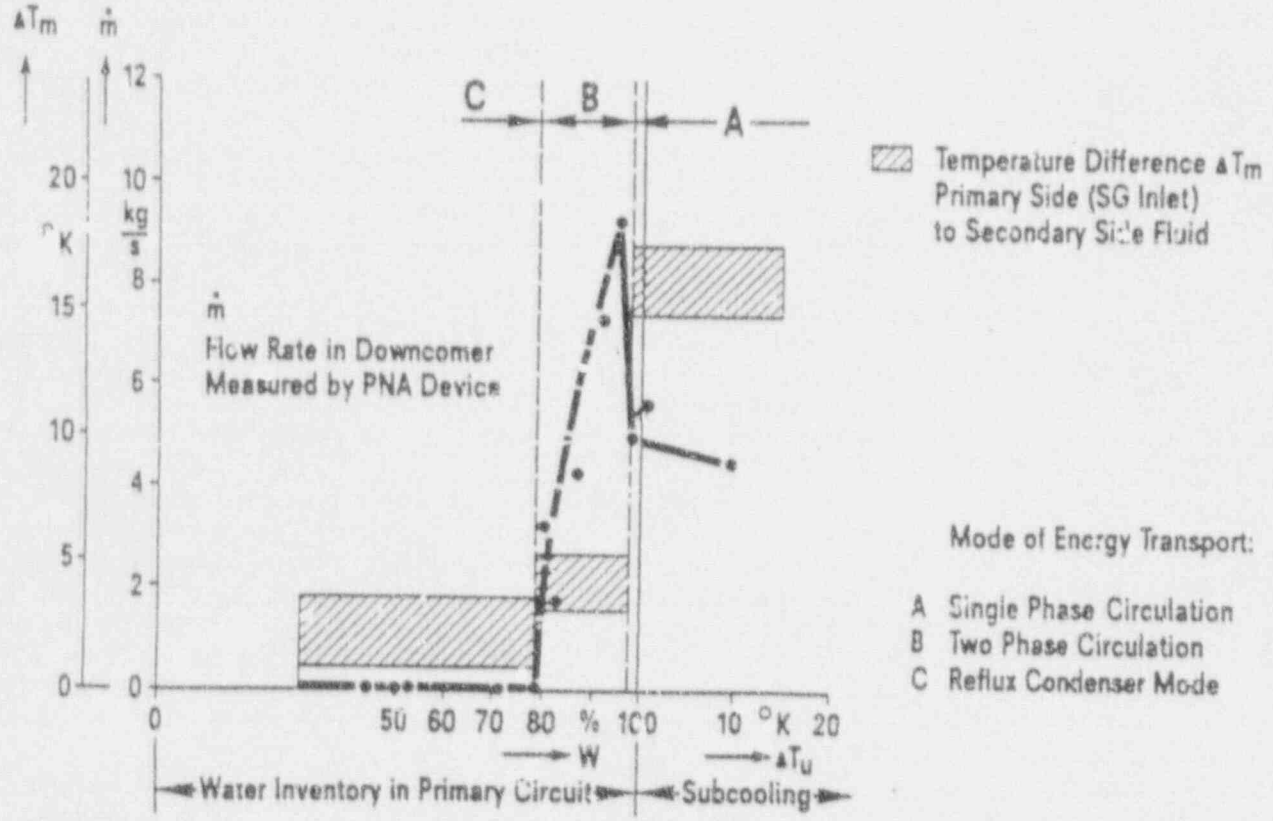

Figure 2-3. Modes of energy transport observed in the PKL test facility.[23]

subcooling decrease, the core vapor generation rate increases, and voids collect in the vessel upper head. As the inventory is further reduced, the hot leg eventually saturates; as voids enter the hot leg nozzle from the vessel upper head. Up to this point the mass flow rate and loop temperature difference behavior have remained relatively constant. However, the natural circulation behavior changes significantly once voids enter the vertical sections of the hot legs and the upflow sides of the steam generator U-tubes. The hot side density is sharply reduced because of the presence of the voids, while the cold side density has not yet been significantly affected. Consequently, the buoyancy effect is enhanced, resulting in a higher loop mass flow rate. The mass flow rate peaks when voids occupy almost the entire upflow sides of the U-tubes, and single-phase liquid exists in the downflow sides of the U-tubes and in the cold leg. This situation corresponds to the maximum hot-to-cold side density difference in the loop. Once voids pass over the top of the steam generator U-tubes into the downflow side, the buoyancy effect is reduced and the mass flow rate likewise decreases.[20] Further inventory reductions result in the drop of the two-phase mixture below the tops of the steam generator U-tubes, interrupting the two-phase flow and initiating reflux condensation. During the two-phase flow mode, the primary-to-secondary temperature difference decreases because of the enhanced heat transfer resulting from vapor condensation. This effect is also observed in the reflux condensation mode where condensation heat transfer is the primary means of decay heat removal.[23]

During reflux condensation, vapor generated in the core is condensed on the inner surface of the steam generator U-tubes. In the upflow sides of the U-tubes, a counter-current flow of vapor and condensate is established. Condensate collects on the inner surface of the steam generator U-tubes and flows back to the core via the hot leg, while vapor continues to flow over the U-tube upper bend. In the downflow side of the U-tubes, vapor and condensate flow into the cold leg suction piping. Experiments have shown an approximately equal split between the condensation in the upflow and in the downflow sides of the U-tubes.[19,20,24] Figure 2-4 illustrates this phenomenon in a single U-tube. The effects of flooding, liquid hold-up, and oscillatory U tube flow may be observed in counter-current type flow situations.[20,25,26] These effects will be addressed in subsequent sections.

In OTSG plants, single-phase natural circulation and the initial stages of two-phase natural circulation are similar to that of UTSG plants. However, during the latter stages of two-phase natural circulation voids may collect in the "candy cane" or U-bend region of the upper hot leg, and disrupt the flow. This flow interruption may delay the onset of boiling condensation and result in the temporary loss of the steam generator as a heat sink. Figure 2-5 (see Reference 27) schematically illustrates the liquid distribution leading to flow interruption and also demonstrates why this event is less likely in the UTSG. In the OTSG, a steam bubble may interrupt flow when the primary liquid level is above the secondary side emergency feedwater spray elevation. The secondary liquid level is thus unable to condense the primary steam bubble and the primary and secondary liquid temperatures may equilibrate, resulting in a temporary loss of the steam generator as a heat sink. In the UTSG, vapor blockages may occupy the upper U-bends of some steam generator U-tubes, but the tops of the U-tubes are normally below the secondary liquid level, keeping the steam generator in a heat sink mode.

During interrupted flow in an OTSG, "spillover" occurs when compression of the steam bubble (due to system pressurization following the loss of the steam generator as a heat sink) allows the primary liquid level in the upflow side of the hot leg to reach the top of the U-bend. Figure 2-6 is a schematic description of the primary liquid distribution just prior to spillover. Spillover results in a recoupling of the primary and secondary sides, and continuous two-phase natural circulation will be reestablished until void blockages reform and the flow is once again interrupted. This cyclic behavior is called intermittent circulation.[28] With no further loss of reactor primary coolant this intermittent behavior would continue indefinitely, as long as secondary coolant flow

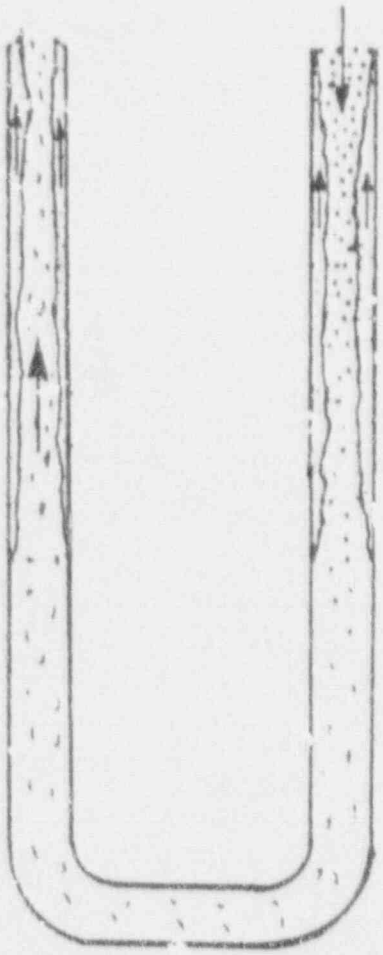

Figure 2-4. U-tube liquid distribution during reflux condensation.

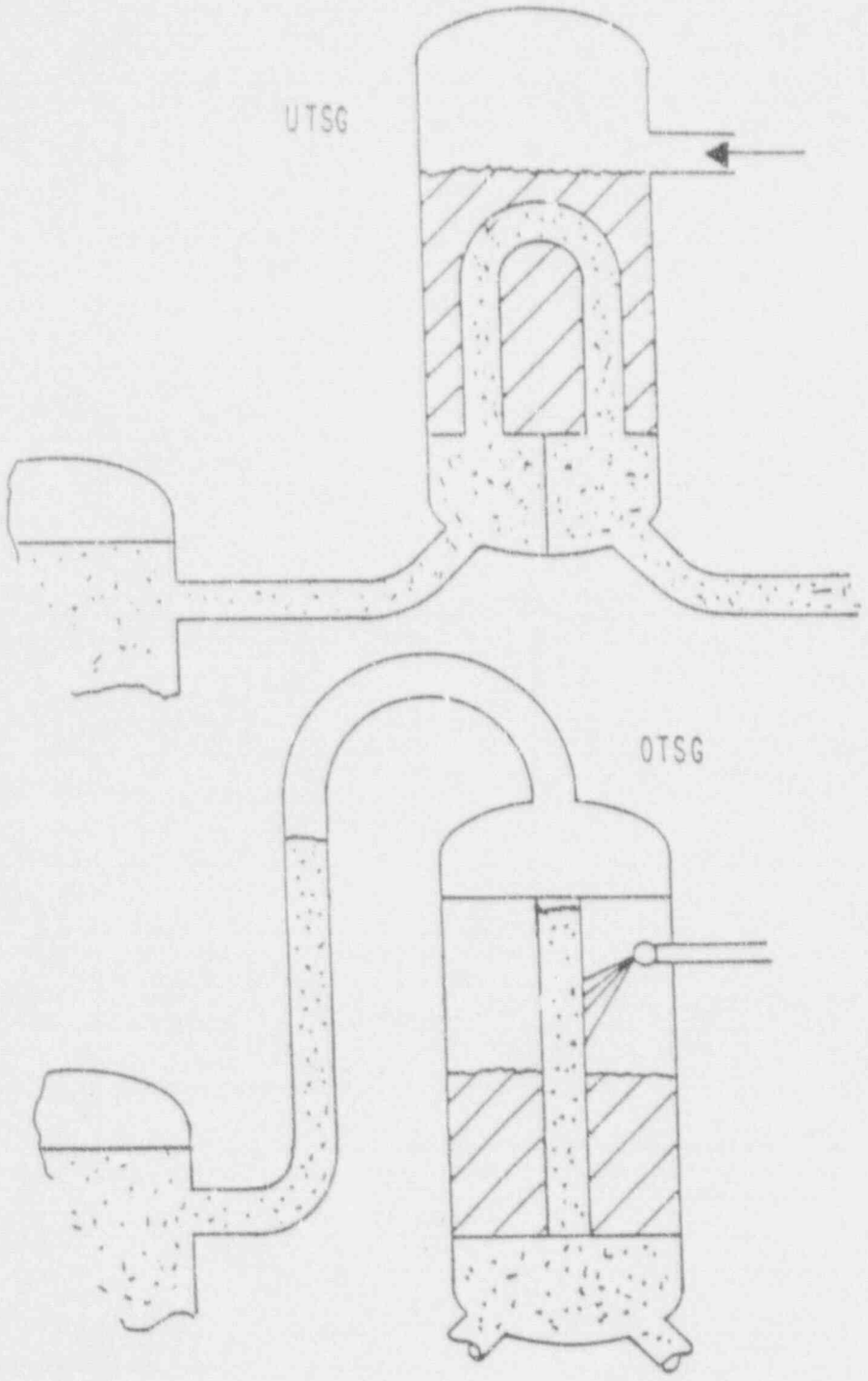

Figure 2-5. Sketch comparing effect of geometry on potential heat sink for two-phase natural circulation.[27]

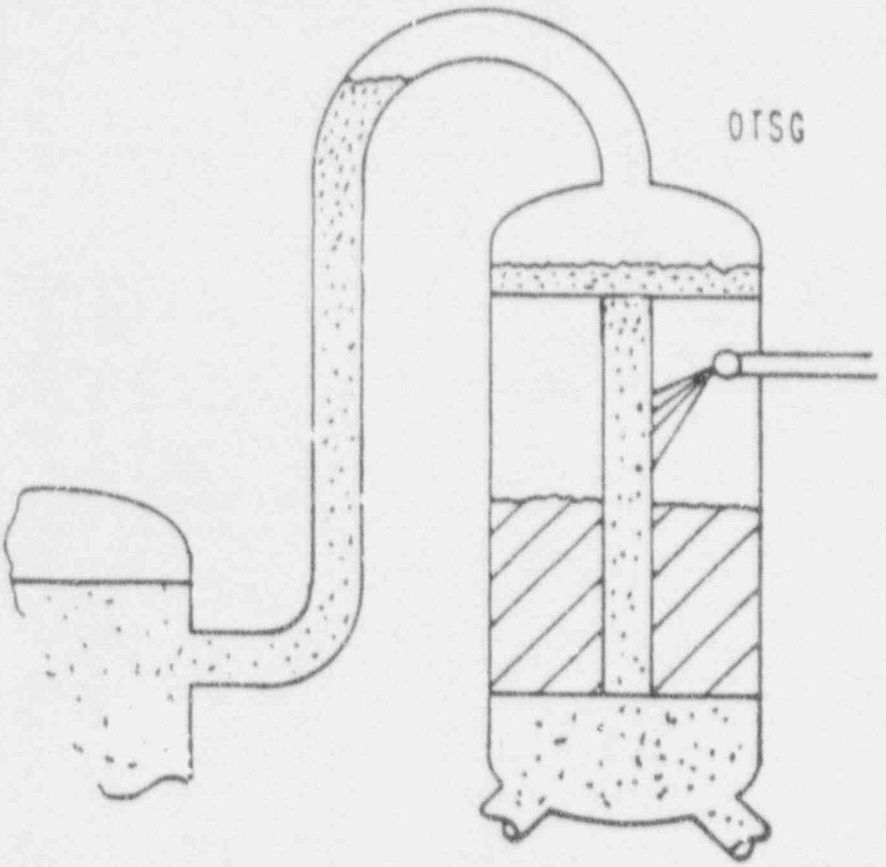

Figure 2-6. Liquid distribution in a OTSG just prior to spillover.[27]

was maintained. Eventually, sufficient loss of primary inventory results in a steam generator primary liquid level that is low enough to initiate the boiling condensation mode of natural circulation.

In the case of a OTSG, such periods of intermittent circulation do not allow the presentation of a continuous flow map such as Figure 2-3. Instead, pressure response data can be used to indicate regions of different natural circulation behavior. Figure 2-7 indicates periods of draining and depressurization to saturation, two-phase natural circulation, interrupted flow, and boiling condensation. Single-phase natural circulation occurs during the early period of draining and depressurization, and in any later post refill cooldown period. Periods of continuous two-phase natural circulation can occur before and after boiling condensation.

Figure 2-8 depicts the liquid distribution in a OTSG loop during boiling condensation. Because this type of boiling condensation requires the primary level to be lower than the secondary level within the steam generator, the configuration shown in this figure is called "pool" boiling condensation. A second type of boiling condensation mode, called Emergency Feedwater (EFW) boiling condensation [sometimes also referred to as Auxiliary Feedwater (AFW) boiling condensation], occurs when the steam generator primary liquid level is greater than the secondary level, but a primary condensing surface exists below the EFW sparger spray location. Both types of boiling condensation are effective means of decay heat removal. Figure 2-9 shows the loop liquid distribution for a single tube during EFW boiling condensation. Figure 2-9 is perhaps overly simplistic in that liquid distribution during EFW boiling condensation will actually vary from tube to tube depending on the proximity of the tube to the EFW sparger spray, the EFW flow rate, and the secondary vapor upflow.[29,30] EFW liquid distribution is dependent upon the secondary vapor upflow when the flooding line is approached. Secondary side flooding may occur at the tube support plates in OTSGs.[29,30]

The preceding discussion of natural circulation phenomena was simplified by considering only the basic natural circulation responses. It is noted as a prelude to subsequent sections that many issues related to natural circulation have not yet been addressed. For example, nonuniform flow, multi-loop effects, secondary side effects, and noncondensable gases can have significant influences on the effectiveness and behavior of natural circulation cooling. Because of the importance of these issues, they will be addressed relative to each natural circulation mode in the sections that follow.

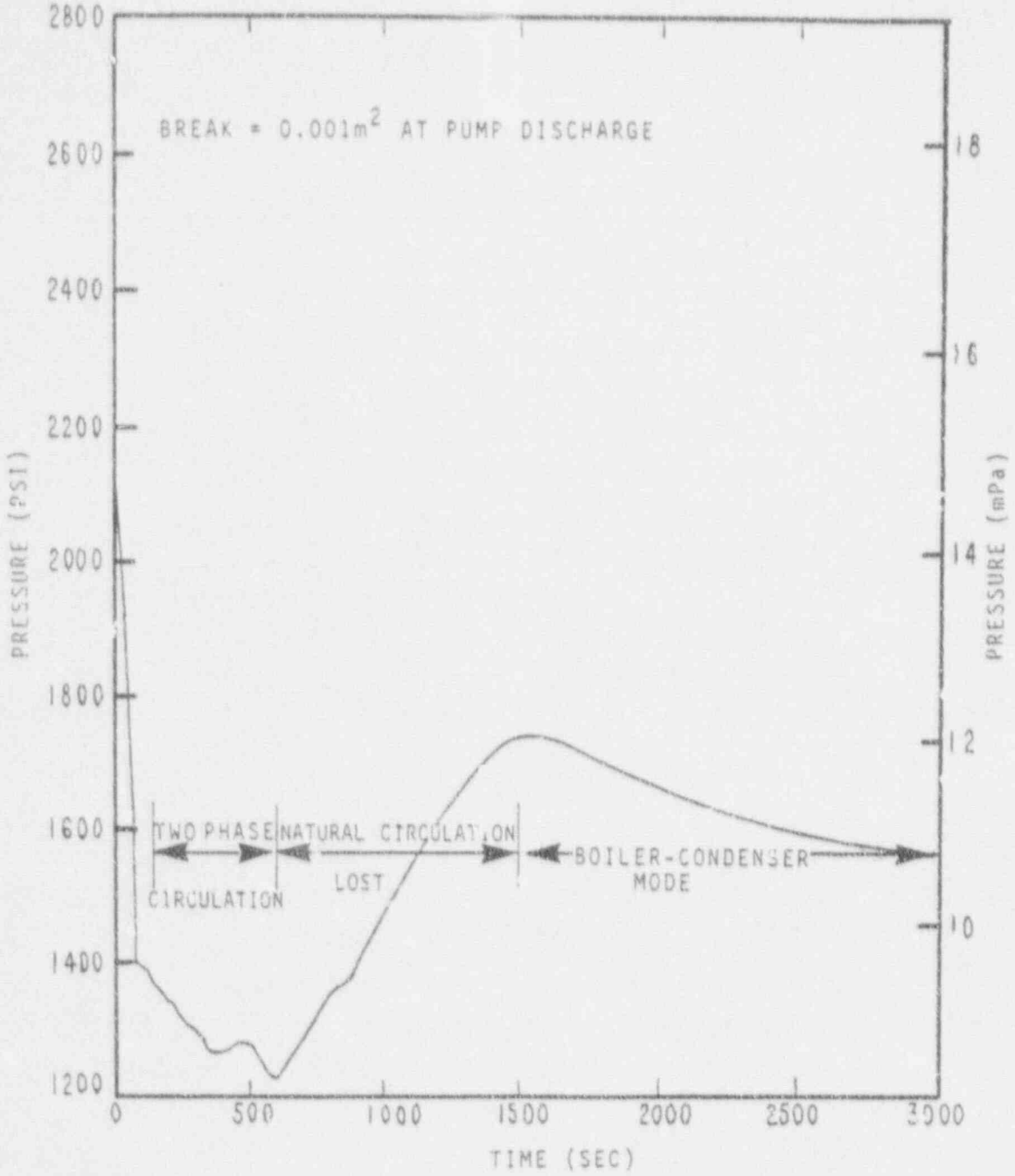

Figure 2-7. Pressure response and natural circulation modes during Small Break Loss-of-Coolant Accident (SBLOCA) transient for OTSG plants.[27]

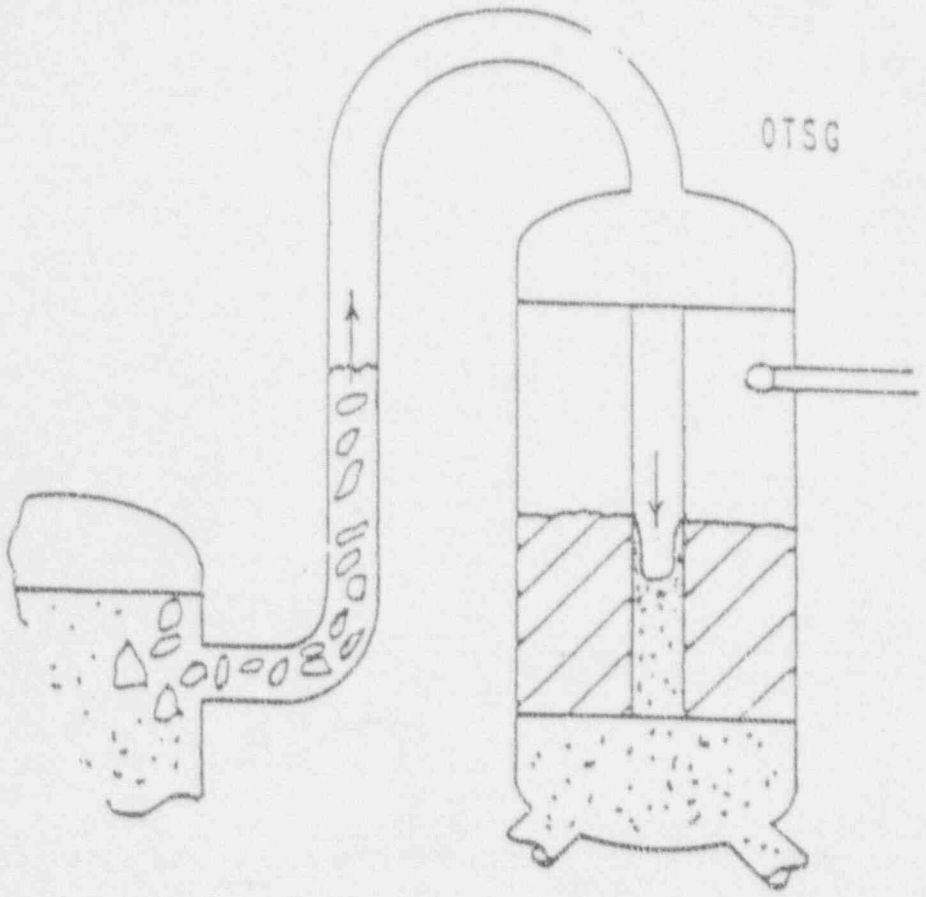

Figure 2-8. OTSG liquid levels during pool boiling condensation.[27]

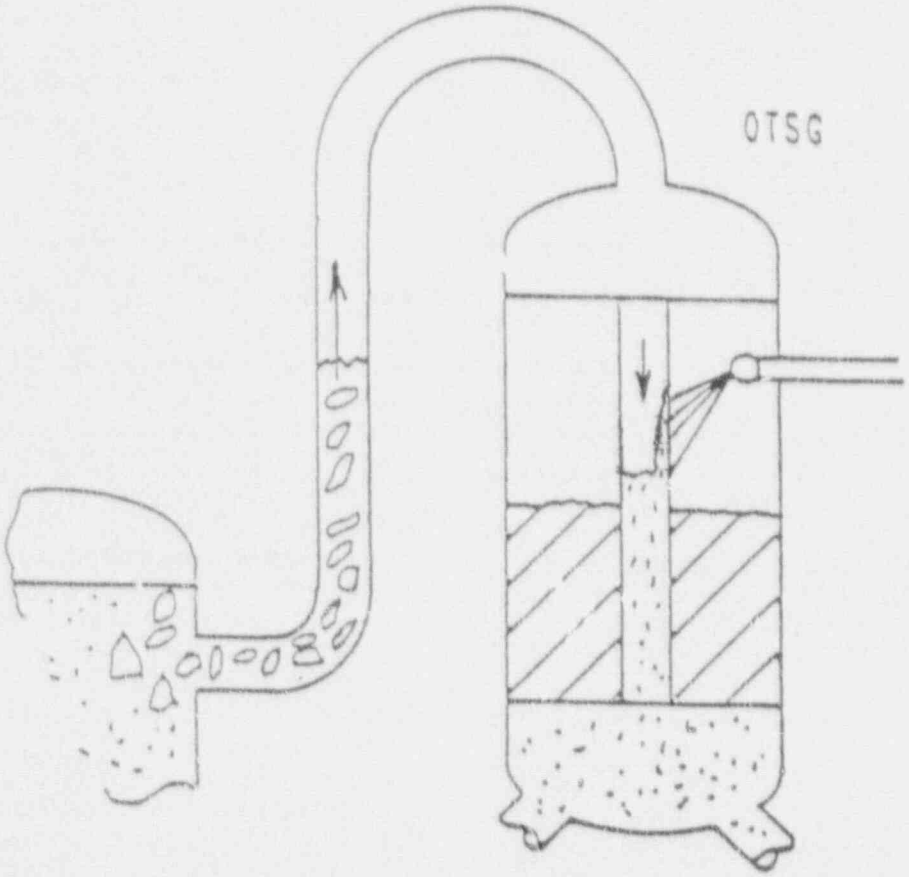

Figure 2-9. OTSG liquid levels during EFW boiling condensation.[27]

3. SINGLE-PHASE NATURAL CIRCULATION

3.1 Introduction

The purpose of this section is to synthesize available data into a format that will enable the prediction of single-phase natural circulation system behavior under various operating conditions. The general characteristics of single-phase natural circulation will be addressed first in order to provide a reference base for discussing more specific phenomena. Also, a discussion of the calculation of steady state single-phase natural circulation using expressions derived from the simplified mass, momentum, and energy equations is included.

Examples of general characteristics of single-phase natural circulation include loop mass flow rate behavior, typical system parameter responses (temperature, pressure, etc.), and primary-to-secondary heat transfer behavior. Once the general characteristics of single-phase natural circulation have been established, specific phenomena associated with certain abnormal conditions are identified and discussed. For example, issues such as noncondensable gases, secondary side conditions, and non-uniform flow are addressed with regard to their effects on single-phase natural circulation. Operating limits and uncertainties associated with these specific phenomena are emphasized. Finally, a brief summary of important single-phase natural circulation behavior will conclude this section.

3.2 General Characteristics

Single-phase natural circulation was described in Section 2 as the flow of an essentially subcooled liquid in the primary loop, driven only by liquid density differences between the hot and cold regions of the primary loop. The CE Owners Group Emergency Procedures Guidelines[31] expands this generic description with the additional characteristics listed as follows:

1. During single-phase natural circulation, hot-to-cold leg temperature differences in the primary loop are less than the normal full power operating condition.
2. Single-phase natural circulation is characterized by decreasing cold leg temperatures.
3. Single-phase natural circulation is characterized by stable or slowly decreasing hot leg temperatures.
4. During single-phase natural circulation, there should only be small differences between the hot leg and core exit thermocouple readings.

These characteristics also give insight into the detection of single-phase natural circulation through the use of available plant temperature data. They imply the existence of a primary loop temperature hierarchy, which is characteristic of single-phase natural circulation, as opposed to the other modes of natural circulation. Figures 3-1 and 3-2 demonstrate this temperature hierarchy in a test conducted in the Electric Power Research Institute/Stanford Research Institute (EPRI/SRI) four-loop test facility.[32] Only one loop was active during this constant power (12.1 kW) test. The temperature hierarchy consisted of the upper vessel, the hot leg, the steam generator (U-tube), the lower vessel, and finally the cold leg.[32] The steam generator U-tube temperature shown in Figure 3-2 was measured in one of the six U-tubes at the top of the heat exchanger. Comparing Figures 3-1 and 3-2 indicates that the lower vessel temperature is higher than the cold leg temperature. In fact, the lower vessel often precedes the cold leg in the temperature hierarchy due to heat gained through the downcomer.[32] Additional evidence of the existence of this temperature hierarchy is presented in Figure 3-3, which illustrates the loop temperature distribution during the single-phase natural circulation period of Semiscale test S-NH-1.[33]

Many SBLOCA experiments[19,20,23,33,34] have demonstrated that single-phase natural circulation persists in the primary loop until the lower level of the voids in the vessel upper head drops to the hot leg nozzle elevation. Once the level of voids reaches this elevation, voids enter the hot leg and two-phase natural circulation is initiated. Table 3-1 shows a

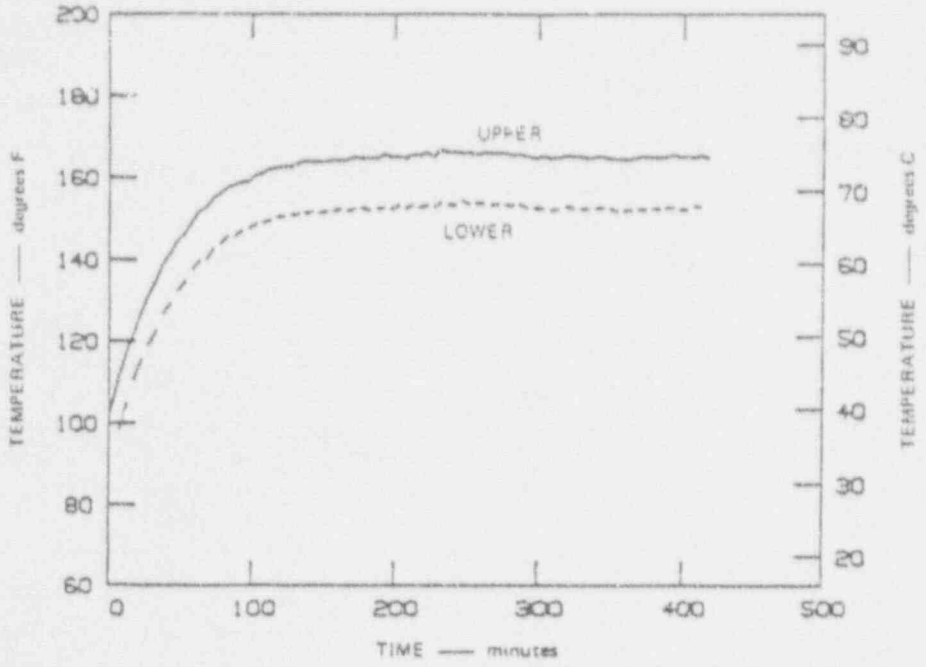

Figure 3-1. Vessel temperatures in a EPRI/SRI single-phase natural circulation test.[32]

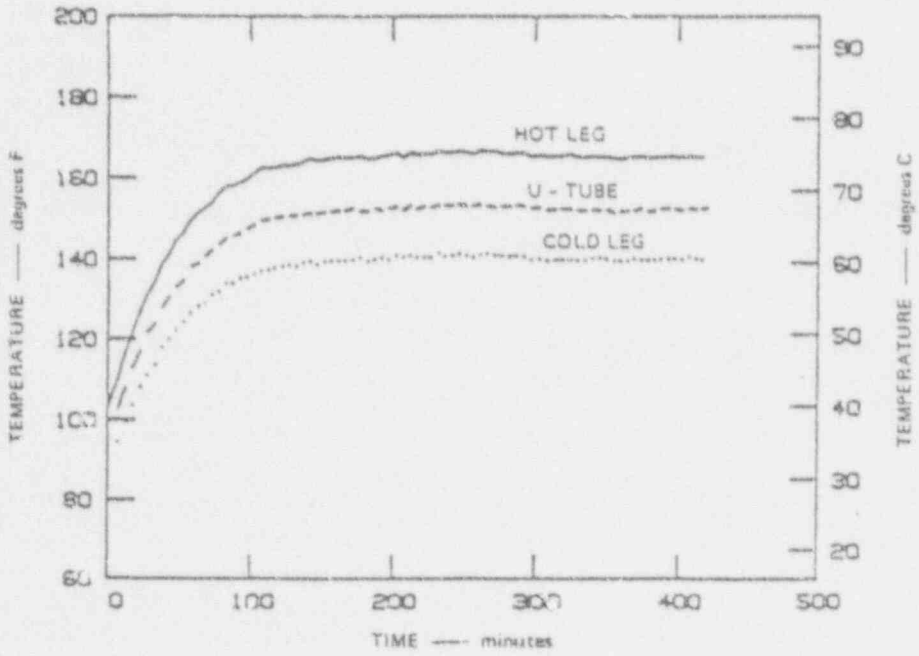

Figure 3-2. Primary A-Loop temperatures in a EPRI/SRI single-phase natural circulation test.[32]

BLSG Primary Tube
Temperature Distribution

Upflow

Longest Length U-Tube	Shortest Length U-Tube
555 (61)	559 (61)
552 (137)	553 (137)
547 (213)	550 (213)
544 (404)	544 (404)
540 (556)	541 (556)
539 (709)	540 (709)
538 (886)	

Downflow

Longest Length U-Tube	Shortest Length U-Tube
538 (99)	537 (99)
537 (404)	535 (404)
538 (709)	

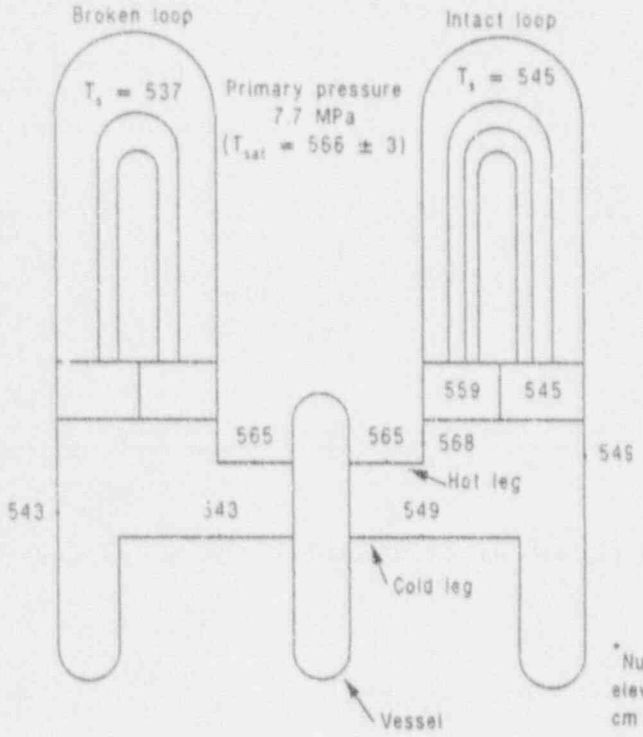

ILSG Primary Tube
Temperature Distribution

Upflow

Longest Length U-Tube	Shortest Length U-Tube
555 (211)	561 (84)
550 (452)	545 (815)

Downflow

Longest Length U-Tube	Shortest Length U-Tube
545 (211)	546 (211)
538 (785)	547 (668)

*Number in parentheses is elevation above tube sheet in cm for primary fluid temperature measurement

(Uncertainty ± 3 K)*

Figure 3-3. Fluid temperature distribution (in degrees K) during Semiscale test S-NH-1 at 250 seconds.[33]

Table 3-1. Comparison of primary mass inventory versus significant inflection poi..ts in the loop mass flow rate as found in PKL. Semiscale, and LSTF natural circulation experiments.[20]

Facility	Scaled Core Power (%)	Last, Lowest Single-Phase Flow Inventory (%)	Inventory at the maximum two-phase flow rate (%)	Zero Flow Inventory (%)
PKL	1.5	99.0	95.0	80.0
Semiscale	1.5	94.0	86.0	70.0
LSTF	2.0	96.0	85.0	70.0
Semiscale	3.0	96.0	88.0	65.0
LSTF	5.0	91.0	80.0	64.0
Semiscale	5.0	94.0	84.0	No Data

comparison of significant inflection points in the loop mass flow rate versus primary mass inventory as found in experiments conducted in the PKL, Semiscale, and LSTF test facilities.[20] Of particular interest to this section is the column entitled "Last, Lowest, Single-Phase Flow Inventory." Comparisons of PKL, Semiscale, and LSTF mass flow versus primary mass inventory are shown in Figure 3-4.[20] Note that the mass flow rates in Figure 3-4 have been scaled by the ratio of the respective power scaling factors using the Semi-scale scaling factor as the base.[20] The important point is that although the scaling factors for these facilities range from 1/48 (LSTF) to 1/1705 (Semiscale) (the PKL scaling factor is 1/134), the qualitative behavior of the loop mass flow rate versus primary mass inventory is nearly the same. Differences in the point of transition between single-phase and two-phase natural circulation for the three test facilities can be attributable to several factors, including: differences in the vessel upper head and hot leg nozzle geometries, different core power levels, different system pressures, and different secondary side conditions. In general, experiments have shown that the occurrence of a given natural circulation mode is primarily a function of the primary mass inventory, with weak dependencies on the other factors mentioned above.

The dominant heat transfer mechanism in single-phase natural circulation cooling is convection. Heat generated by the core is convected away from the reactor vessel through the hot leg to the steam generator (heat sink) via the subcooled primary liquid. Heat is transferred from the primary side to the secondary side in the steam generator. The cooling cycle is completed when the cooled primary liquid flows back to the reactor vessel through the cold leg.

The amount of heat removed from the core through single-phase natural circulation cooling is normally the amount produced by decay heat power levels (≤5% core power). However, an Anticipated Transient Without Scram (ATWS) experiment in the Loss-of-Fluid Test (LOFT) facility[35] demonstrated that single-phase natural circulation can accommodate heat generation greater than the decay heat. It was concluded in this experiment that single-phase natural circulation is capable of adequate cooling up to approximately 18% of full power.

3.3 Analytical Expressions

As stated previously, during single-phase natural circulation, the primary heat transfer mechanism is convection. Therefore, the primary loop mass flow rate is an essential parameter in determining the heat removal capability of single-phase natural circulation cooling. Correlated expressions for the steady state mass flow rate and core temperature difference have been derived for single-phase natural circulation in a PWR by Zvirin et al.[34,36] For turbulent flow, these expressions are given by

$$W = \left[\frac{2\rho_l^2 \beta g \Delta L P}{c\ R}\right]^{\frac{1}{3}} \tag{3-1}$$

$$\Delta T_R = \left(\frac{P}{\rho_l c R}\right)^{\frac{2}{3}} \left[\frac{R}{2g\beta\Delta L}\right]^{\frac{1}{3}} \tag{3-2}$$

If the flow is laminar, the following expressions apply

$$W = \left[\frac{2\rho_l \beta g \Delta L P}{cr}\right]^{\frac{1}{2}} \tag{3-3}$$

$$\Delta T_R = \left[\frac{rP}{2\beta g \Delta L \rho_l c}\right]^{\frac{1}{2}} \tag{3-4}$$

where

W = mass flow rate

β = temperature coefficient for volume expansion at average coolant temperature

g = acceleration of gravity

ΔL = equivalent driving head; for UTSG, the elevation difference between axial midplane of core and axial midplane of active tube

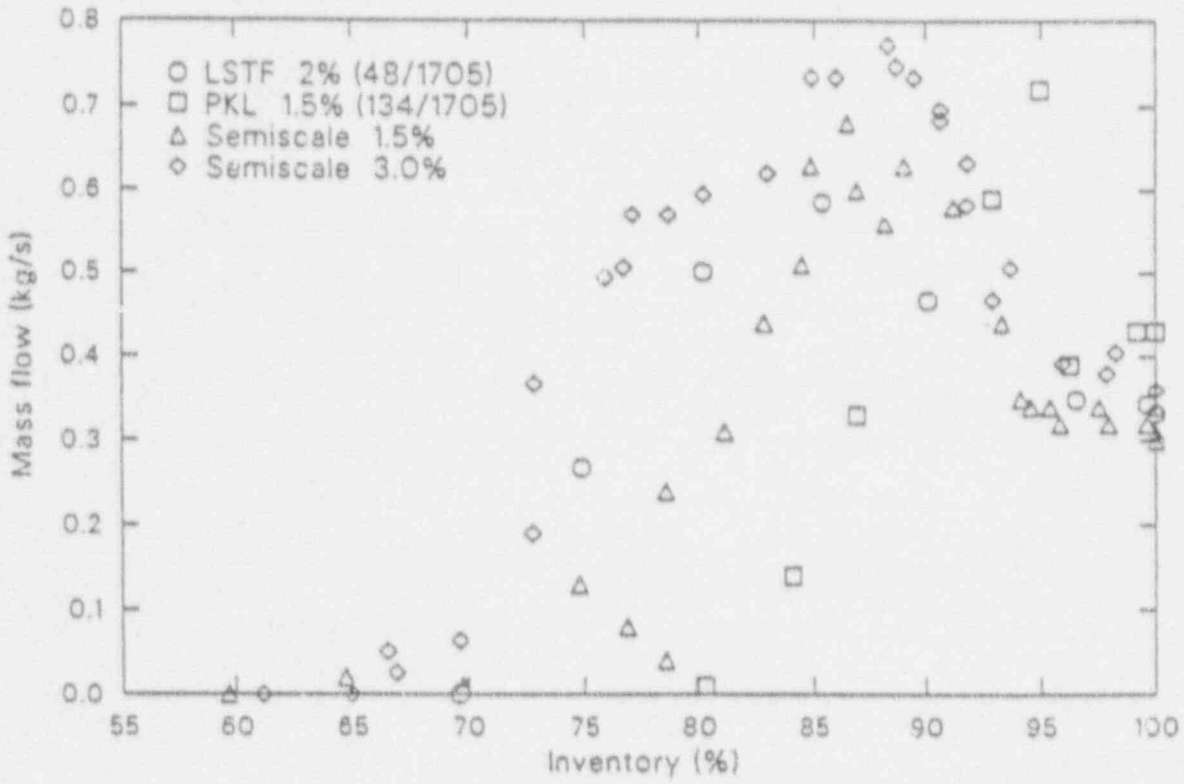

Figure 3-4. Comparison of LSTF, PKL, and Semiscale loop flows, 1.5% - 3.0% power.[20]

bundle; for OTSG,[37,38] the elevation difference between axial midplane of the core and the axial location of the steam generator thermal center (location of average temperature)

P = input power

ρ_l = reference density. Density of coolant at average coolant temperature

c = coolant specific heat at constant pressure at average coolant temperature

R = overall flow resistance parameter for the flow path defined by the sum of the frictional and form losses (turbulent flow)

r = overall flow resistance parameter for the flow path defined by the sum of the frictional and form losses (laminar flow)

ΔT_R = core temperature difference.

In the derivation of the above expressions, conventional one-dimensional mass, momentum, and energy formulations were used. The average cross-sectional temperature was assumed to be equal to the mixed mean temperature and the Boussinesq approximation (i.e., the density is considered constant in the governing equations except for the buoyancy force term) was used. The density in the buoyancy term is assumed to vary linearly with temperature according to

$$\rho = \rho_l \left[1.0 - \beta (T - T_l) \right] \tag{3-5}$$

where ρ_l and T_l are the reference density and temperature. All other fluid properties were considered as constant values, which is justified for small temperature variations.

For steady state, the time dependent terms in the governing equations disappear[34] and the momentum equation reduces to

$$\frac{1}{2} R \frac{W^2}{\rho_l} = - g \oint \rho \, dz \tag{3-6}$$

for turbulent flow, or

$$r W = - g \oint \rho \, dz \tag{3-7}$$

for laminar flow. Note that R (or r) is the total flow resistance parameter defined by the sum of the frictional and form losses

$$R = \oint \frac{f ds}{D A^2} = \sum_{i_{tubes}} f_i \frac{L_i}{D_i A_i^2} + \sum_{j_{form}} \frac{K_j}{A_j^2} \tag{3-8}$$

where the f_i are the friction coefficients in the tubes, L_i are the tube lengths, the A_i are the tube cross-sectional areas, the D_i are the hydraulic diameters, and the K_j factors determine the various form losses in the components of the loop.[34] Note that the friction coefficients and factors depend on the Reynolds number of the flow. The overall resistance parameter can be determined for multiple loops by evaluating resistance subfactors for the vessel and loops individually.[39]

The energy equations for the loop components were simplified using an equivalent "driving head" instead of the density integral, an overall heat balance for the core rather than the formal energy equation, and by requiring that no heat losses occur between the core and the heat exchanger ($\Delta T_R = T_h - T_c$).

Zvrin assumed that the temperature distributions of the primary fluid in the core and in the heat exchanger were linear.[34] Although more accurate temperature distributions could have been used, comparisons of results from models based on linear temperature distributions with results from models based on more exact approximations showed only small deviations,[34,40] thus justifying the linear approximation.

Previous research[34,41] and PWR plant data[18] were used to test the accuracy of the preceding expressions for the mass flow rate and the core temperature difference. Reference 39 indicated that these expressions agreed with data from a variety of loops and PWRs to within 30%. Reference 36 indicates differences between measured data from experiments and plants and calculated values (using the above expressions) are between 17% and 23%. When using these expressions, keep in mind the simplifying assumptions discussed in the previous paragraph and regard them as approximate expressions, not exact solutions.

In the case of a UTSG rejecting decay heat, the major primary-to-secondary heat transfer occurs near the bottom of the upflow sides of the U-tubes. The heat transfer rate decreases gradually along the length of the U-tubes. The result is an almost negligible amount of heat transfer along the downflow side of the U-tubes, compared with the amount occurring along the U-tube upflow side. The existence of nonuniform U-tube flow[19,20,26,32,33,42,43] suggests a corresponding nonuniform heat transfer behavior from one U-tube to another. Thus, Koizumi et al. concluded that it was better to define an overall heat transfer coefficient representing the average fluid-to-fluid thermal resistance based upon the heat transfer area below the secondary collapsed liquid level.[42] This overall heat transfer coefficient, K_e, is given by

$$Q = K_e F R \Delta T \qquad (3\text{-}9)$$

where Q is the total heat transfer rate, F is the total heat transfer area of the steam generator U-tubes (based on U-tube inner diameter), and R is the ratio of the heat transfer area below the collapsed secondary liquid level to the total heat transfer area; ΔT is a logarithmic mean temperature difference based upon the inlet and outlet steam generator plena fluid temperatures (T_{PI} and T_{PE}, respectively) and the secondary fluid temperature (T_S), which is assumed constant.[42] ΔT is expressed as

$$\Delta T = \frac{(T_{PI} - T_S) - (T_{PE} - T_S)}{\ln\left[\frac{T_{PI} - T_S}{T_{PE} - T_S}\right]} \qquad (3\text{-}10)$$

Figure 3-5 (see Reference 42) demonstrates the behavior of K_e as a function of the secondary collapsed liquid level for several different test conditions. For the five percent core power, single-phase natural circulation curve in Figure 3-5, Ke varies between 1.2 kW/(m^{2}K) and 2.0 kW/(m^{2}K) [211.5 Btu/(hft^{2}F) to 352.4 Btu/(hft^{2}F)].

The data uncertainty in Figure 3-5 stems mainly from temperature measurements. Note that the largest uncertainties are prevalent when the secondary collapsed liquid level is high and the effective heat transfer area is large. In this situation, the primary-to-secondary temperature differences are small, resulting in large data measurement uncertainties. Conversely, when the secondary collapsed liquid level is low and the effective heat transfer area is small, the primary-to-secondary temperature difference rises to compensate for the reduced heat transfer area. Consequently, the data measurement uncertainties are reduced.

The overall heat transfer coefficient, K_e, is dependent upon the local overall heat transfer coefficient, H. H consists of three terms: (a) heat transfer at the inner surface of the U-tube wall, (b) heat conduction in the U-tube wall, and (c) heat transfer at the outer surface of the U-tube wall, i.e.

$$\frac{2\pi}{H} = \frac{1}{h_1(D_1/2)} + \frac{1}{k_w}\ln\left(\frac{D_2}{D_1}\right) + \frac{1}{h_2(D_2/2)} \qquad (3\text{-}11)$$

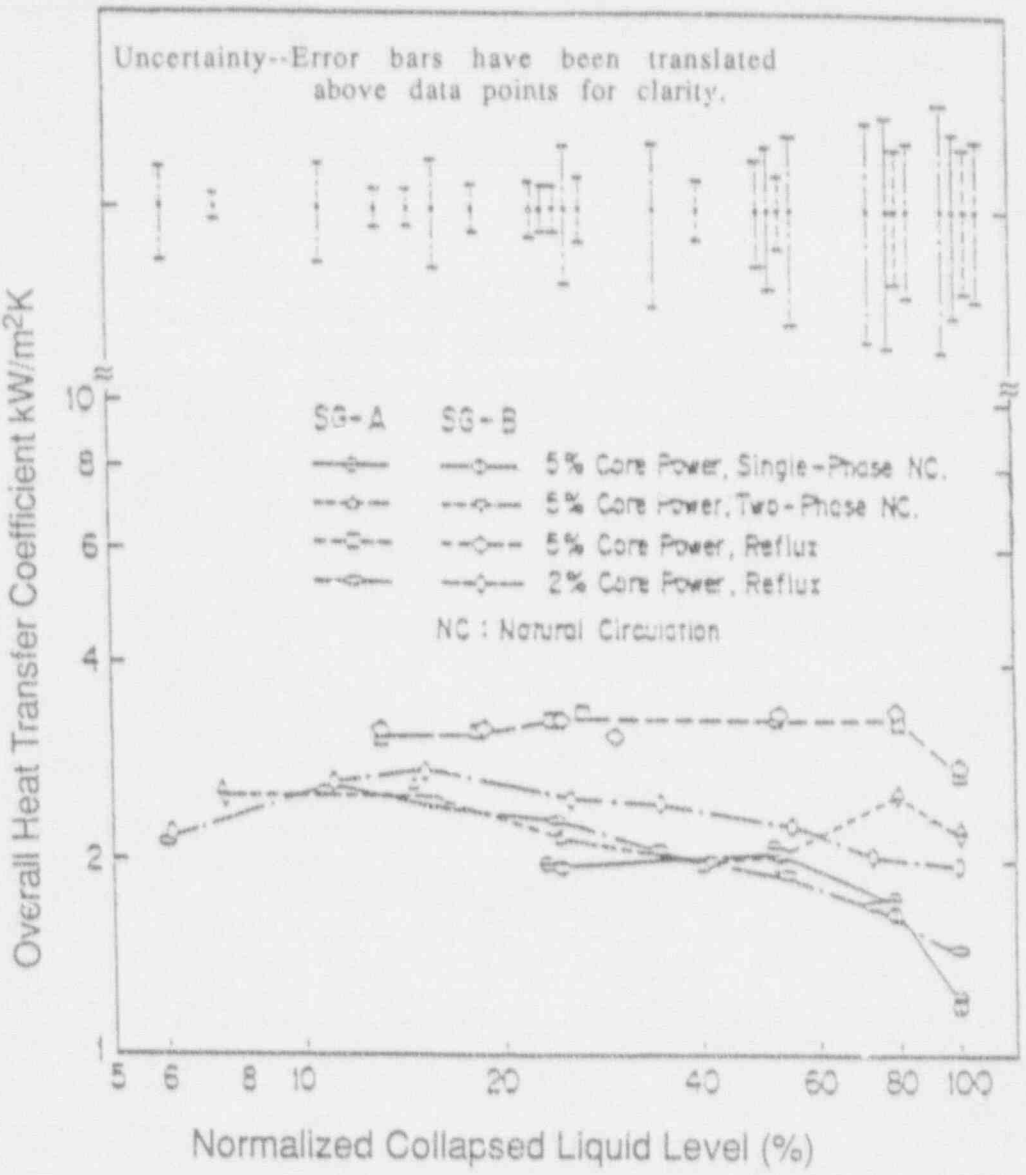

Figure 3-5. LSTF observed primary-to-secondary overall heat transfer coefficient, defined with collapsed liquid level.[42]

where h_1 is the heat transfer coefficient inside the steam generator U-tubes, h_2 is the heat transfer coefficient outside the steam generator U-tubes, D_1 is the inner U-tube diameter, D_2 the outer U-tube diameter, and k_w is the metal thermal conductivity of the U-tube wall.[42] Koizumi et al. claim that Ke is reliably applicable to a full-scale PWR, but warn that a correction should be incorporated by multiplying the Ke results presented in Figure 3-5 by the ratio of the local overall heat transfer coefficient of the full-scale PWR and the local overall heat transfer coefficient of the LSTF. This correction accounts for differences in U-tube wall thickness and metal thermal conductivity between the LSTF and the full-scale PWR.[42] Thus, Ke can be used to evaluate heat transfer rates during each mode of natural circulation. It can also be used in estimating the lower limit on the steam generator secondary side liquid level necessary for adequate core heat removal.

In the case of a OTSG, the primary-to-secondary heat transfer occurs primarily in the upper elevations of the steam generator. Single-phase natural circulation data from the University of Maryland College Park (UMCP) facility are shown in Figure 3-6.[44] This figure is a plot of the overall heat transfer coefficient (UA) versus the hot leg mass flow rate (W_{HL}) during steady-state, single-phase natural circulation conditions. These data were used to correlate the heat transfer coefficient in terms of dimensionless parameters. This correlation takes the following form

$$Nu = 0.028 \frac{Gz}{(Re\ Pr)^{0.08}} \qquad (3\text{-}12)$$

where Nu is the Nusselt number, Re is the Reynolds number, Pr is the Prandtl number, and Gz is the Greatz number $\left(Gz = \frac{RePrD}{L}\right)$.[44] Equation 3-12 defines the heat transfer coefficient per total number of heat exchanger tubes. The correlation of Equation 3-12 is valid for water at temperatures not exceeding 121°C (250°F) and pressures between 241 KPa and 586 KPa (35 psi and 85 psi). Thus, Equation 3-12 is not applicable to full-scale PWRs, but it could be useful in code assessment purposes or comparisons with other low-pressure, low-temperature test facility data.

3.4 Influence of Noncondensable Gases

The effect of noncondensable gases in a PWR loop during single-phase natural circulation is an important issue. The presence of noncondensables in the primary loop may impede or even stagnate the natural circulation flow, thereby significantly reducing or terminating the heat removal capability of the steam generators. Noncondensable gases can be introduced into the primary system through safety injection and by fuel degradation. For example, hydrogen from the pressurizer vapor space, air dissolved in the refueling water, and nitrogen from the accumulators (once they are depleted of water), are several sources of noncondensable gases. In addition, helium may enter the primary flow system if breaching of cladding occurs.[19,31,45]

The majority of research concerning issues related to noncondensable gases has been with regard to the two-phase and reflux/boiling condensation modes of natural circulation. These topics are addressed in later sections. The presence of noncondensables during single-phase natural circulation has not received as much attention as the other two modes, but research addressing this issue has been conducted.[41,45,46,47,48,49] However, these references deal only with the UTSG geometry. Although many similarities exist between single-phase natural circulation responses in UTSG and OTSG plants, caution should be exercised in extending the effects of noncondensable gases in UTSG plants to those of OTSG plants.

Figure 3-7 shows the thermal hydraulic response during a single-phase, noncondensable gas experiment conducted by Cha and Jin in a two-loop test facility modeled after a PWR with a UTSG geometry [Korean Atomic Energy Research Institute (KAERI)].[45] Nitrogen gas was injected into the hot leg of the one active loop in discrete amounts, each approximately 0.26% of the primary volume. The successive nitrogen injections resulted in increased vessel temperatures and decreased

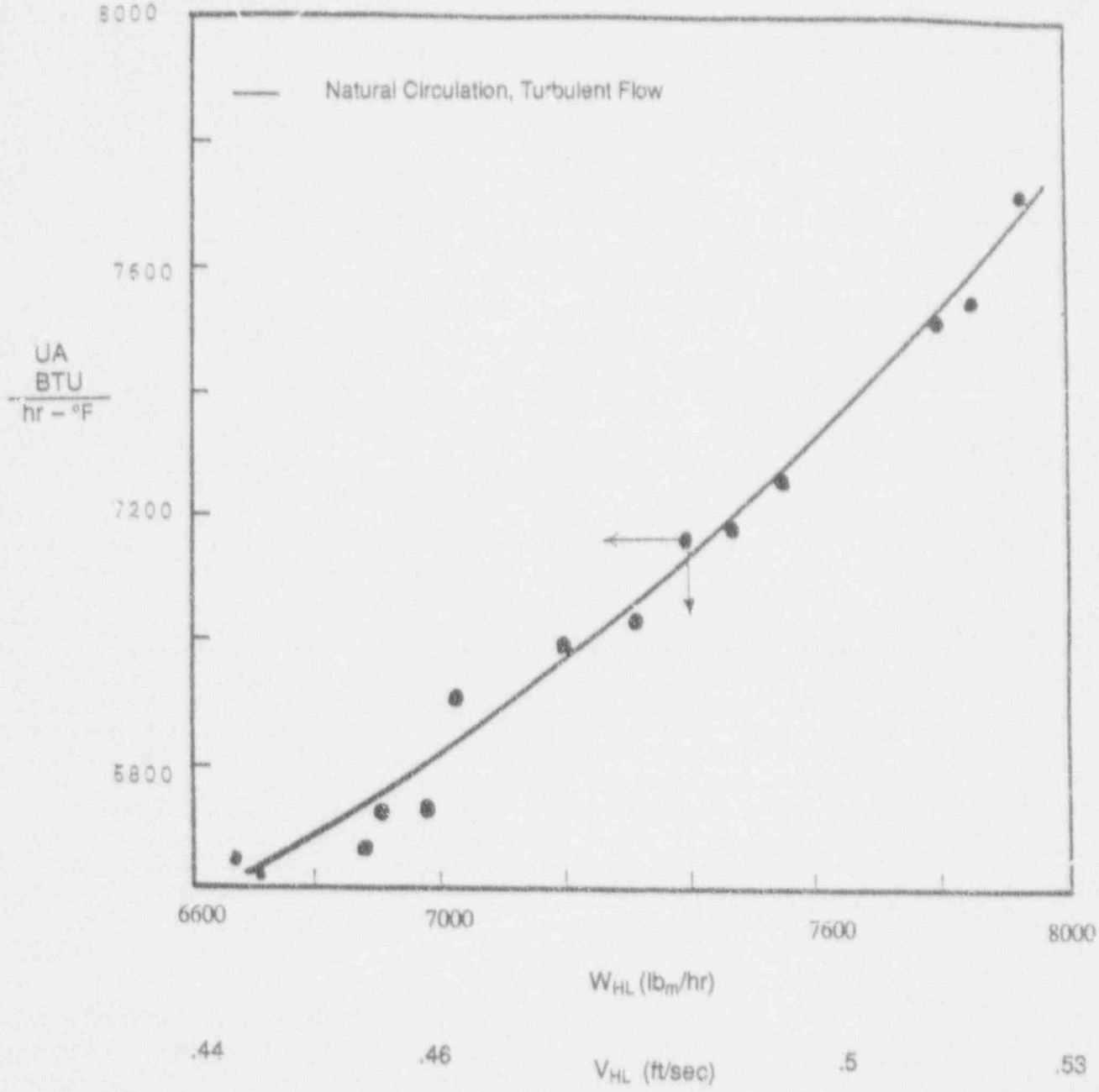

Figure 3-6. UMCP heat exchanger overall heat transfer coefficient versus hot leg mass flow rate (velocity) under steady state and single-phase conditions.[44]

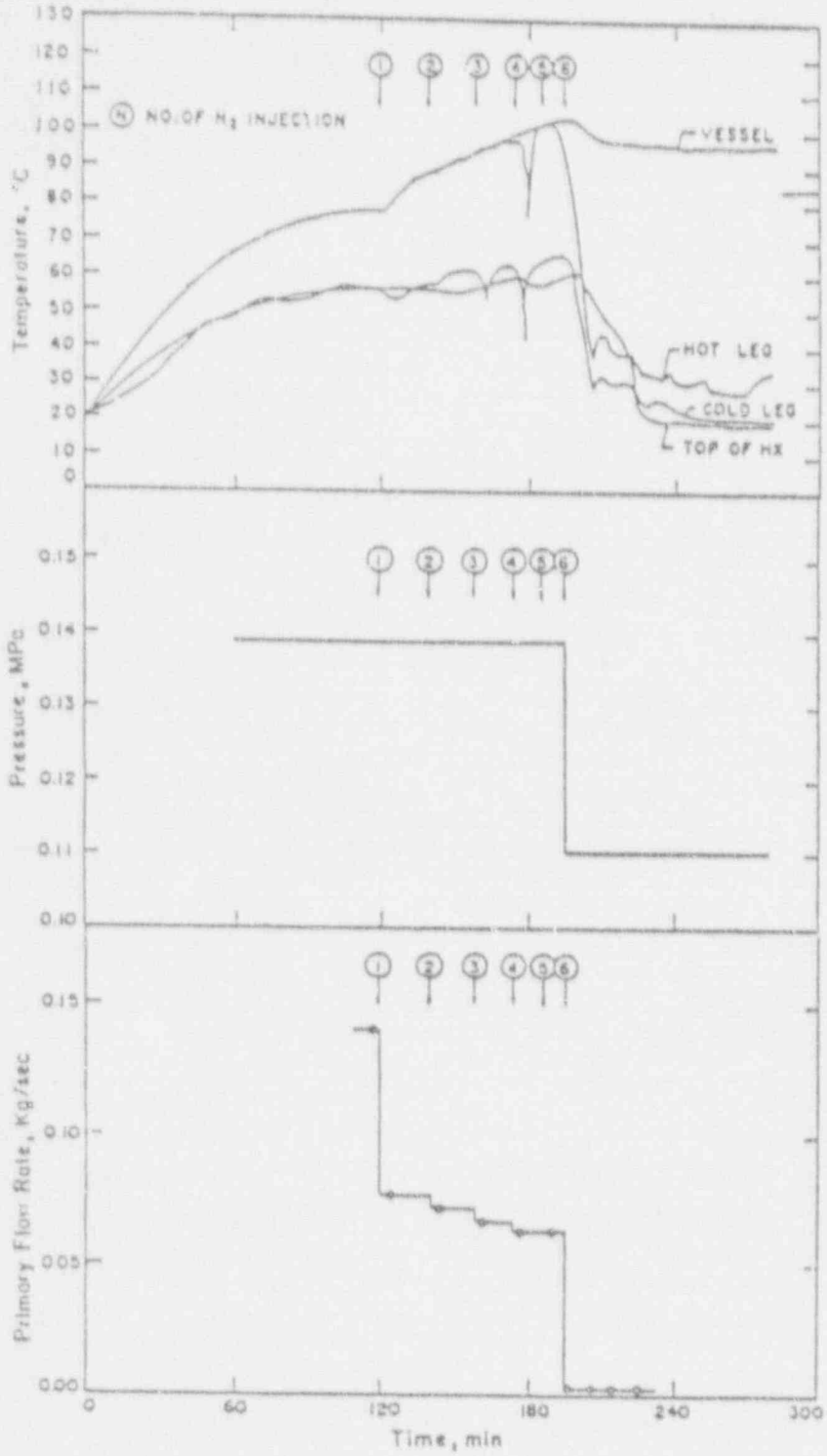

Figure 3-7. Effect of noncondensable gas on single-phase natural circulation with a single active loop in a KAERI test facility.[45]

loop flow rates. After the sixth injection, the flow stagnated (approximately 1.56% nitrogen gas in the primary system). Note that the pressure measurements in this facility were obtained from a single absolute pressure transducer in the vessel upper head. Thus, the pressure readings in Figures 3-7 and 3-8 simply represent the hydrostatic pressure at that location. A drop in pressure indicates an increase in the amount of voids (vapor or noncondensable gas) in the upper elevations of the loop.[45]

Flow stagnation also occurred in a single active test loop at EPRI/SRI following the injection of helium gas directly into the top of the steam generator U-tubes.[46] Injection of helium gas directly into the hot leg of the Full-Length-Emergency-Cooling-Heat-Transfer-Separate-Effects-and-Systems-Effects-Test (FLECHT-SEASET) facility during single-phase natural circulation stalled certain U-tubes, but the loop flow did not stagnate.[49] Successive non-condensable gas injections resulted in gas blockages only in certain U-tubes, and the noncondensables from additional injections tended to migrate to the already stalled U-tubes.[49] During hot leg nitrogen gas injections in the four-loop PKL-III facility, it was found that the rate of injection determined whether loop flow stall would occur.[47] Slow rates of injection resulted in a more heterogeneous gas distribution so that flow stall did not occur in all U-tubes. Faster rates of injection lead to a more homogeneous gas distributions in the steam generator inlet plenum and flow stall in all U-tubes was possible.[47]

Results obtained from the FLECHT-SEASET facility,[49] the EPRI/SRI four loop facility,[48] and the PKL-III facility[47] indicate that single-phase natural circulation remains stable for noncondensable gas injections into the vessel upper plenum and the cold leg. However, PKL-III tests also demonstrated that large amounts of noncondensable gas can eventually fill the vessel upper head and upper plenum. When this occurs noncondensable gas will be forced into all the loops at the same time, leading to possible flow and heat transfer interruption.[47]

During loss or reduction of single-phase natural circulation in the PKL-III tests, the primary system self-adjusted to compensate for the adverse effects of the noncondensable gas. The system responded to compensate for lost heat transfer with flow and heat transfer increases in undisturbed U-tubes, and pressure and temperature increases that compressed gas volumes sufficiently to reactivate some lost heat transfer surfaces.[47] If core heat-up occurs, steam will be produced and the natural circulation driving head will increase. This two-phase loop density gradient may be sufficient to restart flow in the blocked U-tubes.[47]

A second test conducted by Cha & Jin, (KAERI) used two active primary loops, with nitrogen gas injected into the hot leg of one of these loops.[45] The total accumulated nitrogen gas amounted to about 4.5% of the primary system volume, yet complete flow stagnation did not occur. The thermal hydraulic response during this test is shown in Figure 3-8. Note that after the seventh nitrogen injection, the temperature response in the hot leg, cold leg, and top of the steam generator decoupled from the vessel temperature. This suggests that a change in flow also occurred. The sharp divergence between the hot leg and vessel temperatures shortly after the seventh injection suggests the occurrence of at least a partial flow interruption. During this period, noncondensable gas bubbles may have blocked some of the U-tube upper bends. Just before the eighth nitrogen injection, it appears that normal heat transfer from the primary to secondary systems reoccurred, possibly due to some clearing of noncondensable gas blockages in the U-tube upper bends. Note that after the eighth injection this pattern is repeated.

A third test conducted by Cha & Jin consisted of the injection of nitrogen gas into the hot legs of both active loops.[45] They found that an amount of nitrogen gas approximately equivalent to 2% of the system volume interrupted the single-phase natural circulation flow in both loops.

The diverse results discussed above demonstrate that the issues regarding the effects of

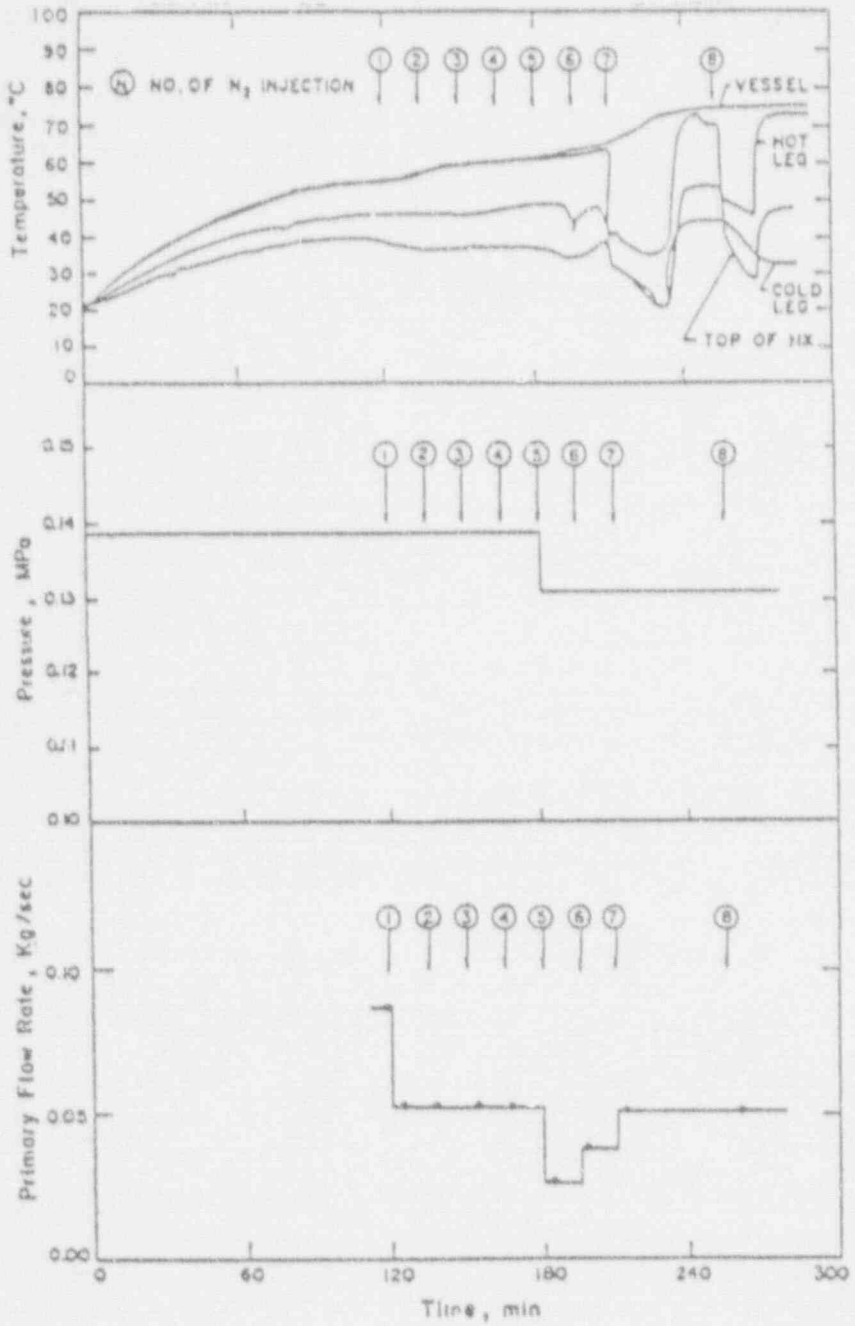

Figure 3-8. Effect of noncondensable gas on single-phase natural circulation with two active loops in a KAERI test facility.[45]

noncondensable gases on single-phase natural circulation remain to be fully quantified. Uncertainties exist regarding the effects of parameters such as:

- The location of the noncondensable gas source
- The amount of noncondensable gas in the system
- The rate of noncondensable gas injection
- The type of noncondensable gas (i.e., effects due to the solubility of the gas in water, the density of the gas compared to steam, etc.)
- The number of active primary loops
- The migration of the noncondensable gases in the primary system.

It is difficult to draw general conclusions from the results presented, but it would seem that upper plenum or cold leg injection would tend to accumulate noncondensable gas in the upper head first, leading to an accommodation of greater amounts than if injected in the hot leg or U-tube entrance. These injection locations also allow sufficient mixing and diffusion of the gases to preclude their accumulation in the U-tube upper bends; whereas hot leg[45] or direct U-tube[46] injection may not allow sufficient mixing and diffusion.

It appears that single-phase flow interruption due to the presence of noncondensable gases is more likely when there is only one active primary loop.[45,46] Observations also indicate that mixing and diffusion of the noncondensable gases can be effective in preventing the accumulation of noncondensable gases in the U-tube upper bends, and that the rate of gas injection may determine whether flow stall is possible. The upper limits on the amounts of noncondensables that can be accommodated by the system (without the loss of single-phase natural circulation) depends on the combined effects of the parameters mentioned in the last display list.

3.5 Effects Due to Secondary Side Conditions

The transfer of heat from the core to the secondary side of the steam generator during single-phase natural circulation depends on conditions in both the primary loop and the secondary side of the steam generator. In previous sections, the factors affecting the primary loop were emphasized. In this section, the effects that secondary side conditions can have upon the natural circulation flow and heat transfer are discussed. Some of the important secondary side parameters are the temperature, flow rate, and liquid level. These parameters directly affect the heat transfer through the steam generator tubes. However, other factors can also affect the local conditions on the secondary side of the steam generator tubes. The procedures used to regulate the feedwater and emergency feedwater flows (and temperatures) during a transient affect the overall heat transfer and/or local heat transfer. In addition, relief valve behavior can affect secondary levels, flow rates, and temperatures. For example, isolation of a steam generator secondary side will lower the flow rate on the secondary side of the tubes, thus decreasing the heat transfer. This can affect the natural circulation in the primary loop.

Experiments have demonstrated that the stability of single-phase natural circulation flow is strongly dependent upon secondary side liquid level. Low secondary liquid levels have resulted in an oscillatory type of flow behavior in several experimental investigations.[19,22,42] Because the primary means of heat removal during single phase natural circulation is convection, flow oscillations can strongly affect the heat removal effectiveness. Thus, the effects of low secondary liquid levels on single-phase natural circulation are very important. Investigations concerning single-phase natural circulation have been performed at many facilities including EPRI/SRI,[22] Large-Scale Test Facility (LSTF,[42] PKL-III,[50] Boucle d'Etudes ThermoHydrauliques Système (BETHSY),[51] and LOFT.[35] The results of several of these single-phase experiments are discussed as follows.

Work performed by EPRI/SRI in an experimental two-loop facility (modeled after a PWR with an OTSG geometry) discovered oscillatory single-phase flow behavior at low secondary liquid levels.[22] Figure 3-9 presents the upper vessel temperature trace for equilibrium states corresponding to different core power and secondary liquid levels (measured from the hot leg centerline elevation). Note the oscillations at the lowest two constant secondary liquid levels. It was found that the on-off behavior of the EFW pumps (in maintaining the secondary levels) and the low secondary liquid levels were the contributing factors leading to this behavior. Figure 3-10 shows the corresponding temperature traces for a wetted steam generator tube, and for the cold legs in each loop, during the time of reduced secondary liquid levels. The low temperatures of the upper trace correspond to the injection of the cold EFW spray. Note that all three temperature traces are in phase with each other. Thus, in maintaining secondary liquid level, the cold EFW spray resulted in primary flow oscillations in both loops. It can be seen in Figure 3-10 that the amplitude of oscillations increases as the secondary liquid level decreases; whereas the frequency of the oscillations decreases as the secondary liquid level decreases.

Single-phase U-tube oscillatory flow behavior at low secondary levels was detected in experiments conducted in the LSTF.[42] Figure 3-11 presents the temperature traces of three U-tubes representing the long, medium, and short length U-tubes, respectively. Note that immediately after the termination of forced circulation the temperature in the longest U-tube dropped significantly. In fact, the temperature in this U-tube became almost equal to the secondary temperature, suggesting a flow stall/reverse phenomena (this phenomena will be discussed in the next section). However, at a low secondary level (approximately 24% of the original 100% inventory), the flow in this longest U-tube experienced large fluctuations. Note also the increase in the temperature of the short and middle length U-tubes at this particular secondary inventory value. These effects suggest a degradation in the primary-to-secondary heat transfer at this low secondary liquid level.

Recent experiments conducted at the PKL-III test facility have also investigated the effects of low secondary liquid levels on the effectiveness of primary-to-secondary heat transfer.[50] The objective of the PKL-III Loss of Feedwater Test was to demonstrate that a single UTSG can remove the residual heat during a hot standby condition even at low secondary levels. It was designed to determine the minimum secondary level for removal of a decay heat of approximately 1.7% of full power. The test was initiated from a state of normal single-phase natural circulation in each of the four loops. Three of the primary loops were then isolated on both the feedwater and main steam sides. After a new steady state period was reached, the feedwater to the remaining steam generator was terminated, resulting in a boiloff of the secondary liquid.[50]

Natural circulation did not cease in the three isolated loops. The 53K primary-to-secondary temperature difference in the single active loop produced a net gravitational force that was sufficient to drive single-phase natural circulation flow in all four loops. However, the flow rates in the three isolated loops were about one-third that of the active loop. Time response data for secondary liquid level, primary and secondary side steam generator pressure, pressurizer liquid level, and primary mass flow rate are given in Figures 3-12 and 3-13. Figure 3-13 demonstrates the reduction of the secondary liquid level in the nonisolated steam generator and the corresponding response of the pressurizer liquid level and primary mass flow.[50] Note that for secondary liquid levels above 3 meters (9.84 ft), there are few changes in the flow behavior. However, once the secondary liquid level dropped below 3 meters (9.84 ft), the temperature and pressure of the primary mass flow increased and the mass flow rate in the nonisolated loop decreased. Because of the large energy storage capacity of the isolated steam generators, the primary pressure and temperature rise was gradual. These effects are shown in Figures 3-12 and 3-13. Note that feedwater flow was restarted once the secondary level reached 0.6 meters (1.97 ft), thus checking the increases in temperature and pressure and the decrease in the mass flow rate in the nonisolated loop.[50] This experiment demonstrated that a 1.7% decay heat level can

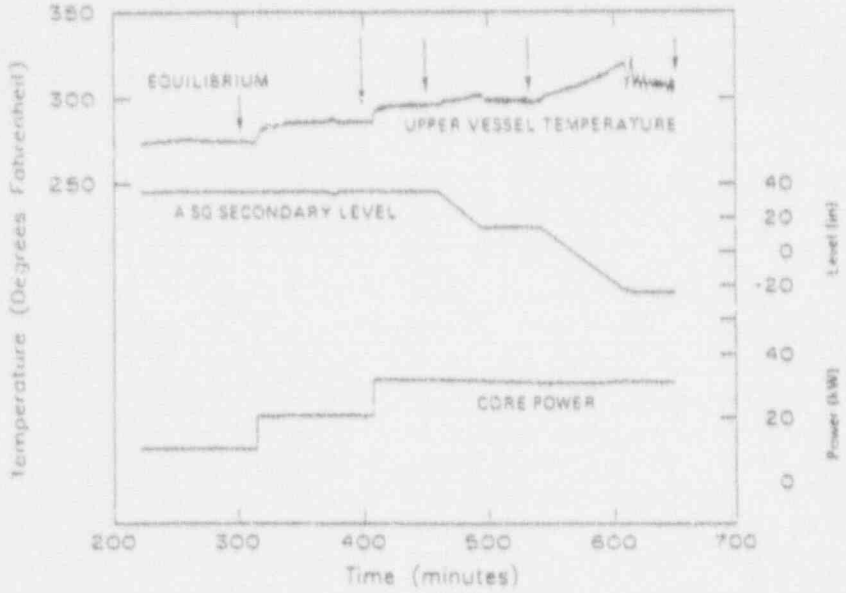

Figure 3-9. Vessel temperature, secondary level, and core power during EPRI/SRI single-phase natural circulation test.[22]

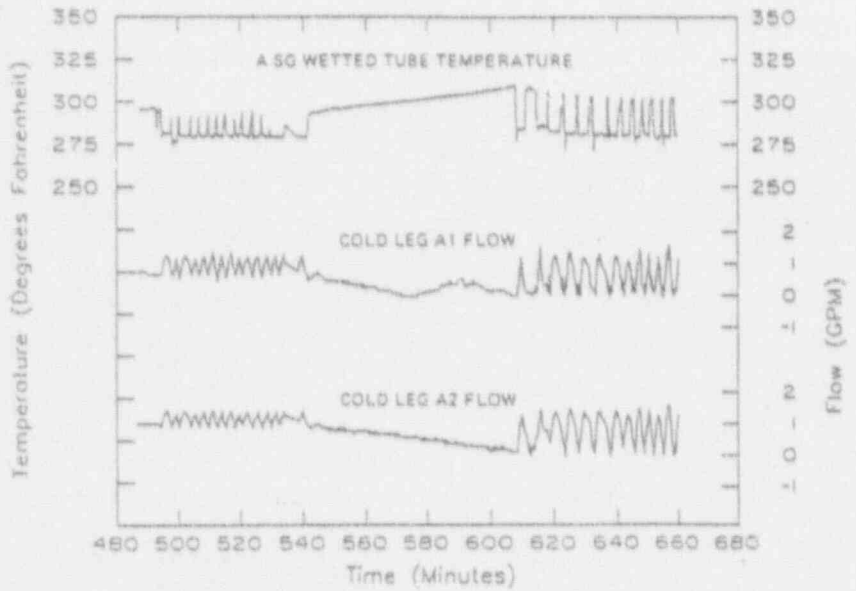

Figure 3-10. Effect of EFW injection on loop flow during single-phase natural circulation with reduced secondary liquid levels in an EPRI/SRI test facility.[22]

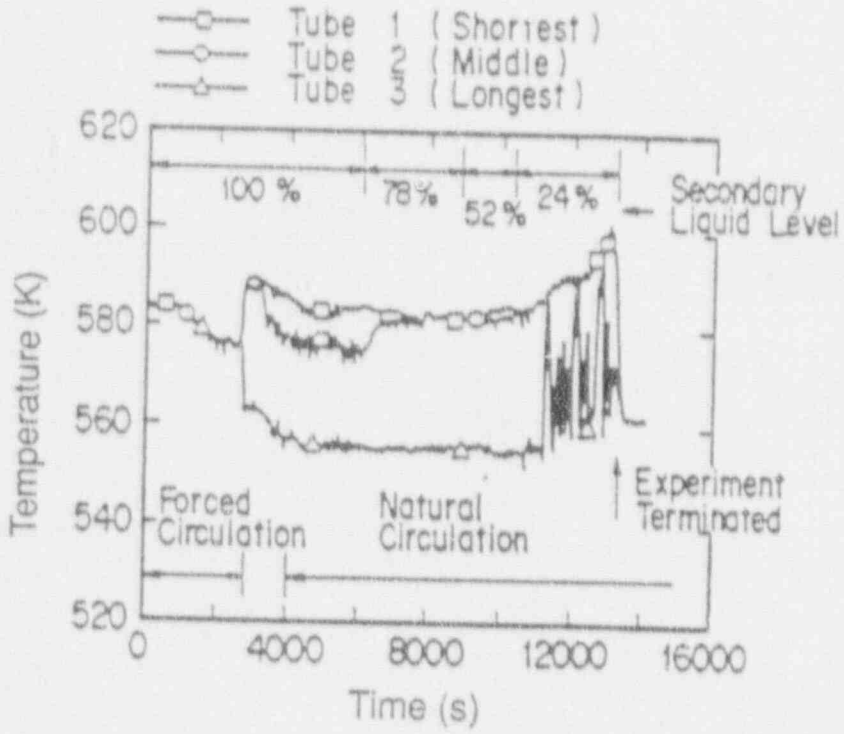

Figure 3-11. Fluid temperatures in steam generator U-tubes during a LSTF single-phase natural circulation test.[42]

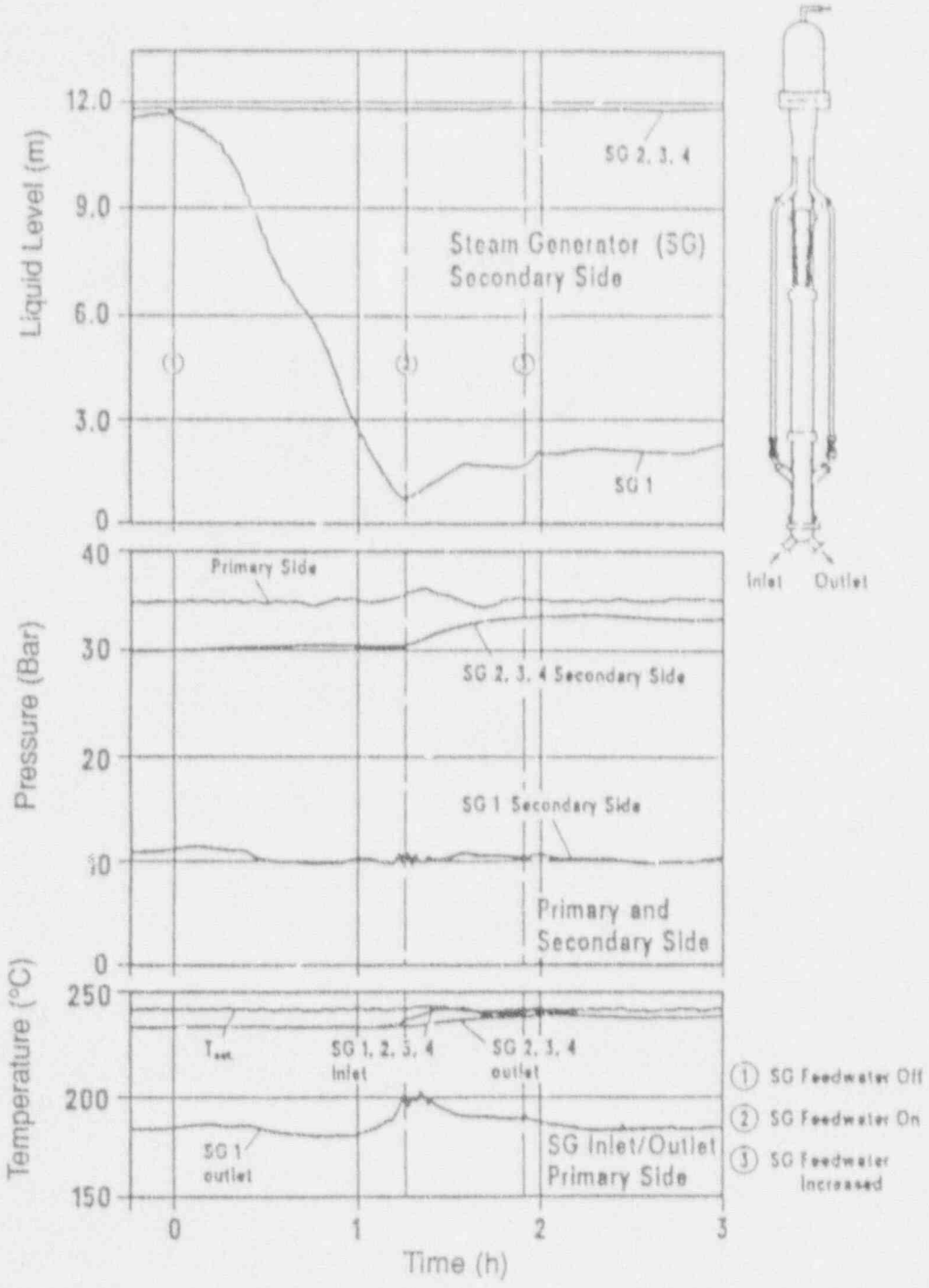

Figure 3-12. Time response data for secondary liquid level, primary and secondary side steam generator pressure, and steam generator inlet/outlet primary temperatures in PKL-III.[50]

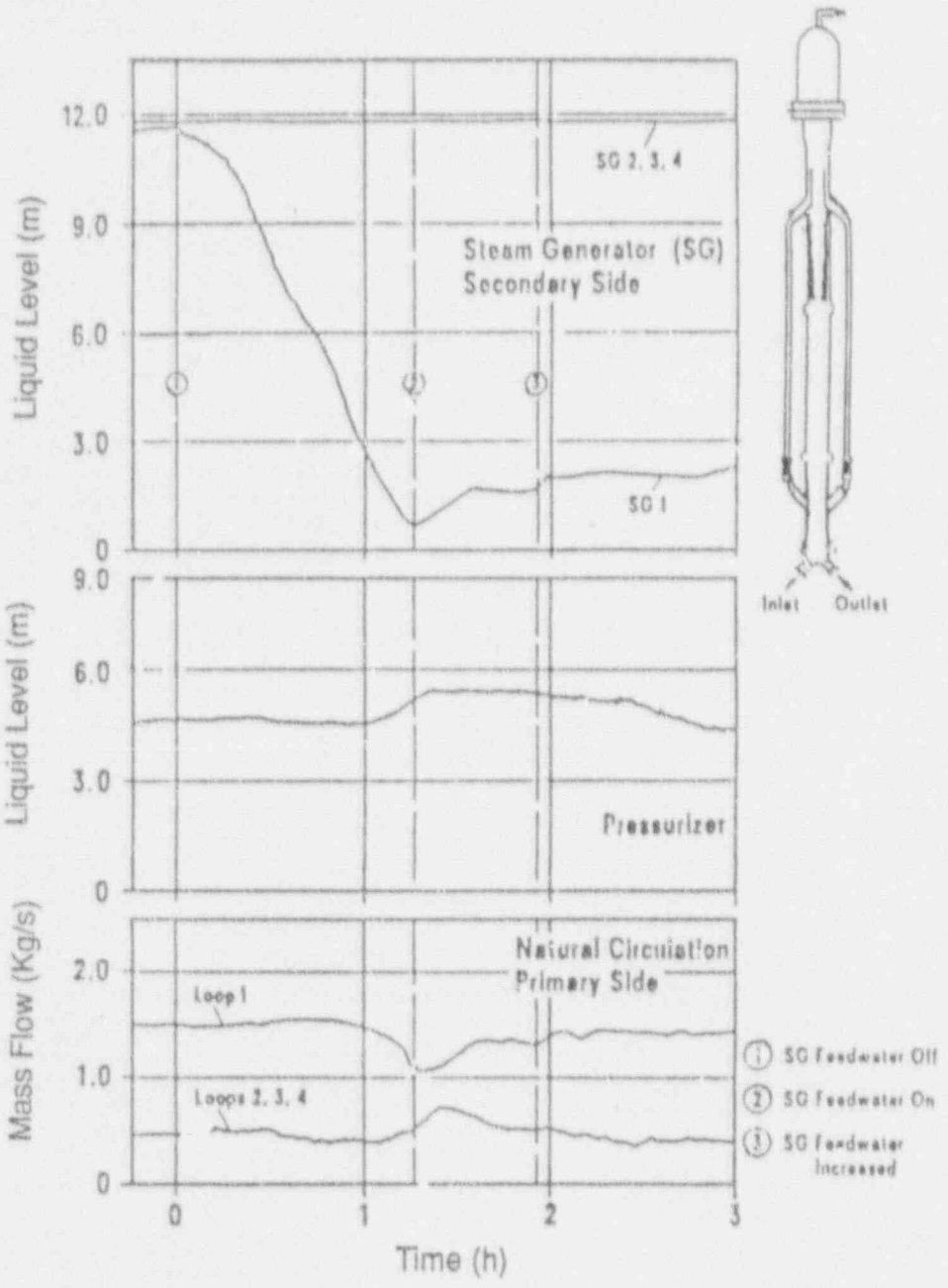

Figure 3-13. Time response data for pressurizer and secondary liquid levels and primary mass flow rate in PKL-III, a Loss of Feedwater Test .[50]

be removed by a single steam generator under steady state conditions as long as a minimum secondary liquid level of 3 meters (9.84 ft) and a primary-to-secondary temperature difference of 53K were maintained. It was noted by Umminger et al. that the minimum secondary level required to remove a given amount of heat is only meaningful if a minimum primary-to-secondary temperature difference is also specified.[50] Umminger et al. also observed that natural circulation flow was not terminated in the isolated loops.[50] The observed degradation in the primary-to-secondary heat transfer during single-phase natural circulation at low secondary liquid levels is also supported by recent experiments conducted in the BETHSY facility.[51]

Single-phase natural circulation experiments conducted in the LOFT facility demonstrated the effectiveness of secondary steam and feed operations in maintaining the steam generator in a heat sink mode.[7] Single-phase natural circulation can be maintained (or regained) in many situations by reducing the secondary temperature and pressure. This method will be addressed in greater detail in the two-phase natural circulation section.

Thermal stratification on the secondary side can also affect the efficiency of single-phase natural circulation cooling. In the case of a UTSG, the majority of the heat transfer occurs in the lower elevations of the steam generator. Consequently, secondary liquid is heated from below and buoyancy effects cause the secondary side to be well mixed. As a result, virtually all of the secondary liquid will be available as a heat sink. In the case of a OTSG, warming of the secondary liquid occurs at the top of the steam generator, which can lead to thermal stratification in the secondary side. Thermal stratification can effectively reduce the liquid available for use as a heat sink.

3.6 Nonuniform Flow

Flow in the single-phase mode of natural circulation can be classified as either uniform or nonuniform, and as steady or unsteady. The term unsteady implies changes over time, and nonuniform implies changes due to location. Thus, one term relates to the dimension of time and the other to the dimension of space. The most common types of single-phase nonuniform behavior are nonuniform multi-loop flow and (in the case of a UTSG geometry) nonuniform U-tube flow. Single-phase natural circulation unsteadiness normally occurs only during transitional flow periods. Otherwise, the flow in single-phase natural circulation can generally be considered as quasi-steady. For example, the transition from forced circulation to single-phase natural circulation is often accompanied by decoupled loop behavior. In this situation, the heat removal is often shifted from loop to loop because of loop stalling, unbalanced loop conditions, etc.[33] This results in coolant flow that is both unsteady and nonuniform. The complex switching of natural circulation modes between loops is another example of unsteady, nonuniform flow on a loop-to-loop basis.[33] Because the other major type of nonuniform flow (nonuniform U-tube flow) is more specifically related to single-phase natural circulation, it will be the main focus of this section's discussion. An understanding of single-phase, nonuniform U-tube flow behavior is a preliminary step in the investigation of the more complex U-tube phenomena associated with the two-phase mode of natural circulation, as discussed in Section 4.6.

Nonuniform U-tube flow during single-phase natural circulation is primarily due to flow stall and flow reversal in the longest length U-tubes. During single-phase natural circulation, the majority of the heat transfer occurs near the bottom of the upflow sides of the U-tubes. As a result, a column of dense fluid forms in the upflow side of the U-tubes. This dense fluid must be forced over the U-tube bends by the net driving force between the thermal centers of the primary loop. This driving force may not be sufficient in the longer U-tubes because the length of the dense upflow-side liquid column will be greater than in the shorter tubes.[20] A second contributing factor in the flow stall/reversal phenomena is the frictional losses that result as the primary fluid flows through the U-tubes, which are even more significant when occurring in the longer U-tubes.[26] Therefore, it is possible that in some instances, the resultant sum of these opposing forces may be sufficient to overcome the net driving force of the flow. For example, in the

LSTF, 2% power single-phase natural circulation test, the pressure in the outlet plenum of the steam generator was greater than that of the inlet plenum. This resulted in a pressure gradient force between the U-tube inlet and outlet plena that opposed the normal flow direction, causing flow stall and reversal in the longest U-tubes.[20,26] Flow stall occurs only when an exact force balance exists. Therefore, U-tube flow stall is a metastable state in which a small disturbance in the force balance results in the reestablishment of forward flow or the initiation of reverse flow.[20]

Experiments in the LSTF,[20] the Loop Blowdown Investigation (LOBI) facility,[52,53] and the Semiscale facility[24] have observed flow stall and flow reversal in the longest instrumented U-tubes. Figure 3-14 is a schematic showing different types of U-tube flow behavior versus the primary mass inventory for different length U-tubes in each of the two loops of the LSTF.[26] Note that flow reversal occurs only in the longest U-tubes during single-phase natural circulation.

In some instances, once reversed flow was established in a U-tube, it persisted until the peak mass flow rate occurred during the two-phase mode of natural circulation.[20] This observation is consistent with an analytical and experimental investigation by Sanders, in which it was shown that parallel flow in the tubes of a UTSG can be unstable for certain power levels.[43] This conclusion was derived from the results of a mathematical model based on the one-dimensional Oberbeck-Boussinesq equations.[43] Sanders made the following assumptions in deriving the U-tube flow equations:

- Density differences were considered only in the gravitational body force term.
- Density changes were due to changes in temperature only. This temperature dependence is given by

$$\rho(T) = \rho_0(1 - \beta(T - T_s)) \qquad (3\text{-}13)$$

where β is the coefficient of thermal expansion, T_s is the secondary side temperature, and ρ_0 is the density at T_s.

- Heat conduction in the liquid was neglected.
- Temperature changes along the flow path were not considered for friction or heat transfer coefficients.
- Heat generated by friction was neglected.

An important consequence of the preceding assumptions was that the tube velocity, v, remained constant over the length of a U-tube.[43] Stability was investigated by first imposing a small-scale disturbance upon the basic solution, and then linearizing the governing differential equations with respect to the disturbed solution. These equations were then integrated and solved for the pressure and temperature disturbances in terms of the constant tube velocity, v, and the small scale velocity disturbance. In order to investigate the stability of parallel flow, two U-tubes were analyzed. Instabilities were found by assuming different velocity disturbances in each of the U-tubes. Next, the condition of equal pressures at the tube exits was enforced. This yielded an expression for the system eigenvalue... The sign of this eigenvalue determined whether the flow was stable (negative eigenvalue) or unstable (positive eigenvalue). Criticality (neutral stability) was characterized by a zero eigenvalue. The expression derived by Sanders characterizing criticality (neutral stability) was given as

$$\frac{\rho_0 L\left(f + \frac{v}{2}\frac{df}{dv}\right)}{D\left(1 - \frac{v}{\lambda}\frac{d\lambda}{dv}\right)} = \frac{1 - z\left(1 + 2\frac{\lambda L}{2v}\right)}{1 + \frac{2h}{L}\frac{\lambda L}{2v}(1 + z) - z}$$

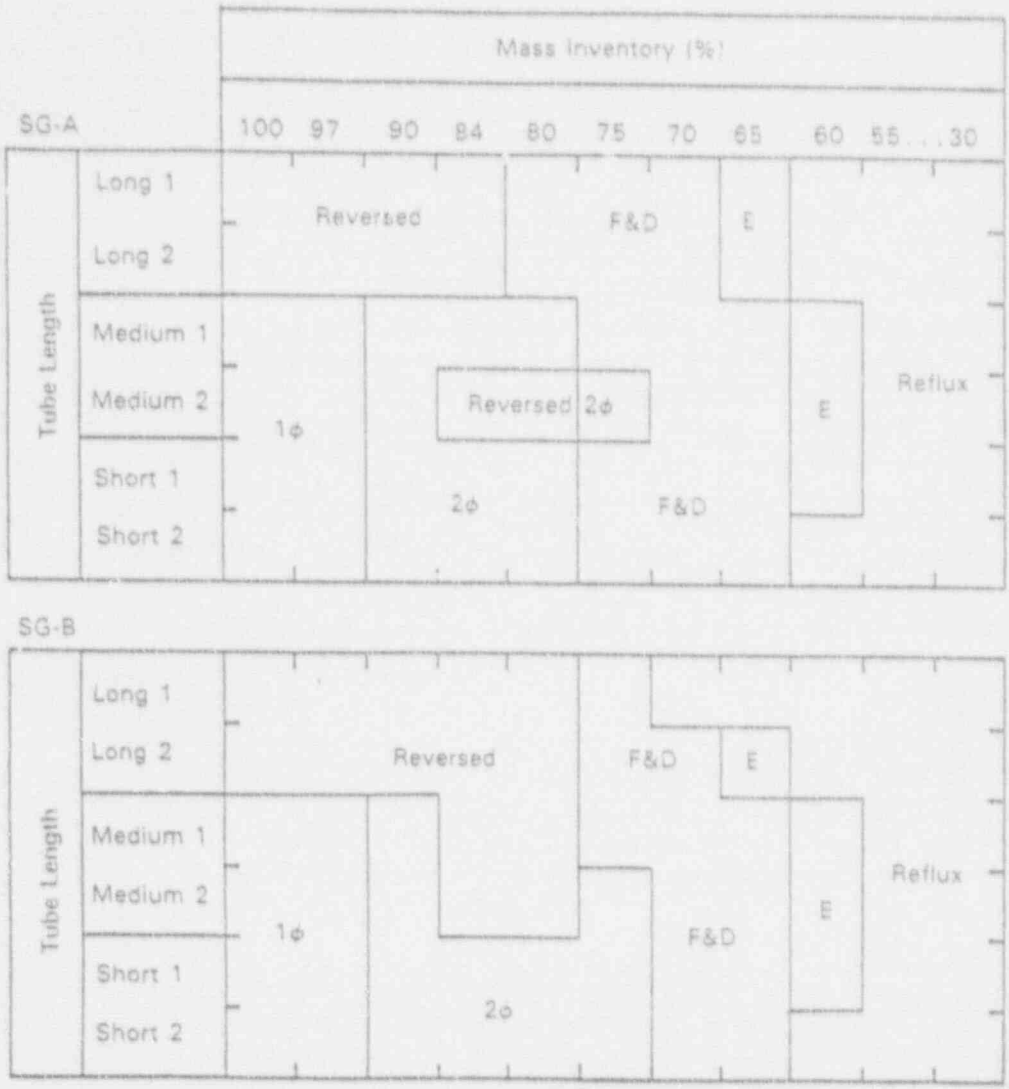

Figure 3-14. LSTF U-tube flow modes versus primary system mass inventory (1φ= single-phase, 2φ= two-phase, F&D = cyclic fill and dump, E = tube emptying).[26]

where

$$z = \exp\left(-\frac{\lambda L}{2v}\right) \qquad (3\text{-}14)$$

D = U-tube inner diameter

f = friction coefficient in U-tube

F = friction coefficient for total primary circuit

h = distance between center of core heat input and upper surface of steam generator tube plate

L = average length of U-tube

λ = ratio of U-tube wall heat transfer to heat capacity of water

ρ_0 = Density at primary side pressure and secondary side temperature.

A second stability analysis by Sanders, similar to the one just described, demonstrated that stability can be obtained with reversed flow in some of the U-tubes.[43]

Figure 3-15 shows the conditions for criticality and the zones of stability for parallel flow in U-tubes.[43] The results shown in Figure 3-15 were computed using Equation 3-14.[43] Note that stability of parallel flow depends primarily upon the height of the steam generators (h) with respect to the center of core heat input, and the ratio of the friction in the U-tubes to the friction in the whole circuit (f/F). High steam generators and little circuit friction lead to stable parallel flow in the U-tubes. For a given plant with specified dimensions and friction coefficients, stability depends upon the heat input, which is directly related to the flow velocity, v.[43]

U-tube flow reversal was observed during experiments in the LSTF[20,26] and the LOBI facility.[52,53] During reversed U-tube flow, differential pressure measurements at both facilities indicated that the pressure in the steam generator outlet plenum was greater than the pressure in the steam generator inlet plenum.[20,26,43] This observation is consistent with Sanders' theory, which predicts that when parallel flow in the U-tubes becomes unstable, the pressure in the steam generator outlet plena is greater than the pressure in the steam generator inlet plena. Physically, this phenomenon is due to the density differences in the liquid in the upflow and downflow sides of the U-tube. This pressure increase in the forward flow direction is the most important parameter for determining if U-tube reversed flow is possible.[43]

Reversed flow was observed in the LOBI facility,[43] but Sanders' theory did not predict this behavior. However, this discrepancy could be due to the limitations of the mathematical model, some of which are listed as follows:

- The use of simple models for U-tube friction and heat transfer
- The theory did not account for different friction in U-tubes of different length
- The influence of the position of different U-tubes in the inlet plena was not considered
- Flow mixing in the steam generator plena was not studied.

Sanders concluded that although instability was not predicted by his theory, it was still the mechanism causing the observed reversed flow in some steam generator U-tubes.[43]

The detection of reversed U-tube flow can normally be accomplished from the observation of the steam generator inlet temperature. The steam generator inlet temperature will be reduced if flow reversal occurs in a U-tube, because of the flow of cooled primary liquid back into the steam generator inlet plenum via

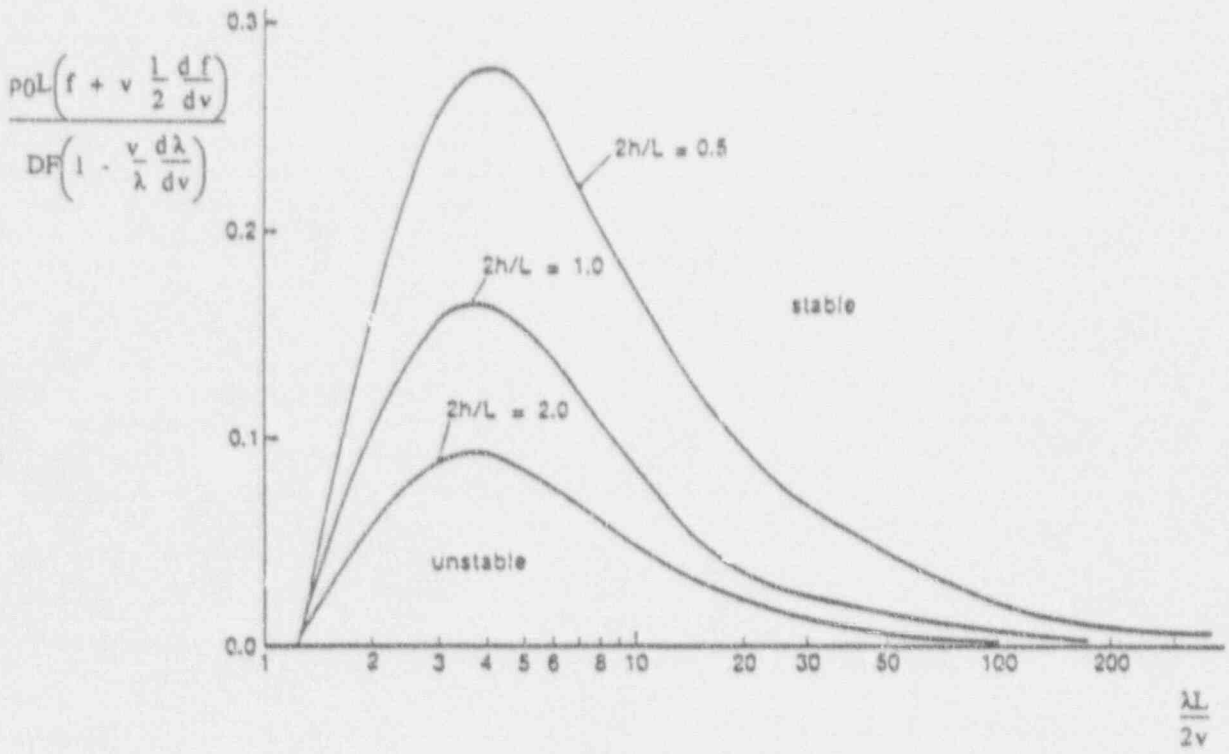

Figure 3-15. Conditions for criticality and zones of stability for parallel flow in U-tubes.[43]

the reversed-flow U-tube. Thus, if flow reversal is occurring, the steam generator inlet plenum temperature will be lower than the hot leg temperature.[20,33] Figure 3-16 shows a temperature drop of approximately 4 K in the steam generator inlet plenum after 13,000 s due to the reversed flow in the longest U-tubes during a LSTF experiment.[26] Figure 3-17 is a corresponding schematic diagram that shows a representative U-tube temperature distribution during this situation. Note that the longest length U-tube temperature is nearly equal to the secondary temperature at all U-tube elevations.[20]

Single-phase natural circulation experiments have shown that the U-tubes with normal flow direction provided a sufficient heat transfer area for removing core power from the primary, even with the nonuniform U-tube behavior.[26] Although the loop flow rates were sufficient to keep the core well cooled, they were smaller than if forward flow existed in all the steam generator U-tubes.[20] This observation may explain why thermal-hydraulic system codes sometimes overpredict single-phase mass flow rates in UTSG plants when single U-tube steam generator models are used.[20,26] This topic will be discussed further in Section 6.2.

In summary, it should be emphasized that the single-phase natural circulation will not cease or undergo interruptions in the presence of tube-to-tube flow reversals or instabilities within the loop.[54] Although reversed single-phase flow in steam generator U-tubes may not be a significant reactor safety concern, modelling this phenomena could be a useful test case for reactor safety codes.

3.7 Summary

The effectiveness of single-phase natural circulation cooling has been discussed with regard to various PWR plant operating conditions. The general characteristics associated with single-phase natural circulation have been described; and analytical expressions, useful in predicting single-phase behavior, have been presented. The influences on single-phase natural circulation behavior of such parameters as noncondensable gases, secondary side conditions, and nonuniform flow have been studied. The general characteristics of single-phase natural circulation were described in Section 3.2. It was noted that this mode of natural circulation persists during a transient until the level of voids in the vessel upper head drops to the hot leg nozzle elevation. The dominant heat transfer mechanism during this mode is convection, making the loop flow rate the most important parameter governing heat removal. Single-phase natural circulation was effective enough to provide adequate cooling for power levels up to 18% of full power in the LOFT facility.[35]

Approximate analytical expressions that assist in predicting general single-phase natural circulation response were given in Section 3.3, including expressions for the loop mass flow rate, core temperature differential, and overall primary-to-secondary heat transfer coefficients.

Section 3.4 demonstrated that the presence of noncondensable gases may impede or even stagnate single-phase natural circulation, especially if there is only one active primary loop. Important parameters in determining the effectiveness of single-phase natural circulation in the presence of noncondensable gases include:

- The injection location of the noncondensable gas source
- The total amount of noncondensable gas in the system
- The rate of noncondensable gas injection
- The type of noncondensable gas
- The number of active primary loops
- The migration of the noncondensable gases in the primary system.

The effect of secondary side conditions on single-phase natural circulation behavior was studied in Section 3.5. It was demonstrated that the stability of single-phase natural circulation

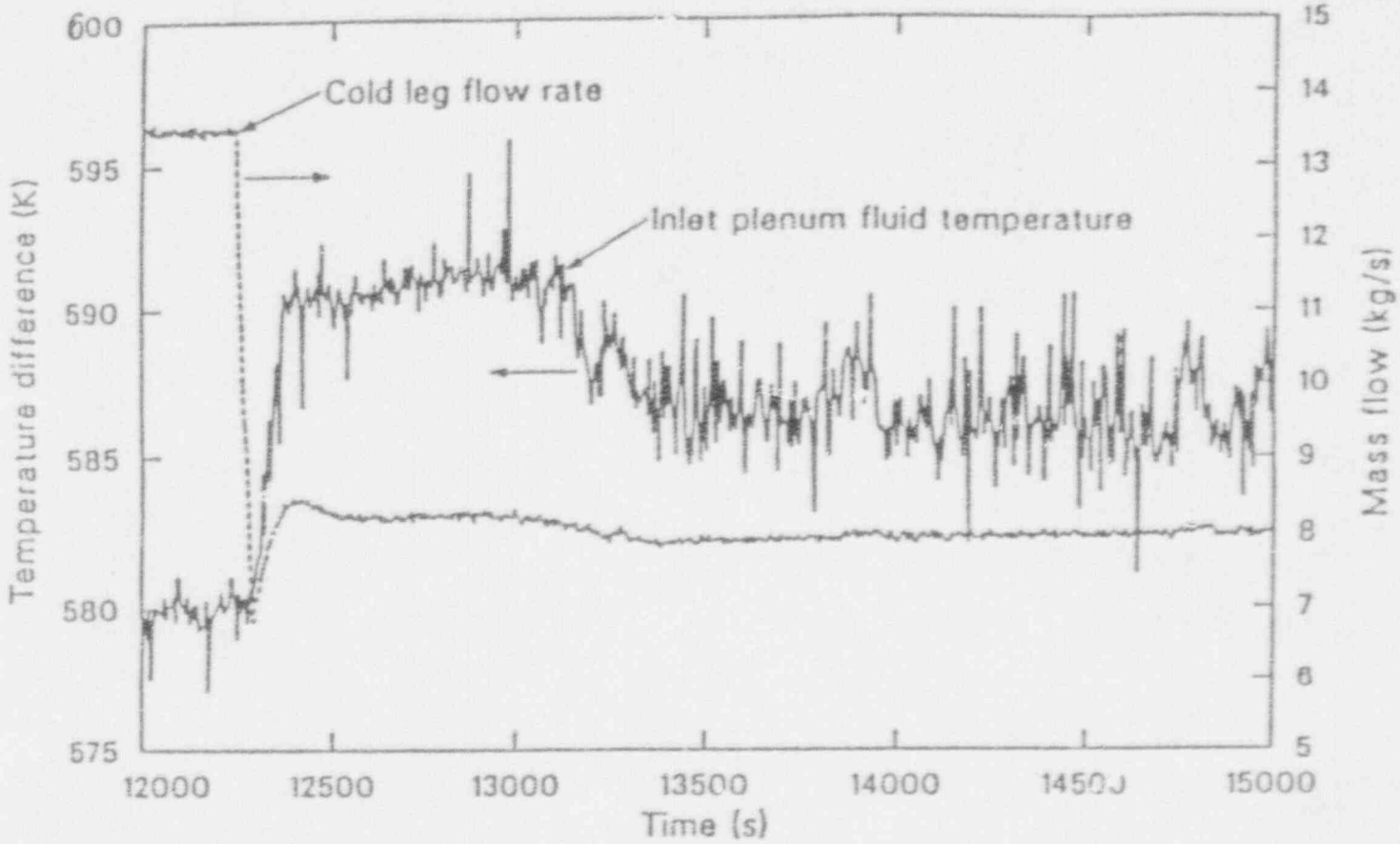

Figure 3-16. Influence of reversed U-tube flow on steam generator inlet plenum temperature in the LSTF.[40]

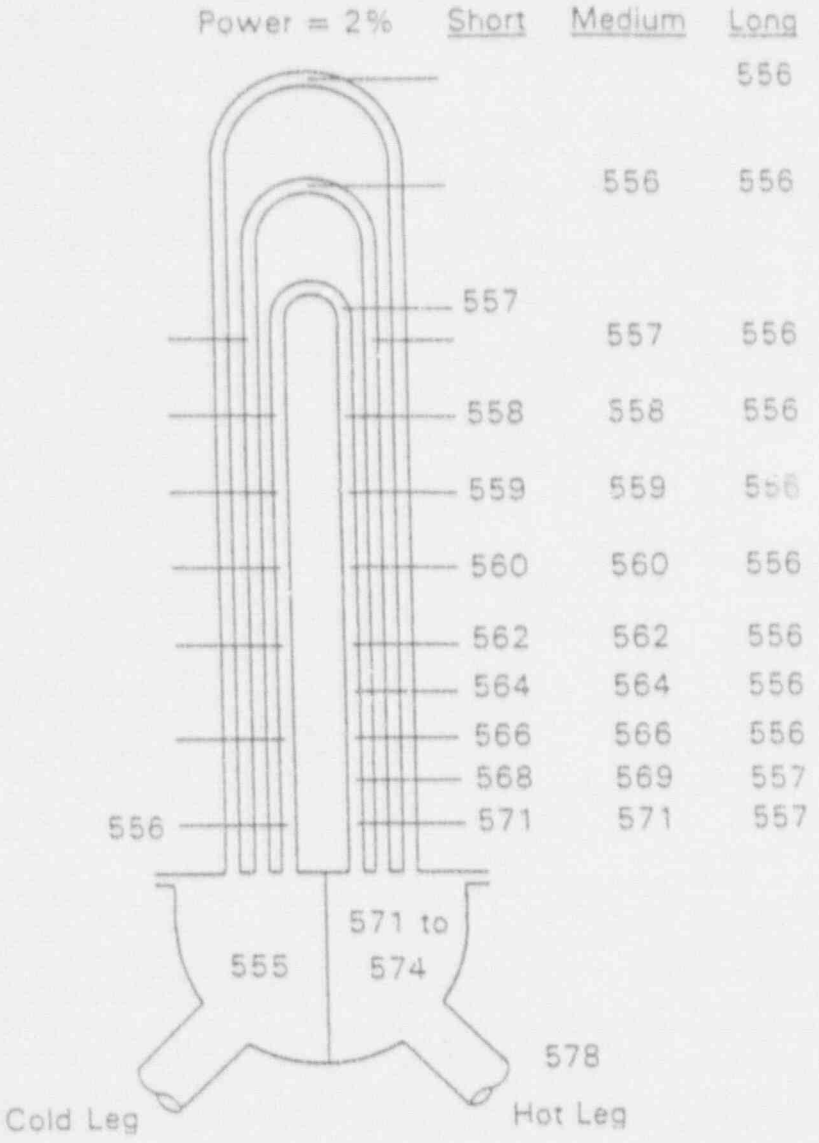

Figure 3-17. U-tube fluid temperature distribution during single-phase natural circulation in the LSTF.[20]

flow is dependent on secondary side liquid levels. In the case of plantms with OTSGs, primary flow oscillations may be caused by the on/off behavior of EFW pumps or by nonuniform EFW tube wetting. It was also noted that secondary side steam and feed operations are effective in maintaining a steam generator in a heat sink mode.

Section 3.6 addressed the issue of non-uniform single-phase natural circulation flow. The discussion primarily dealt with non-uniform flow in the tubes of a UTSG. It was pointed out that flow stall and/or reversal may occur in the longer U-tubes of a UTSG. However, it was emphasized that single-phase natural circulation will not cease or experience interruptions due to these tube-to-tube flow nonuniformities. The modelling of this phenomenon may serve as a useful test case for reactor safety codes.

Single-phase natural circulation is generally an effective and dependable means for removing decay heat in PWRs with either OTSG or UTSG designs. However, it was pointed out that abnormal conditions may compromise the heat removal ability of the single-phase mode of natural circulation.

4. TWO-PHASE NATURAL CIRCULATION

4.1 Introduction

During two-phase natural circulation, vapor generated in the core enters the hot leg and flows with the saturated liquid to the steam generator, where the vapor is condensed. A continuous primary loop flow of a liquid and vapor mixture is defined as the mode of two-phase natural circulation. This normally persists until the amount of voids in the primary loop increases to the point where continuous two-phase flow no longer exists in the upper U-bends of the UTSGs or in the hot leg upper "candy cane" bend leading to the OTSGs. By definition, when this occurs, the two-phase mode of natural circulation is terminated in the case of a UTSG, or interrupted in the case of a OTSG. Flow interruption in a OTSG plant may be followed by an intermittent type of circulation. If there is a sufficient loss of coolant from the primary system, this may later result in boiling condensation. In the case of a UTSG plant, the termination of two-phase natural circulation is usually immediately followed by the onset of reflux condensation.

Two-phase natural circulation behavior can be much more complicated than single-phase natural circulation behavior. Items such as flow nonuniformity, secondary side effects, effects of noncondensable gases, and heat transfer characteristics are important during two-phase natural circulation and will be discussed. Other phenomena such as steam generator inlet flooding, vent valve behavior in plants with OTSGs, and thermal stratification can also influence two-phase natural circulation behavior.

Section 4.2 will discuss general characteristics of two-phase natural circulation. Correlated expressions, which help quantify two-phase natural circulation behavior, will be presented in Section 4.3. Section 4.4 addresses the influence of noncondensable gases on the characteristic two-phase natural circulation response. Section 4.5 investigates the role of secondary side parameters in determining primary two-phase natural circulation behavior. Section 4.6 discusses nonuniform behavior associated with two-phase natural circulation and Section 4.7 summarizes the important phenomena associated with two-phase natural circulation.

4.2 General Characteristics

Density gradients in the two-phase mode of natural circulation are determined by both the primary void distribution and the loop temperature differences. The natural circulation behavior changes significantly as the hot side density is reduced by an increasing hot side void fraction. As long as the cold side density is not reduced by voids, the buoyancy effect is enhanced by the increased hot side void fraction, and a higher loop mass flow rate will result. The loop mass flow rate is the most important parameter affecting heat removal from the core during two-phase natural circulation.[21]

4.2.1 UTSG Plants

For plants with UTSGs, the peak mass flow rate in the primary loop occurs when voids occupy most of the volume in the upflow sides of the U-tubes, and single-phase liquid occupies most of the volume in the downflow sides of the U-tubes. This void distribution corresponds to the maximum hot-to-cold side density difference in the loop. Once voids flow over the U-tube bends into the downflow sides of the U-tubes, the buoyancy effect is reduced and the mass flow rate decreases.[20] This effect is illustrated in Figure 4-1, a representative flow map which presents mass flow rate versus primary mass inventory percentage from the PKL, LSTF, and Semiscale natural circulation experiments.[20] Initially, as the mass inventory is reduced, voids appear in the upflow sides of the U-tubes, the loop density gradient is enhanced, and the mass flow increases. After further primary mass inventory reductions, the mass flow rate reaches a peak value once voids reach the tops of the U-tubes. Still further inventory reductions force voids into the downflow sides of the U-tubes, reducing the net gravitational force, and decreasing the mass flow rate. Table 4-1 shows the observed ranges of primary mass inventories

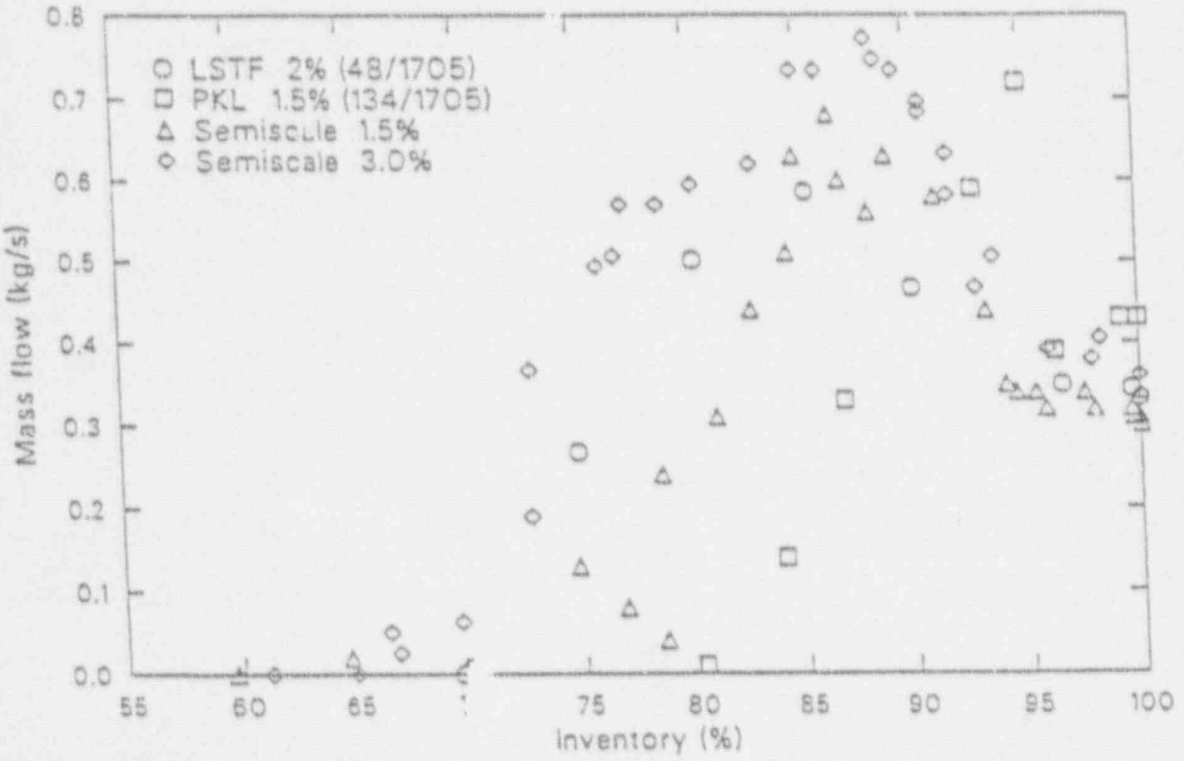

Figure 4-1. LSTF, PKL, and Semiscale mass flow rates as a function of primary mass inventory.[20]

Table 4-1. Comparison of significant primary mass inventory inflection points as found in PKL, Semiscale, and LSTF experiments [20]

Facility	% Break Area / Core Area	Last Single-Phase Flow Inventory (%)	Inventory at the Maximum Two-Phase Flow Rate (%)	Zero Flow Inventory (%)
PKL	1.5	99.0	85.0	80.0
Semiscale	1.5	94.0	86.0	70.0
LSTF	2.0	96.0	85.0	70.0
Semiscale	3.0	96.0	88.0	65.0
LSTF	5.0	91.0	80.0	64.0
Semiscale	5.0	94.0	84.0	No data

for the occurrence of two-phase natural circulation in the PKL, LSTF, and Semiscale natural circulation experiments. For example, two-phase natural circulation occurred during the LSTF 2.0% power experiment when primary mass inventories ranged between 96% and 70%.

4.2.2 OTSG Plants

The loop mass flow rate behavior in OTSG plants during two-phase natural circulation is not easily described. As long as the voids are entrained in the continuous liquid-vapor flow and pass through the U-bend region of the upper hot leg into the steam generator tubes, the flow behavior is similar to that in the UTSG plants. However, if the voids increase sufficiently such that they collect in the upper U-bend, or "candy cane," region of the hot leg, flow interruption may occur. This phenomenon can result in a cyclic flow behavior. Pressurization, due to loss of the steam generator as a heat sink, compresses the steam bubble until the liquid level reaches the top of the U-bend. Once a liquid bridge is formed between the hot leg upflow and downflow sides, spillover and reestablishment of continuous two-phase natural circulation will occur until void blockages interrupt the flow once again. This cyclic behavior has been labeled intermittent circulation[28] and can sometimes occur over extended periods of time. In test facilities with OTSGs, periodic interruptions of two-phase natural circulation have been frequently observed.[28,55,56]

Sufficient loss of primary mass inventory during intermittent circulation will cause the two-phase and/or intermittent circulation to be succeeded by the boiling condensation mode of natural circulation. Depressurization of the primary system during boiling condensation may allow high-pressure safety injection (HPSI) to initiate system refill. Two-phase natural circulation and/or intermittent circulation can reoccur after boiling condensation if the primary liquid inventory is increased sufficiently during refill.

4.2.3 Summary of Two-Phase Characteristics

In summary, voids generated in the core are condensed in the steam generators during the two-phase mode of natural circulation. In the steam generators, heat transfer acts primarily to reduce the amount of voids, rather than reduce the temperature of the fluid. Thus, the temperature difference between the hot and cold regions in two-phase natural circulation is smaller than the characteristic single-phase natural circulation temperature difference. The primary-to-secondary temperature difference is also smaller during two-phase natural circulation than during single-phase natural circulation, as shown in Figure 4-2 for a UTSG design.[40]

Reductions in primary mass inventory result in increased loop mass flow rates as long as the cold side density is not reduced by voids. As voids reduce the cold side density, the loop mass flow rate decreases. This can continue until the loop mass flow rate approaches zero. Once continuous two-phase flow no longer exists in the upper U-bends of the UTSGs or the hot leg upper heads leading to the OTSGs, the two-phase mode of natural circulation will be terminated or interrupted.

4.3 Correlated Expressions for Two-Phase Natural Circulation

The mass flow rate in the primary loop is the most important parameter governing heat removal from the core for both single- and two-phase modes of natural circulation. In PWR model tests, the loop mass flow rate has been shown to be directly related to the mass inventory in the primary coolant system.[19,40,57] Correlated expressions for single-phase natural circulation were given in Section 3.3. The following discussion includes correlated expressions used to describe two-phase natural circulation in PWRs.

The simplified primary loop conditions for two-phase natural circulation are depicted in Figure 4-3.[21] This figure shows a liquid-filled cold leg, downcomer, and lower plenum. Void formation begins a distance, L', above the bottom of the core. Voids are present in the upper vessel, the hot leg, and the steam generator. The thermal length (ΔL), the saturation elevation (L'), and the core length (L_c) are indicated in this figure.

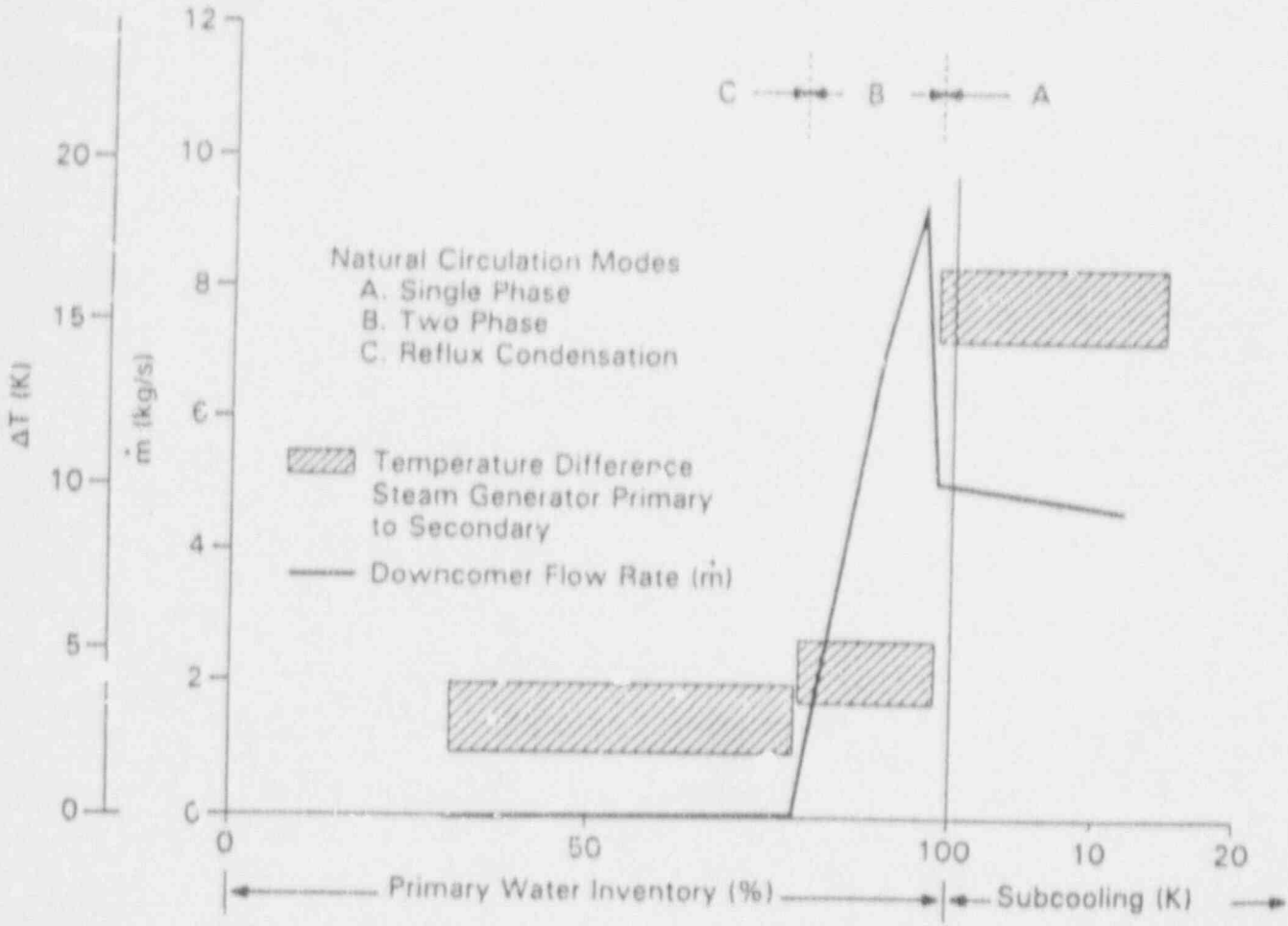

Figure 4-2. PKL mass flow rates and primary-to-secondary temperature differences as functions of the primary mass inventory.[23]

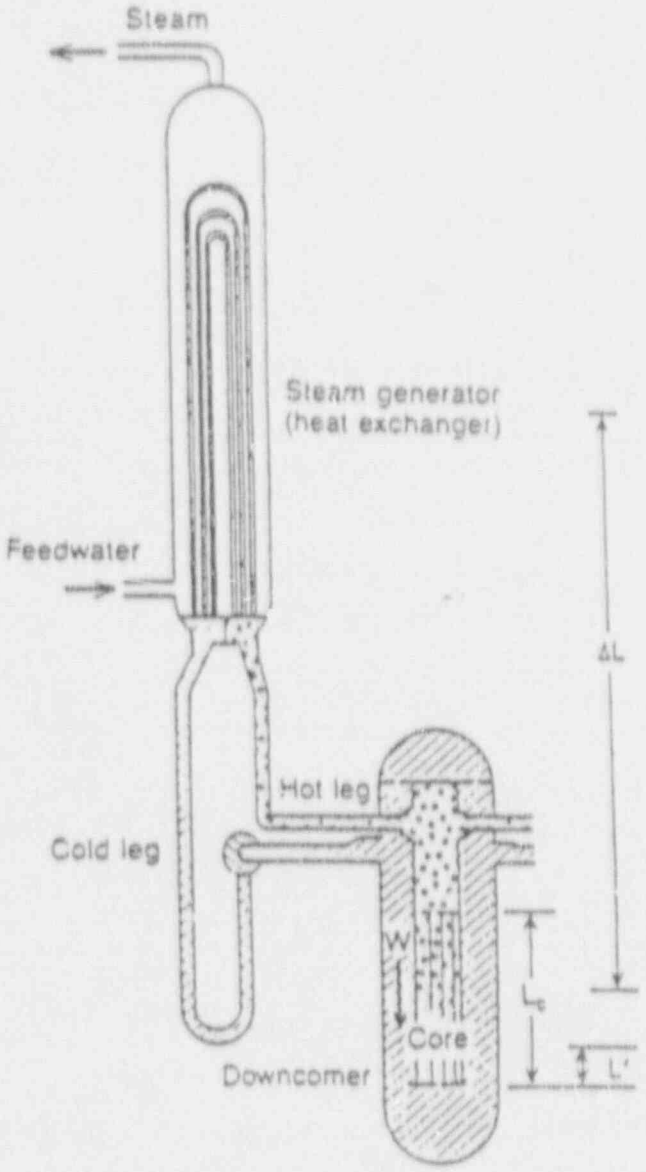

Figure 4-3. Typical PWR system with -tube steam generators.[21]

4.3.1 Mass Flow Rate

Various expressions describing two-phase natural circulation phenomena have been developed.[21,58] The fundamental assumption that the flow in two-phase natural circulation is quasi-steady leads to an expression for the two-phase natural circulation mass flow rate that is similar to the single-phase expression given by Equation 3-1.[58] In the two-phase derivation, the small two-phase density change

$$\Delta\rho = \frac{P}{Qh_{fg}} \qquad (4\text{-}1)$$

is used in place of the single-phase expression

$$\Delta\rho = \frac{\beta P}{Qc} \qquad (4\text{-}2)$$

where

- Q = volumetric flow rate
- P = core power
- h_{fg} = latent heat of vaporization
- β = fluid coefficient of thermal expansion
- c = fluid specific heat capacity.

The two-phase derivation results in the following expression for the mass flow rate:[58]

$$W = \left[\frac{2\,\bar{\rho}^{2}\,g\,\Delta L\,P}{h_{fg}\,R}\right]^{\frac{1}{3}} \qquad (4\text{-}3)$$

where

- W = mass flow rate
- g = acceleration of gravity
- ΔL = thermal length (elevation difference between core and steam generator thermal centers)
- $\bar{\rho}$ = average loop two-phase density
- R = equivalent two-phase flow resistance parameter.

Note, however, that use of the above expression assumes knowledge of the average loop two-phase density and two-phase flow resistance parameter, which may be difficult to obtain in some instances.

A more detailed formulation for the two-phase mass flow rate in terms of the primary fractional mass inventory was derived by Duffey and Sursock.[21] This derivation also assumed the natural circulation process to be quasi-steady.[21] Note that this assumption is supported by test data from SBLOCA experiments.[19,49,57] For a PWR with UTSGs, Duffey and Sursock observed that when the mass flow rate, W, is plotted versus the normalized mass inventory, I, the maximum mass flow rate occurs during two-phase natural circulation. This peak flow rate is caused by void formation on the hot side of the loop, which in turn increases the loop natural circulation driving force. The subsequent decrease in the mass flow rate (following mass inventory reductions) is caused by voids entering the cold side of the loop and reducing the loop natural circulation driving force. Based on these observations, Duffey and Sursock identified four distinct primary mass inventory regions over which the mass flow rate exhibits significantly different behavior. Then they developed expressions for the coolant inventory at transition points in terms of void and system volume fractions. The first region occurs when the fractional mass inventory is approximately one (a liquid full system). The flow is single phase and the expressions in Section 3.3 can be used to estimate the mass flow rate. Two-phase flow is divided into two regions, one in which the mass flow rate is increasing, and the other in which the mass flow rate is decreasing. The two-phase flow regions are separated at the peak two-phase mass flow rate. The fractional mass inventory at this point is designated as I_m. Thus, the range of the second fractional mass inventory region is $I_m < I < 1$. The range of the third mass inventory region is $I_R < I < I_m$, where I_R is the fractional mass inventory at the point where reflux condensation just begins. Thus, reflux condensation occurs in the fourth fractional mass inventory region. Note that the mass flow

rate is very small in this region. The expressions for I_m and I_{IC}, as defined by Duffey and Sursock, are given as

$$I_{IC} = 1 - \alpha_1(V_1 + V_2) \quad (4\text{-}4)$$

$$I_m = \frac{V_2 + (V_1)(I_{IC})}{V_1 + V_2} \quad (4\text{-}5)$$

where

α_1 = void fraction for the hot side regions

V_1 = fractional volume of core, upper plenum, hot leg, and hot side of the steam generator

V_2 = fractional volume of the cold side of steam generator, pump, and downcomer.

Note that α_1 must be known at the transitional point where reflux condensation just begins, before either I_{IC} or I_m can be calculated. When reflux is established, the primary loop is saturated, and the mass flow rate is near zero. Note that during reflux, there is a nonzero flow of steam (and returning liquid). However, because there is flow in both the hot and cold legs (negative liquid flow in the hot leg, positive liquid flow in the cold leg) the "loop" mass flow is physically small. The following expressions may be used to estimate α_1 at the point where reflux condensation begins[21]

$$\alpha_1 = \frac{\bar{\alpha}_c (V_1) + (\alpha_o - \bar{\alpha}_c)(V_u)}{V_1} \quad (4\text{-}6)$$

$$\bar{\alpha}_c = \frac{1}{C_o(1 - \gamma)}\left[1 - \frac{\ln(1 + P^*)}{P^*}\right] \quad (4\text{-}7)$$

$$\alpha_o = \frac{1}{C_o(1 - \gamma)}\frac{P^*}{1 - P^*} \quad (4\text{-}8)$$

$$P^* = \frac{C_o P(1 - \gamma)(1 - L_1^*)}{\rho_g h_{fg} A_c \left(V_{gj} + \frac{W C_o}{\rho_l A_c}\right)}$$

$$= \frac{C_o P(1 - \gamma)}{\rho_g h_{fg} A_c V_{gj}} \quad (4\text{-}9)$$

where

A_c = core flow Area

$\bar{\alpha}_c$ = mean void fraction for the core

α_o = maximum core void fraction

C_o = distribution coefficient

γ = density ratio (ρ_g/ρ_l)

h_{fg} = latent heat of vaporization

L_1^* = nondimensional saturation elevation. During reflux condensation the loop is assumed saturated, so $L_1^* = 0$.

P = power (heat input)

P^* = nondimensional power

ρ_g = vapor density

ρ_l = liquid density

V_u = fractional volume of the sum of the upper plenum and hot leg.

V_{gj} = void weighted drift velocity

W = loop mass flow rate (Approximately zero for reflux condensation).

See Reference 21 for the derivation details; only the results of the derivations are presented below. Expressions for the mass flow rate, W, are now given for the two fractional mass inventories covering the two-phase mode of natural circulation

1. $I_m \uparrow I \uparrow 1$

$$W = \hat{W}\left|\frac{I\,(1-I)}{V_1}(1-\gamma) + \psi\left(\frac{W_{1\phi}}{\hat{W}}\right)^2\right|^{\frac{1}{2}} \qquad (4\text{-}10)$$

where

$\hat{W}$ = reference value defined by

$$\frac{\sqrt{2gL}\,\rho_l\,A}{\sqrt{K_l}}$$

A = flow Area

g = acceleration due to gravity

K_l = loss coefficient for single-phase flow

L = height of the system

ρ_l = liquid density

ψ = interpolation parameter
$= \dfrac{1 - I_m}{1 - I_m}$

$W_{1\phi}$ = single-phase loop mass flow rate [see Equation 3-1].

2. $I_{FC} < I < I_{FN}$

$$W = \hat{W}\left|\frac{I\,(I - I_{FC})}{V_2}(1-\gamma)\right|^{\frac{1}{2}} \qquad (4\text{-}11)$$

An estimate for the maximum mass flow rate can be obtained if the following assumptions are made:[21]

- At maximum flow $W >> \dfrac{\rho_l A_C V_{gj}}{C_o}$
- Saturated flow ($L_1^* = 0$)
- The cold side void fraction is zero
- Q^* is much less than one
- Near the maximum flow rate, the two-phase friction multiplier (ϕ) is approximately zero.[21,57]

The resulting expression is given below.[21]

$$W_{max} = \left|\frac{\hat{W}^2(1-\gamma)Q_o}{2C_o\,\gamma\,h_{fg}}\right|^{\frac{1}{3}} \qquad (4\text{-}12)$$

The theory presented above was compared with data from the Semiscale facility,[19,57] and with data from the FLECHT-SEASET facility.[49] These comparisons are shown in Figure 4-4. Duffey and Sursock state that the same approach can be used for PWRs with OTSGs if I_{FC} is defined as the mass inventory fraction corresponding to flow interruption and the volume fraction of the steam generator hot side is taken to be zero.

4.3.2 Overall Heat Transfer Coefficient (UTSG)

In a UTSG, the flow behavior in the primary side during single- and two-phase natural circulation may vary from tube to tube. Consequently, the heat transfer from the primary side to the secondary side may also vary from tube to tube. Therefore, rather than attempting to define local heat transfer coefficients, it is more practical to define an overall heat transfer coefficient by using the inlet and outlet steam generator plena fluid temperatures and the secondary fluid temperature. An expression for this overall UTSG primary to secondary heat transfer coefficient in two-phase flow was defined[42] based on the "effective" heat transfer area (heat transfer area below the collapsed secondary liquid level) as

$$Q = K_e F R\,\Delta T \qquad (4\text{-}13)$$

where

Q = total heat transfer rate

K_e = effective overall heat transfer coefficient defined with heat transfer surface area below collapsed liquid level

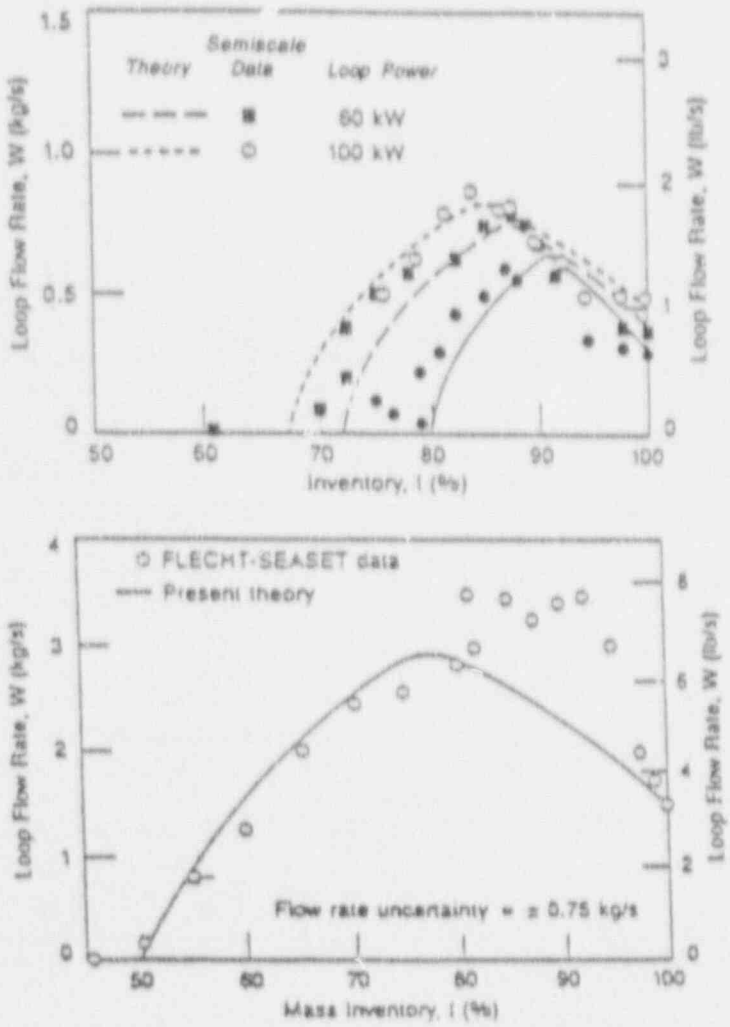

Figure 4-4. Duffey and Sursock's comparison of their theory with Semiscale and FLECHT-SEASET data.[21]

F = total inner surface area of U-tubes in a steam generator

R = ratio of collapsed liquid level height to average height of U-tubes, in secondary side

ΔT = logarithmic mean temperature difference defined by Equation 3-10.

Using the above expression, LSTF data from the ST-SG-02 and ST-SG-03 experiments were used to obtain overall heat transfer coefficients.[42] Figure 4-5 shows that the overall heat transfer coefficient for two-phase natural circulation varied from 2.0 kW/(m^2K) [1141.9 Btu/(hft^{2}F)] to 2.5 kW/(m^2K) [1427.4 Btu/(hft^{2}F)].

Recall from the discussion in Section 3.3 that K_e is dependent upon the local overall heat transfer coefficient defined by Equation 3-11. Thus, a correction should be incorporated in extending these results to a full-scale PWR. This correction consists of multiplying the value of K_e found in the LSTF by the ratio of the local overall heat transfer coefficient of the full scale PWR to the local overall heat transfer coefficient of the LSTF.[42]

4.4 Noncondensable Gases

The effect of noncondensable gases in a PWR loop is an important issue with regard to the effectiveness of two-phase natural circulation cooling. The primary concern in the case of a UTSG plant design is that noncondensable gas will disrupt the two-phase flow by accumulating in the steam generator U-tube upper bends.[19] In the case of a OTSG plant design, the concern is that noncondensables will collect in the "candy cane" region of the hot legs and disrupt the two-phase flow.[59] In Section 3.4, it was pointed out that noncondensable gases can enter the primary loop through safety injection or fuel degradation. Research has concentrated on determining whether noncondensables will migrate to and collect in the upper elevations of the primary loop. There, they may interrupt the two-phase natural circulation flow and jeopardize the effectiveness of the two-phase natural circulation cooling.

4.4.1 UTSG Plants

Experiments conducted in the Semiscale facility,[19,60] the FLECHT-SEASET facility,[41,49,61] and a KAERI experimental test facility[45] have examined the effects of noncondensable gases on two-phase natural circulation behavior in UTSG plant designs. The Semiscale test was designed to determine if nitrogen gas, injected directly into the steam generator inlet piping, would accumulate in the steam generator upper U-bends. The test was initiated from a peak two-phase flow condition (86% primary mass inventory) at 1.5% core power. Discrete amounts of nitrogen gas were then injected directly into the steam generator inlet piping. During this test, the broken loop of the test facility was disconnected so that the primary system consisted of the vessel and a single active loop. Note that in the Semiscale facility, the "broken" loop models a single PWR loop while the "intact" loop models three loops of a PWR. Each of the twelve nitrogen injections (~ 1-2% system volume/injection) were followed by a period of steady operation with adequate core cooling. The total nitrogen volume injected into the primary system amounted to approximately 13% of the primary system volume at the primary temperature and pressure. Figure 4-6 shows the behavior of the primary mass flow and pressure versus the volume of nitrogen in terms of the percent of system volume.[19] Note the immediate drop in the mass flow rate after the first nitrogen injection (1.4% of primary system volume). The mass flow rate fell from its peak two-phase value to a level characteristic of single-phase natural circulation. The initial nitrogen injection resulted in a gas bubble that blocked the flow through the steam generator U-tubes. The initial pressure increase, caused by an interruption of the two-phase natural circulation flow, condensed a large fraction of the voids in the primary loop.[60] System pressurization eventually compressed the gas blockage sufficiently to allow the resumption of a natural circulation condition consisting of single-phase liquid and nitrogen gas bubbles. The condensation of voids effectively reduced the loop driving head, and resulted in the drop in the loop mass flow rate.[60] Smaller reductions in the loop mass flow rate following subsequent nitrogen injections were attributed to increases

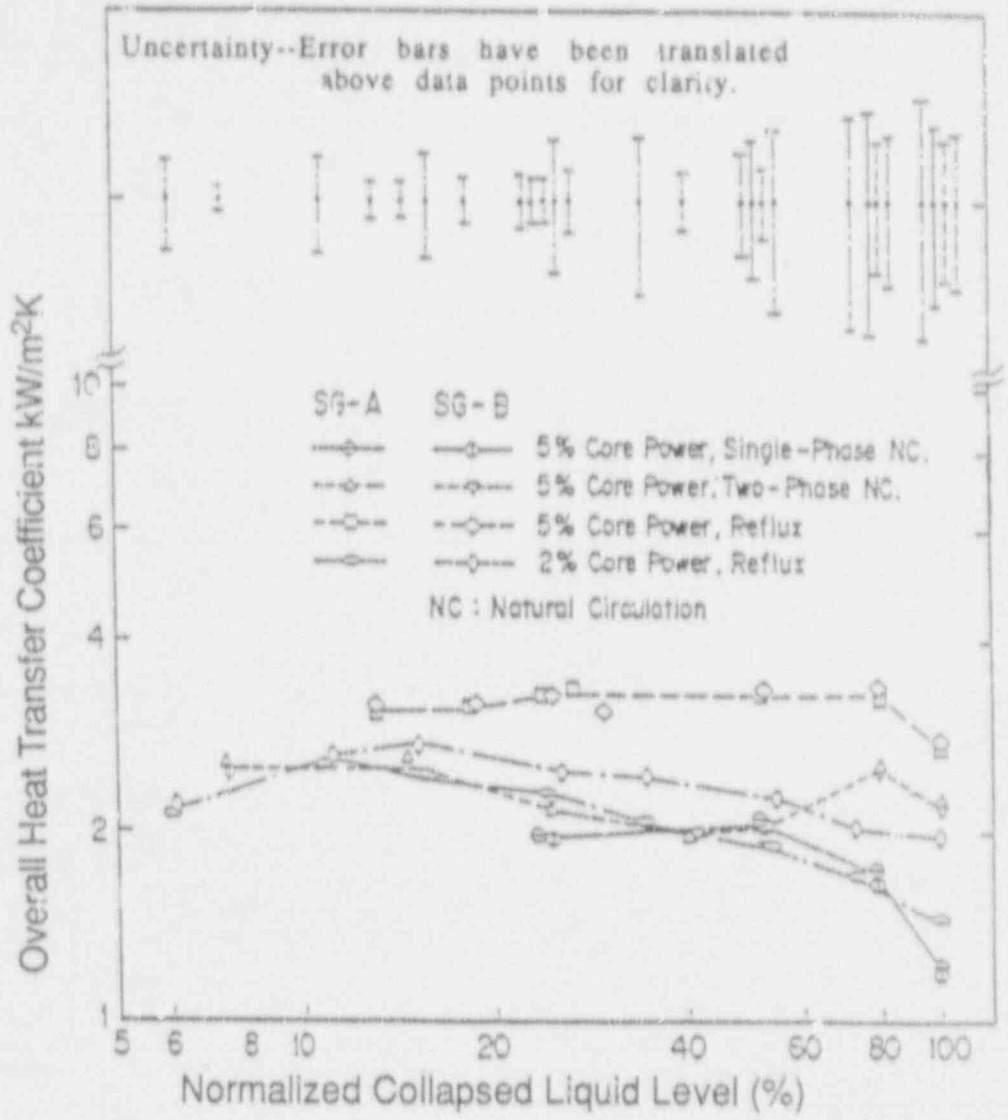

Figure 4-5. LSTF primary-to-secondary heat transfer coefficients based on the effective heat transfer area.[42]

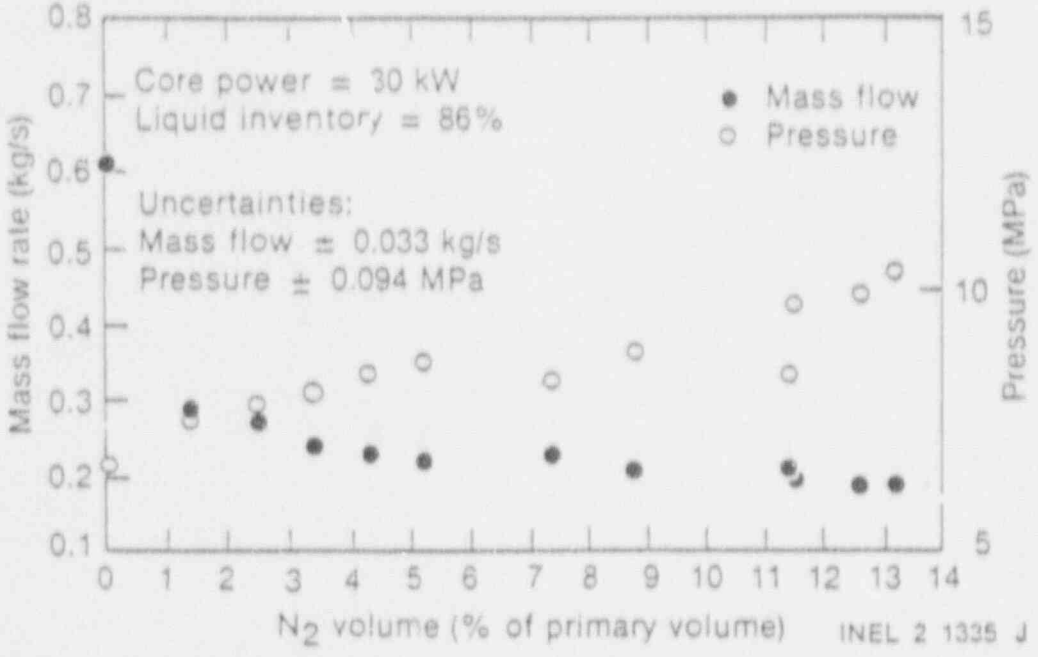

Figure 4-6. Influence of noncondensable gas on two-phase natural circulation observed in the Semiscale facility.[19]

in pressure drop in the loop because of nitrogen gas bubbles in the primary coolant, and to increases in the loop flow resistance which resulted from nitrogen gas blockages in some of the steam generator U-tubes.[60]

Eventually, most of the nitrogen gas injected into the primary system migrated to the vessel upper plenum and to the upper U-bends of several of the steam generator U-tubes. The nitrogen gas in the vessel upper plenum did not influence the mass flow rate. However, nitrogen gas bubbles in the steam generator U-tubes reduced the mass flow rate by increasing the total loop flow resistance by stalling the flow in some of the steam generator U-tubes.[60] Even though some of the U-tubes stalled, the overall primary-to-secondary heat transfer rate was not degraded.[60] The observed Semiscale two-phase natural circulation behavior in the presence of noncondensable gases was corroborated by similar results obtained by KAERI,[45] and in the FLECHT-SEASET facility.[41,49] In the KAERI tests, nitrogen gas was injected into the hot leg of the single active loop of a two-loop test facility.[45] The FLECHT-SEASET noncondensable gas tests consisted of injecting helium gas into both the broken and intact loops of the test system. The broken loop represented a single loop of the four-loop reference PWR, while the intact loop represented the remaining three loops. During the noncondensable FLECHT-SEASET experiments, the broken loop was in a stalled condition so essentially only one loop was active in the primary system.[49]

Faster rates of noncondensable gas injection have resulted in loop flow stalling.[19] In another Semiscale experiment, an injection rate of 0.01% system volume/second was sufficient to cause flow stall in the single active loop. This flow stall behavior was often followed by rapid increases in the system pressure and subsequent compression of the gas blockages. Condensation eventually raises the liquid level in the upflow sides of the steam generator U-tubes to the tops of the upper U-bends. A liquid bridge with the downflow sides of the U-tubes forms, and flow quickly restarts. After flow restart, the noncondensable gas mixes and circulates with the primary coolant. However, as the amount of noncondensable gases increases, flow may not restart in all of the steam generator U-tubes. In this case, noncondensable gas from U-tubes with restarted flow may be redistributed to other stalled U-tubes.[19]

4.4.2 OTSG Plants

Experiments performed by EPRI/SRI[59] investigated the effects of noncondensable gases on two-phase natural circulation in a test facility with a OTSG type plant design. Nitrogen gas volumes up to 1.5% of the system volume at the system temperature and pressure were injected into the lower hot leg of the single active loop. Injection of nitrogen gas caused increases in the temperature and pressure of the primary system. Pressure increases resulted in the condensation of voids in the upflow section of the hot leg which significantly reduced the driving head for the flow. Consequently, the primary system mass flow rate was reduced.[59]

4.4.3 Summary of Effects of Noncondensable Gases on the Primary System

Experiments conducted in facilities with UTSGs[19,45,49,60] and with OTSGs[59] have led to the conclusion that adequate heat rejection is possible with plausible amounts of noncondensable gases during two-phase natural circulation. The important parameters during two-phase natural circulation are the same as those listed for single-phase natural circulation in Section 3.4. However, two-phase natural circulation is more tolerant of noncondensable gases than single-phase natural circulation.[53]

Limits on the amounts of noncondensable gases that can be accommodated by a system are difficult to define. The Semiscale experiments demonstrated that adequate heat removal was possible with nitrogen gas occupying 13% of the total system volume.[19,60] The noncondensable gas experiments conducted by EPRI/SRI concluded that the amount of noncondensable gas that can be accommodated by a system is determined only by the design pressure limits of the system.[59]

Combustion Engineering Owners Group Emergency Procedures Guidelines provides a reference point for estimating this

noncondensable gas limit. They state that the overall primary-to-secondary heat transfer coefficient will be degraded by approximately 3% and the pressure will increase by about 2% due to the presence of a noncondensable gas volume that consists of the sum of the air in the refueling water, hydrogen in the primary coolant, and hydrogen in the pressurizer vapor space.[62] They further conclude that this amount of noncondensable gas in the primary system will not preclude the transition from two-phase natural circulation to single-phase natural circulation.[62]

4.5 Effects Due to Secondary Side Conditions

Conditions on the secondary side of the steam generator directly affect the heat transfer from the primary to the secondary through the steam generator tube walls. Previous sections emphasized conditions in the primary loop and their effects upon natural circulation phenomena. This section discusses the effects that secondary side conditions can have on two-phase natural circulation in the primary loop.

A specific concern regarding the steam generator is the consequences that could occur if the secondary side heat sink is lost or degraded during a transient. The primary side may not be sufficiently cooled if primary coolant is being gradually depleted. This could eventually lead to core voiding and dryout.

As was the case for single-phase natural circulation, the main secondary side parameters that directly affect primary-to-secondary heat transfer are the temperature, flow rate, and liquid level. Other factors can indirectly affect the primary-to-secondary heat transfer by influencing these parameters. They include relief valve behavior, feedwater injection, and emergency feedwater behavior during a transient. Procedures used to regulate the secondary side conditions during a transient will indirectly influence the primary-to-secondary heat transfer.

4.5.1 UTSG Plants

Experiments have shown that low secondary inventories can affect two-phase natural circulation.[19,28,42] Also, it has been demonstrated that unbalanced loop secondary side conditions in multiloop systems can lead to flow stall or oscillatory flow behavior in two-phase natural circulation.[55] Results from various experiments investigating these issues are discussed in the following paragraphs.

4.5.1.1 Reduced Secondary Inventory. The Semiscale Mod-2A facility was used to examine the behavior of natural circulation in a PWR geometry.[19] In these experiments, the effect of reduced secondary mass inventory on natural circulation cooling in a UTSG was investigated.

In the Semiscale tests, coolant was drained from the primary system until the peak two-phase mass flow rate was reached (~ 85% mass inventory). The secondary side was maintained at a relatively constant saturation pressure while the secondary liquid level was reduced in discrete increments, and maintained with feed and bleed.[19] Results were obtained for both single- and two-loop configurations, at two different core power levels.

The primary loop mass flow rate as a function of secondary side collapsed liquid level is plotted in Figure 4-7 for the single loop Semiscale configuration.[19] Reduction in secondary side liquid level had no significant effect on mass flow rate for liquid levels greater than 50% of normal. At liquid levels below 50%, the primary mass flow rate decreased and large oscillations in this flow rate were observed. However, heat removal was still adequate.[19] Testing with the two-loop configuration showed behavior qualitatively and quantitatively similar to that for the single-loop system.

In a similar experiment conducted in the LSTF (ST-NC/SG-03), the secondary inventory was reduced in discrete steps under a peak two-phase flow condition (75% mass inventory, 5% core power).[42] The results demonstrated that the

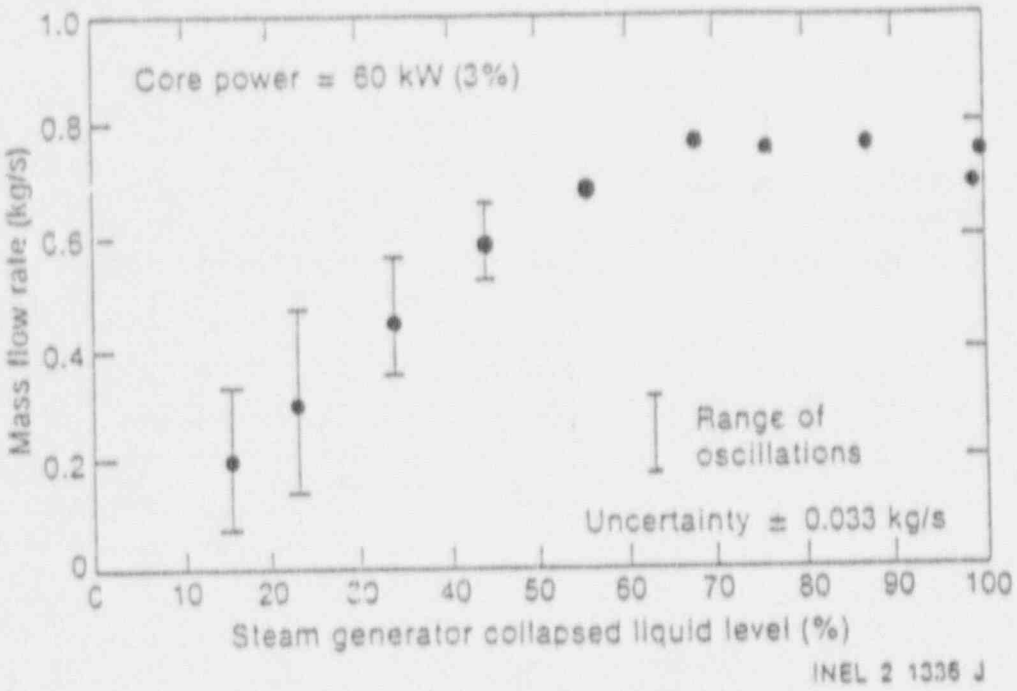

Figure 4-7. Two-phase natural circulation cold leg mass flow rate versus secondary inventory in the Semiscale facility.[19]

effective overall heat transfer coefficients are approximately constant for different secondary collapsed liquid levels. Based on Equation 4-13, this implies that the total heat transfer is directly proportional to the heat transfer area below the collapsed liquid level. Figure 4-5 shows that the value of the overall heat transfer coefficient based on the effective heat transfer area ranged between 2.0 and 2.5 kW/m^2K (1141.9 and 1427.4 Btu/hft^2F) for two-phase natural circulation.[42]

4.5.1.2 Unbalanced Loop Secondary Conditions. During the two-loop Semiscale experiment, the effect of unbalancing the two secondaries was investigated by reducing the liquid level in the broken loop steam generator. This level was reduced in discrete steps while constant conditions were maintained in the intact loop secondary. Note that in this context, the broken loop refers to the small Semiscale loop simulating a single loop in the reference PWR (in this discussion it does not imply a LOCA). Similarly, the intact loop refers to the large loop in the Semiscale facility (which simulates three loops in the reference PWR). A flow reduction occurred in the broken loop primary, but little change took place in the intact loop flow rate. Periodic stalling and unstalling of the broken loop flow occurred at secondary inventories below 50%, as shown in the transient mass flow rate data of Figure 4-8.[19] This oscillatory behavior was due to void formation in the upper U-tube U-bends, which disrupted the flow. Some voids gradually collapsed and caused a rapid restart of the flow, followed by more cycles of void formation and collapse. Figure 4-9 shows the broken loop flow rate and the collapsed liquid levels in the shortest U-tubes upflow and downflow sides. The conditions just prior to flow restart are depicted in Figure 4-10; note that flow was sometimes observed to switch back and forth between the short and long U-tubes.

In a multi-loop system, two conditions appear necessary for oscillatory behavior to occur in one of the loops. First, enough of the steam generator U-tube surfaces must be uncovered to degrade the heat transfer rate and thus allow voids to disrupt the flow in the U-tubes. Second, the degraded steam generator must have a sink temperature lower than the primary system temperature so that voids can be collapsed after flow stall has occurred. It was observed that the oscillatory period shortened and the flow excursions reduced to brief spikes as the secondary level was further reduced.[42]

4.5.2 OTSG Plants

Secondary liquid level is a very important parameter in determining primary-to-secondary heat transfer in plants with OTSGs. A loss of the steam generator as a heat sink is possible if the primary collapsed liquid level is above the secondary collapsed liquid level and EFW is not available. This situation can occur during two-phase natural circulation if a steam bubble forms in the hot leg "candy cane" region and temporarily interrupts the flow. The liquid distribution during flow interruption is illustrated in Figure 2-5.

Action of the injected emergency feedwater can significantly affect natural circulation cooling in PWRs with OTSGs. The degree to which the tubes are wetted by the EFW and the flow distribution over the tubes also affects the heat transfer.[55] These effects depend mainly on the EFW injection rate, and the possibility of secondary side flooding near the tube support plate (TSP). An analytical study predicted the possibility for flow reversal in the unwetted tubes for conditions typical of the MIST facility.[30] It concluded that with a large number of tubes wetted, density differences can cause internal circulation, driving primary flow upwards in the unwetted tubes.[30] It is unknown whether the occurrence of this phenomenon has been verified in the Multiloop Integral System Test (MIST) facility.

In the Once-Through Integral System (OTIS) SBLOCA tests[28], a lower steam generator water level [(3.05 m (10 ft) versus 11.6 m (38 ft)] resulted in a later transition to the boiling condensation mode. This occurred because primary inventory had to be drained until the steam generator primary liquid level fell below the secondary liquid level. Note that in this test, the secondary liquid level control impacted the availability of EFW. Had EFW been available, high-level EFW boiling condensation would have occurred as soon as the steam generator

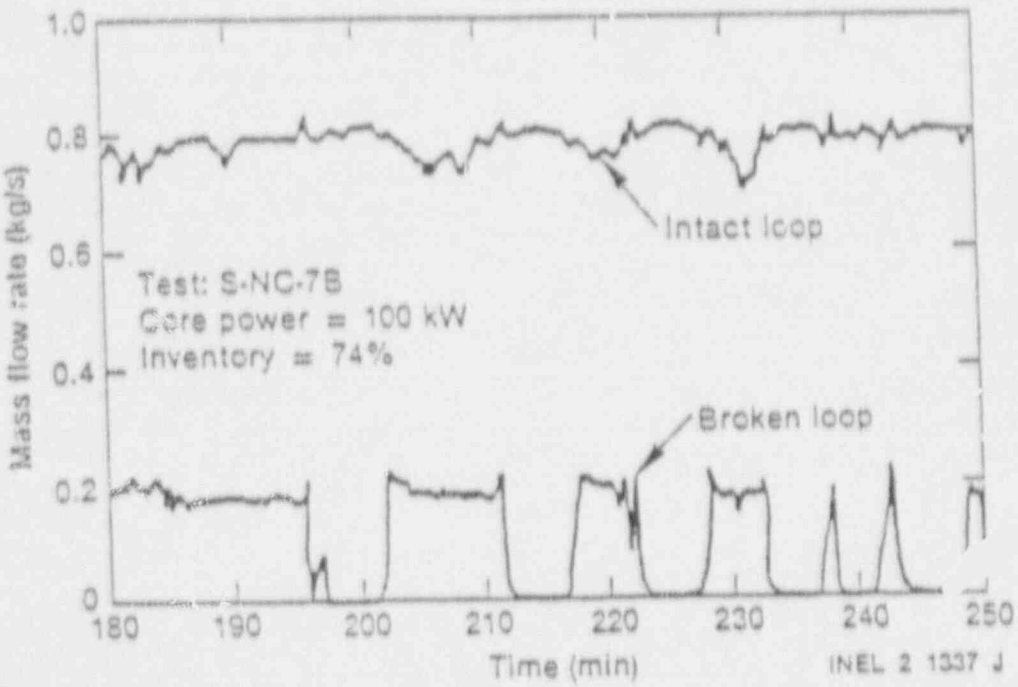

Figure 4-8. Effect of reducing broken loop secondary inventory on the cold leg mass flow rate during Semiscale test S-NC-7B.[19]

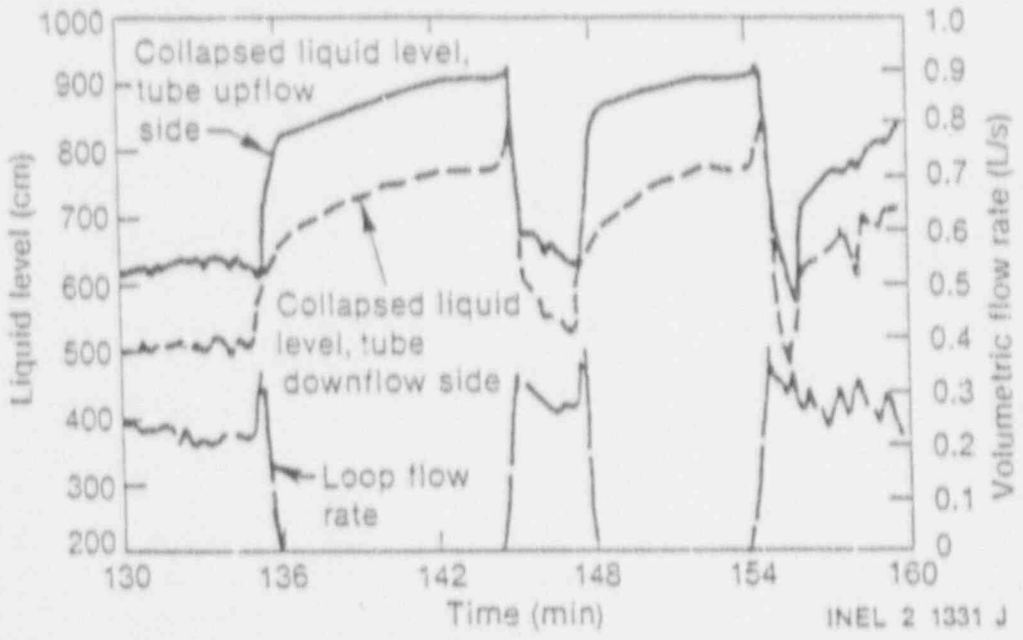

Figure 4-9. Time responses of the collapsed liquid levels in the Semiscale broken loop steam generator U-tubes and the loop flow rate.[19]

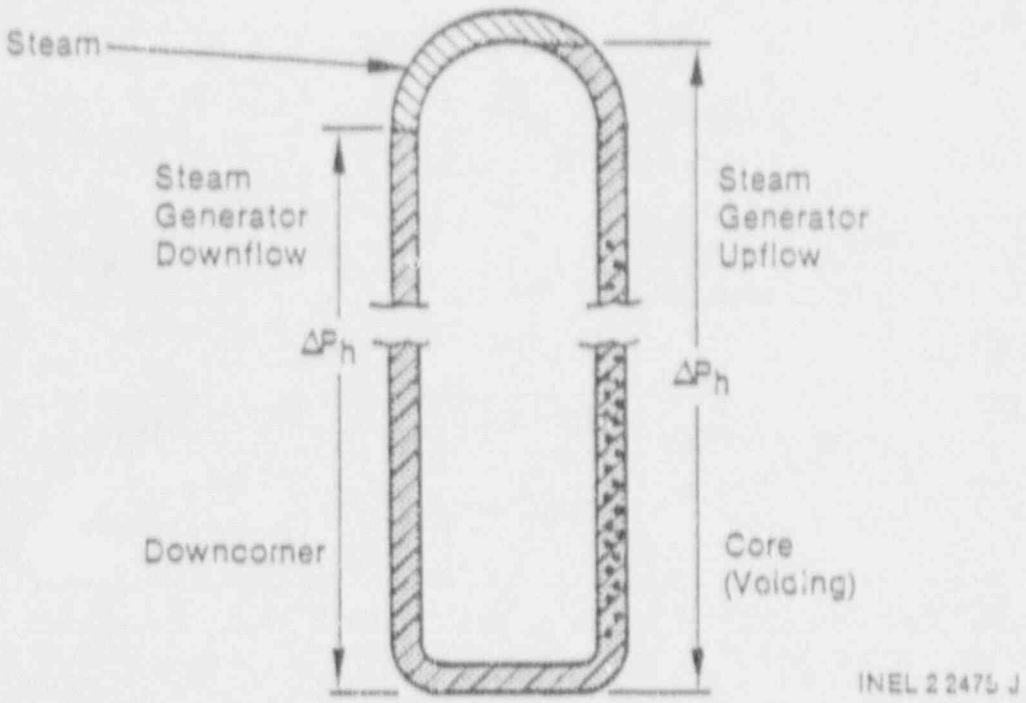

Figure 4-10. Conditions in a U-tube just prior to flow restart.[19]

primary liquid level dropped below the steam generator tubesheet.[28]

4.6 Nonuniform Two-Phase Flow Phenomena

Two-phase natural circulation is subject to two basic types of nonuniformity in flow. The first type is loop nonuniformity, and the second type is U-tube nonuniformity in UTSGs. Both UTSG and OTSG plants can have nonuniform loop flow phenomena. Although it is possible to have nonuniform tube flow phenomena in an OTSG (i.e., due to nonuniform EFW tube wetting[30]), these tubes are of equal length and direction making nonuniform flow less likely than in the case of the UTSG. Therefore, the nonuniform tube flow discussion applies only to the UTSG plants.

4.6.1 Nonuniform U-tube Flow

This discussion concerns nonuniform U-tube flow exhibited in experimental test facilities with UTSGs during two-phase natural circulation.

4.6.1.1 Different U-tube Flow Regimes. Primary mass inventory and U-tube length are two factors that determine U-tube flow behavior. Tests in the LSTF discl d nonuniform U-tube flow under both single a l two-phase modes of natura' circulati Figure 4-11[26] is a U-tube flow regime map t indicates different U-tube flow behavior for different length tubes and for different primary mass inventories (at 2% core power). Note that in the two-phase flow regime (approximately 75% to 90% mass inventory) several different types of U-tube flow can exist in the different length tubes. Consider the flow map for steam generator A as the primary mass inventory is reduced; the longest tubes experienced reversed two-phase flow and a cyclic fill and dump behavior. The medium length tubes experienced forward two-phase flow, reversed two-phase flow, and a cyclic fill and dump behavior. The shortest tubes experienced normal two-phase flow and a cyclic fill and dump behavior.[26]

The fill and dump process, is depicted in Figure 4-12.[26] The filling period in the LSTF test was about 100 s, followed by a quick dump of fluid into the downflow side of the tube. This phenomenon was repeated periodically. During the filling period, the levels in both sides of the U-tube increase as the vapor bubble is condensed [Figure 4-12 (a)]. When the mixture level in the upflow side reaches the top of the U-bend, a quick dump of the mixture begins [Figure 4-12 (b)]. The two-phase mixture flows through the U-tube, with a considerable amount of liquid carryover to the steam generator outlet plenum [Figure 4-12 (c)]. Flow once again stagnates when the void distribution in the U-tube satisfies the U-tube differential pressure common to all U-tubes. After flow stagnation, voids may rise in both sides of the tube to once again form a steam bubble at the top of the U-bend.[26]

Steam-water interphase drag in the hot leg and inlet plenum (not flooding at the U-tube inlet), was determined to be responsible for the high mixture level in the U-tubes during the cyclic fill and dump flow phenomenon. Cyclic fill and dump occurred in the LSTF at 2% core power ($j_g^* \approx 0.16$), which was well below the observed flooding limit ($j_g^* \approx 0.4$). A detailed discussion of the role of interphase drag in natural circulation is found in Reference 63. The frequency and magnitude of the fill and dump flows differed from tube to tube. The longer tubes had longer intervals between dumps, while the level oscillations were largest in the medium-to-long tubes.[26] It was observed that the level oscillations in individual U-tubes did not have a significant impact on the U-tube differential pressure common to all tubes. U-tube differential pressure was fairly constant despite large level oscillations in individual tubes.[26] A reason for this behavior can be deduced from Figure 4-13.[33] This figure, from Semiscale data, shows the levels in the short and long U-tubes consistently oscillated out of phase with each other. Thus, the combined effects from two levels upon U-tube differential pressure tended to cancel, resulting in a fairly constant differential pressure between steam generator plena.

Oscillations in differential pressure between the top of the U-bends and one of the steam generator plena during the later part of the tests was judged to be the result of oscillations in the

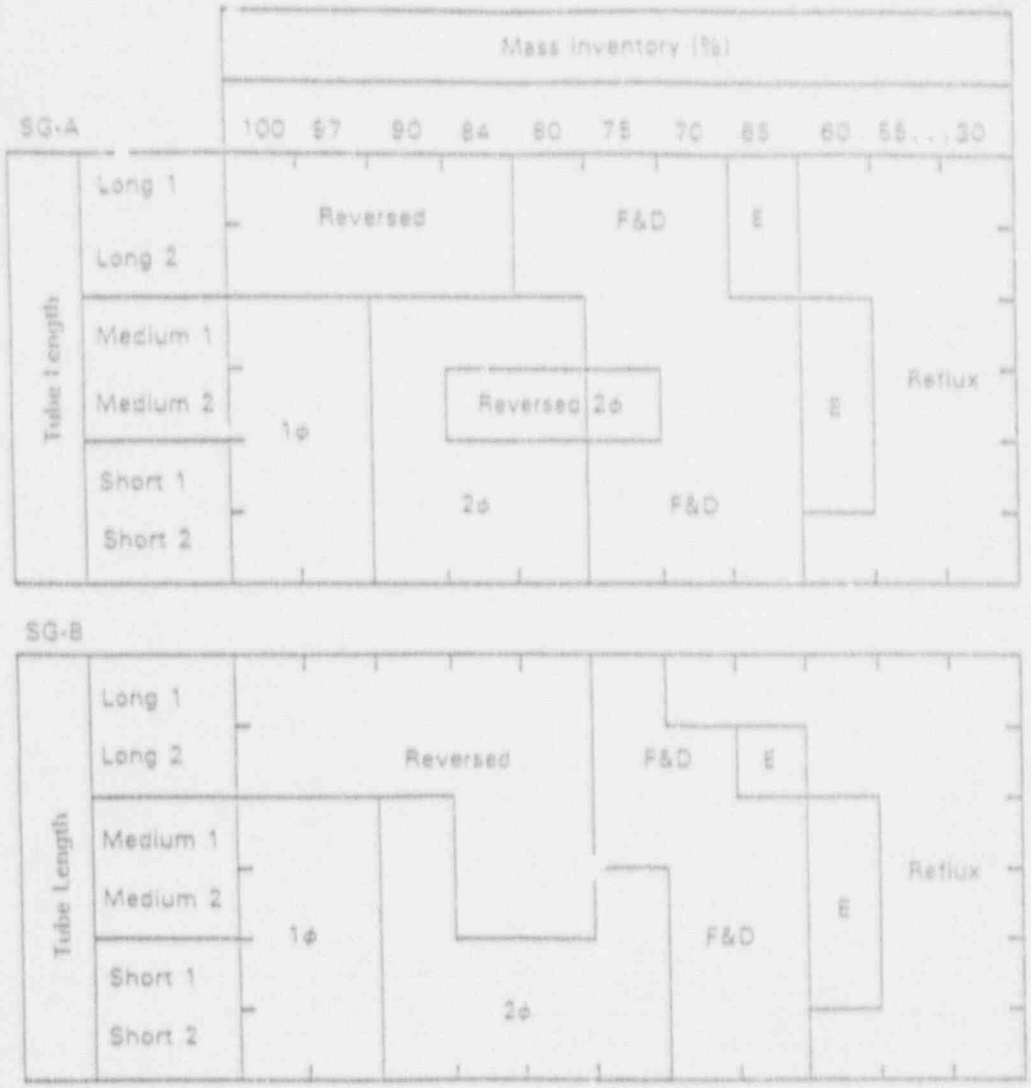

Figure 4-11. LSTF U-tube flow behavior as a function of mass inventory and tube length (1φ=single-phase, 2φ=two-phase, F&D=cyclic fill and dump, E=tube emptying).[26]

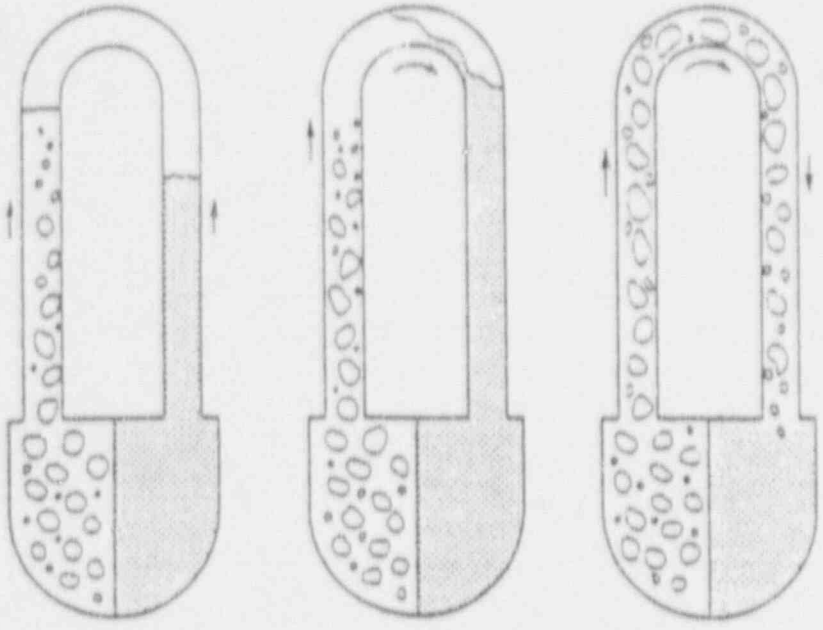

Figure 4-12. Schematic of the U-tube cyclic fill and dump process.[26]

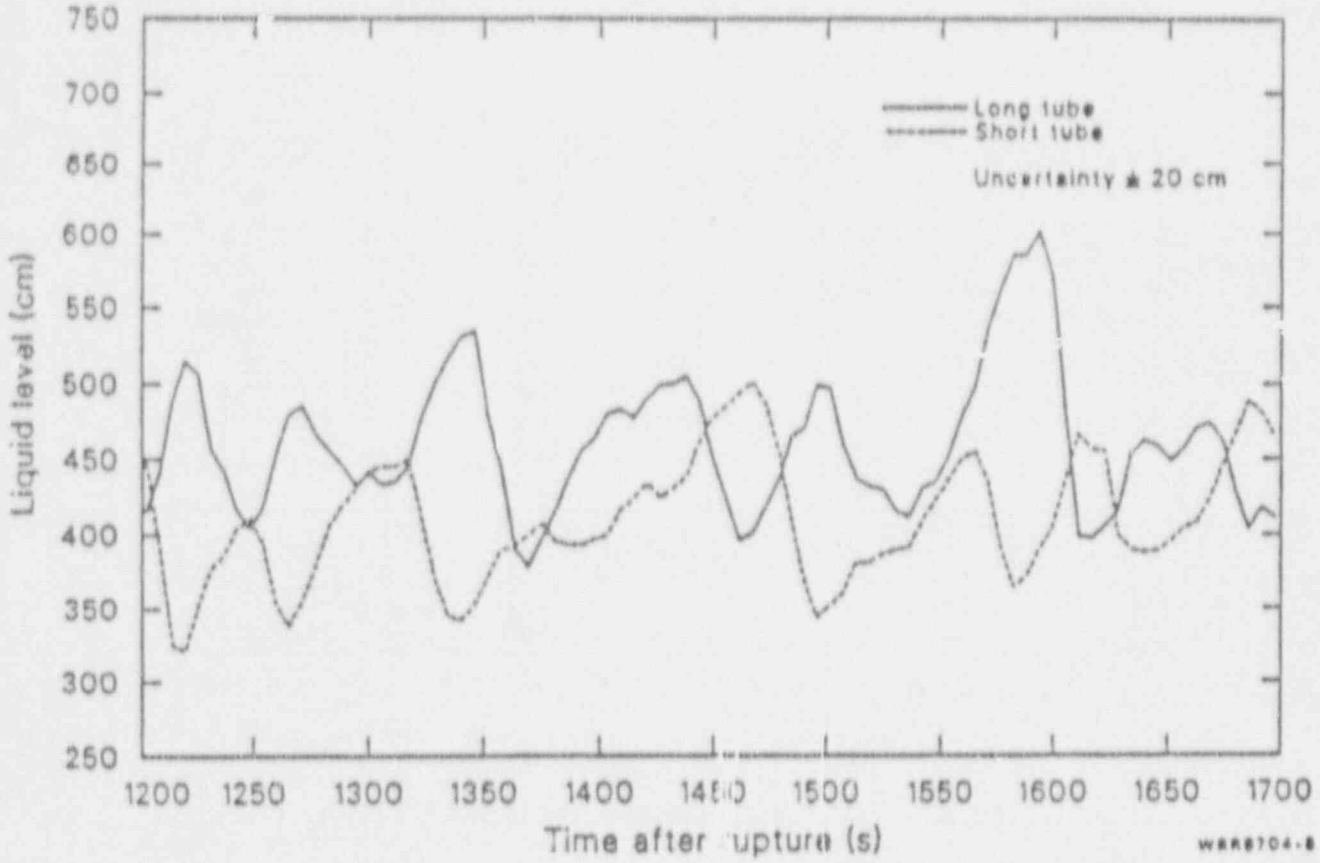

Figure 4-13. U-tube upflow side liquid levels in the broken loop of the Semiscale facility.[33]

U-tube continuous two-phase flow, a fill-and-dump flow pattern in the U-tubes, or a combination of the these phenomena.[20] Note that Semiscale-MOD2 (5% core power) and LOBI-MOD2 (3.5% core power) tests also exhibited oscillatory behavior during two-phase natural circulation.[13,64] U-tube flow stalls and oscillatory differential pressure responses indicate that the cyclic fill and dump phenomena may have also occurred in the Semiscale tests.[20,33] The oscillations in the LOBI facility at 75% mass inventory (transition region between two-phase natural circulation and reflux condensation) were attributed to a syphon condensation phenomena similar to the cyclic fill and dump phenomena described earlier.[64]

At mass inventories between 70% and 55% in the LSTF experiments, the U-tubes emptied of liquid. The transition to the reflux condensation mode of natural circulation occurred in all tubes by the time the mass inventory reached 55%.[26] Figure 4-11 shows that some individual tubes may start reflux before others. For example, in steam generator B, the longer U-tubes began reflux at a mass inventory of approximately 70%, whereas the shorter U-tubes did not begin the reflux condensation mode until the mass inventory was reduced to approximately 60%.

4.6.1.2 Nonuniform U-tube Flow Due to Secondary Side Effects. One cause of nonuniform U-tube flow is a reduced mass inventory in the steam generator secondary side. Semiscale tests showed that large flow oscillations occurred in the primary loop for secondary mass inventories below 50%.[19] These oscillations were apparently caused by rapid accumulation and collapse of voids in the U-bends of the steam generator tubes.[19] However, the oscillations had a negligible effect on core decay heat removal. Testing with a two-loop configuration showed that the loops behaved rather independently, implying the effect of reduced secondary inventory is nonuniform U-tube flow which, in turn, leads to unsteady loop flow.[19]

4.6.1.3 Nonuniform U-tube Flow Due to Noncondensable Gas Effects. A second cause of nonuniform U-tube flow is the presence of noncondensable gases in the steam generator U-tubes. Semiscale tests demonstrated that if noncondensable gas (nitrogen) is injected into the steam generator U-tube inlet at a sufficient rate (0.01% of the system volume/s), nonuniform U-tube flow results.[19] The flow in some tubes stall because of noncondensable gas accumulation in the tube U-bend. The resulting reduced heat removal capability of the steam generator will initiate a rise in pressure that compresses the noncondensable gas bubble. If the gas bubble in a U-tube is compressed sufficiently to allow a liquid bridge to form between the upflow and downflow sides of the U-tube, flow will quickly restart in the U-tube, pushing the noncondensable gas out of the tube. The gas expelled from a tube after flow restart may become well mixed and circulate with the primary coolant; or it may be redistributed to another stalled U-tube, the vessel upper head, the pressurizer, or some other location in the primary loop. The migration tendencies of noncondensable gases in the primary loop during two-phase natural circulation are not completely understood.

4.6.2 Nonuniform Loop Flow

Transition between modes of natural circulation often produces nonuniform loop flow phenomena because of loop stalling, unbalanced loop conditions, etc. Typically, this complex switching of natural circulation modes produces flow conditions that are both unsteady and nonuniform. In transitions from one natural circulation mode to another, nonuniform loop flow can exist in plants with either UTSGs or OTSGs.

4.6.2.1 Nonuniform Loop Flow in UTSG Plants. Section 4.6.1.2 indicated that reducing the secondary mass inventory in the Semiscale facility resulted in large flow oscillations in the primary loop.[19] These oscillations appeared to be caused by nonuniform U-tube flow, namely the rapid accumulation and collapse of voids in the U-bends of the steam generator U-tubes. Nonuniform U-tube flow with a normal secondary liquid level did not have a significant impact on the differential pressure across the steam generator (Section 4.6.1.1). Thus, a reduced secondary mass inventory (less than 50% normal inventory) combined with

nonuniform U-tube behavior may lead to a nonuniform loop flow.[19]

The effect of unbalancing the secondary sides of the two loops in the Semiscale Mod-2A facility was also investigated.[19] The liquid level in the broken loop secondary was reduced in discrete steps while maintaining constant secondary conditions in the intact loop. Below a secondary inventory of 50%, periodic stalling and unstalling of broken loop flow occurred with little effect on the intact loop.[19] The unbalanced secondary sides caused a nonuniform loop flow in the primary system.

4.6.2.2 Nonuniform Loop Flow in OTSG Plants. Experimental evidence indicates that flow instability is common during two-phase natural circulation in OTSG plants. Section 2 discussed the unsteady (intermittent) circulation exhibited in OTSG plants during two-phase natural circulation. The discussion in Section 2 was based on results observed in the OTIS facility.[28] Similar behavior has also been observed by EPRI/SRI in a test facility modelled after Three Mile Island Unit 2 (TMI-2),[22] in the UMCP facility,[65] and in experiments conducted by Argonne National Lab (ANL).[66,67,68,69] The UMCP facility exhibited an intermittent type circulation described as the Interruption-Resumption Mode (IRM).[65] In the EPRI/SRI facility, natural circulation flow changed from a stable to an oscillatory mode at 90% mass inventory.[22] Figure 4-14[22] shows temperature traces at the 90% mass inventory level. The two-phase flows were described as near-single-phase-stable (NSPS) and near-single-phase-oscillatory (NSPO). In the NSPS mode, the core flow is approximately constant; and in the NSPO mode, the two loop flows are in phase and produce oscillatory core flow. At a primary mass inventory of 77%, the two-phase natural circulation was still oscillatory. At 69% inventory, the system settled into a different oscillatory pattern and a slightly higher frequency than the NSPO mode. This latter mode was called very-large-peak-flow (VLPF) natural circulation.[22] Figure 4-15 shows the temperature traces through the 77% and 69% mass inventory periods of time.[22] It is clearly shown that during the VLPF period the two loops were no longer in unison. Thus, nonuniform, unsteady loop flow occurred during the VLPF period.

Alternate flow paths is another potential mechanism for flow irregularity. Reference 65 calls this type of nonuniformity Multi-Channel Instability. In the UMCP facility, alternate flow paths include two complete loops each consisting of two cold legs. Other paths are from the vessel to the upper regions of the downcomer through the reactor vessel vent valves.[65] Thus, several equivalent energy removal flow states can exist and unstable flow can occur when transitions between these flow states are possible.[65]

A third source of nonuniformity in loop flow in OTSG plants is due to flow geometry effects.[65] For example, manometric oscillations between connected liquid legs can be caused when voids form because of primary mass inventory depletion.[65] Manometric type oscillations have been observed in the UMCP facility,[65] the MIST facility,[56] and in experiments conducted by ANL.[66]

4.6.3 Summary of Nonuniform Flow Effects

In summary, nonuniform and nonsteady flows are common in two-phase natural circulation. This includes both nonuniform tube flow in UTSG and nonuniform loop flow in both UTSG and OTSG plants. Investigation of nonuniform primary flow is important for two main reasons: (a) there exists a strong coupling between primary flow and heat transfer during two-phase natural circulation, and (b) flow instabilities may cause operational confusion because most flow instabilities can be observed through temperature and pressure monitors.[65] Therefore, they must be identifiable and understood even if they do not jeopardize adequate core cooling.[65]

In the UTSG plant design, two types of nonuniform flow have been observed in integral test facilities during two-phase natural circulation: nonuniform U-tube flow, and nonuniform loop flow. Types of nonuniform U-tube flow include:

- U-tube flow stall and/or reversal (see Section 3.6)

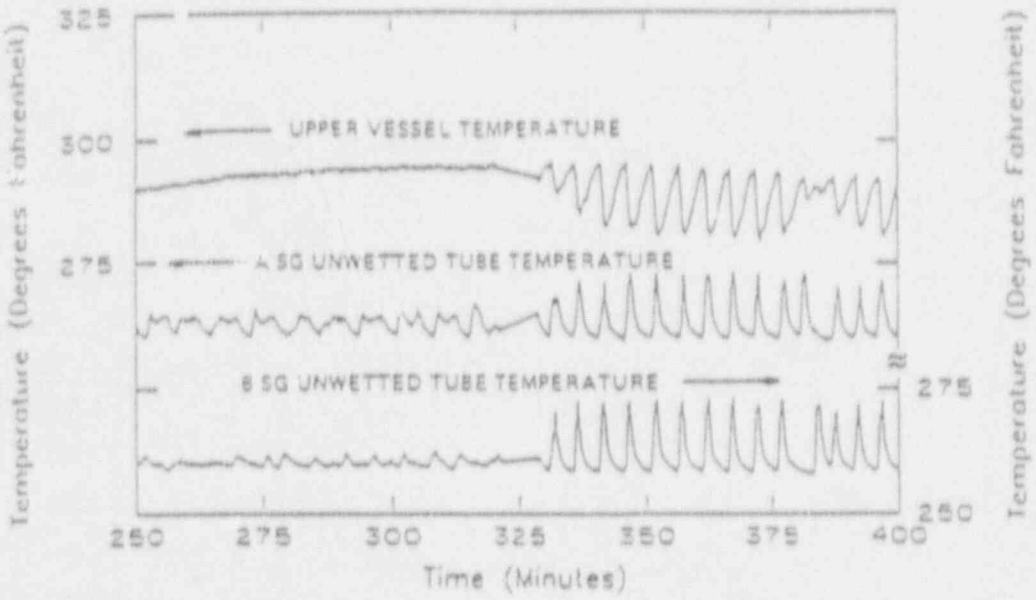

Figure 4-14. Temperature traces during near-single-phase stable and near-single-phase-oscillatory two-phase natural circulation in an EPRI/SIRI test facility.[22]

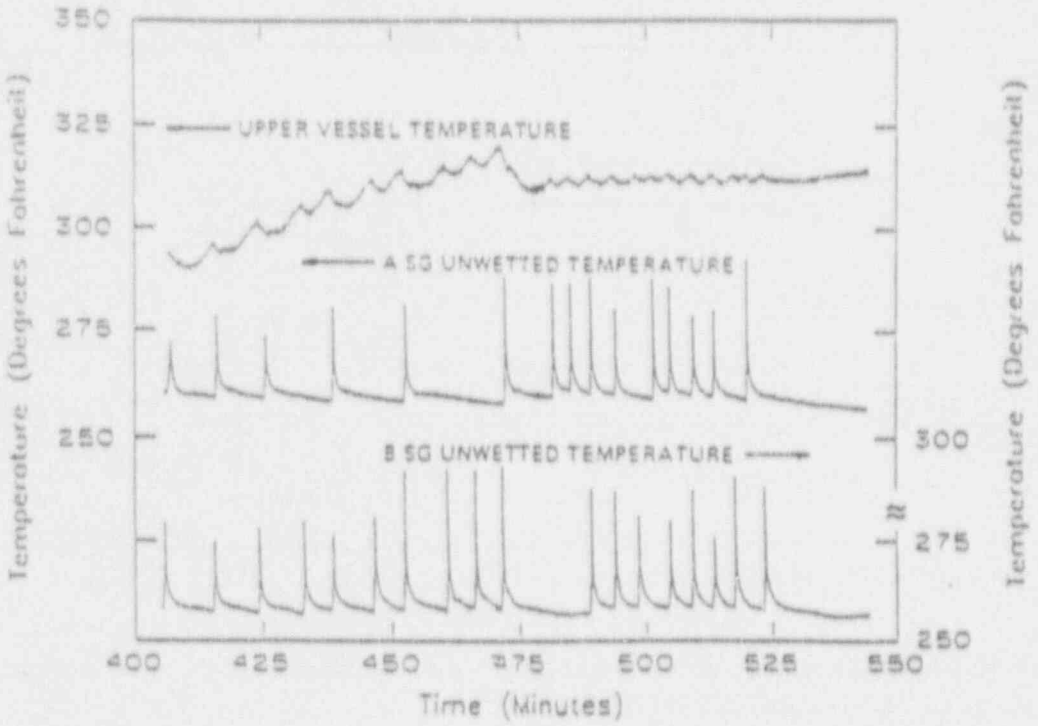

Figure 4-15. Temperatures during very-large-peak-flow mode of two-phase natural circulation in an EPRI/SRI test facility.[22]

- U-tube flow stall caused by noncondensable gas blockages in the steam generator U-tubes (see Section 4.4)
- A cyclic fill and dump flow behavior
- Oscillatory U-tube flow resulting from low secondary liquid levels (see Section 4.5).

Nonuniform flow within a primary circulation loop may be caused by transitions between the different natural circulation modes, unbalanced conditions between different primary circulation loops (i.e., unbalanced secondary conditions), or from nonuniform U-tube flow in one or more primary loops (i.e., cyclic fill and dump behavior).

Nonuniform flow during two-phase natural circulation in plants with OTSG designs results from the following:

- Intermittent circulation (see Sections 2 and 4.2.2).
- Multi-channel instability.
- Flow geometry effects.
- Nonuniform EFW behavior (see Sections 3.5 and 4.5.2).

4.7 Summary

In two-phase natural circulation, vapor is generated in the core and flows along with the saturated liquid to the steam generator where at least some of the vapor is condensed. Density gradients and, hence, the mass flow rate are affected by the presence of voids and by temperature differences in the loop. The most important parameter affecting heat removal from the core during two-phase natural circulation is the loop mass flow rate.

For natural circulation in plants with UTSGs, the mass flow rate in the primary loop reaches its maximum value when voids occupy most of the volume in the upflow sides of the U-tubes, but almost none of the volume in the downflow side. Once voids begin to flow into the downflow side of the U-tubes, the loop mass flow rate decreases. As the primary mass inventory is further reduced, the loop mass flow rate eventually approaches zero and continuous two-phase flow is lost. This defines the transition from two-phase natural circulation to reflux condensation natural circulation.

For plants with OTSGs, flow behavior is similar to that in UTSG plants as long as voids are entrained in the flow and pass into the steam generator tubes. Once voids begin to collect in the upper U-bend region of the hot leg, flow interruption may take place. Depending on conditions in the primary loop and secondary side of the steam generator, flow interruption could last for an extended period of time and/or lead to an intermittent circulation. As primary inventory is lost, two-phase (or intermittent) circulation will be replaced by the boiling condensation mode of natural circulation.

Two-phase natural circulation provides an adequate means of removing decay heat from the core.[55] Because of additional heat transfer through condensation, the required primary-to-secondary temperature difference is not as large during two-phase natural circulation as during single-phase natural circulation.

Correlated expressions for two-phase natural circulation mass flow rate, maximum mass flow rate, and effective overall heat transfer coefficient were presented in Section 4.3.

It was noted in Section 4.4 that noncondensable gases can produce flow stalling in some U-tubes in plants with UTSGs, and can reduce the flow rates in plants with both UTSGs and OTSGs, if present in significant quantities. When noncondensable gases caused complete flow stall during two-phase natural circulation tests, subsequent increases in pressure were observed to compress noncondensable gas blockages so that the natural circulation flow could restart. In comparison with single-phase natural circulation, two-phase natural circulation was found to be more tolerant of noncondensable gases. The effects of noncondensable gases were summarized in Section 4.4.3.

Conditions in the secondary sides of the steam generator can affect primary conditions in two-phase natural circulation. At secondary mass inventories below 50% of normal, oscillatory and/or nonuniform behavior in the primary loop can result. Also, actions of the secondary side feedwater and relief valves can affect primary loop conditions. During two-phase natural circulation, nonuniform and nonsteady flows frequently occur in UTSGs and also in the primary loops of both types of plants. The different types of nonuniform flow behavior occurring in UTSG and OTSG plant designs were summarized in Section 4.6.3.

In summation, two-phase natural circulation behavior can be much more complicated than single-phase natural circulation behavior because of the large number of two-phase flow patterns that can occur within the primary loop.

5. REFLUX CONDENSATION/BOILING CONDENSER NATURAL CIRCULATION

5.1 Introduction

The single- and two-phase modes of natural circulation were discussed in Sections 3 and 4. The third mode of natural circulation occurs when the flow through the steam generators is no longer a continuous two-phase mixture. The fluid distribution is characterized primarily by vapor in the upper elevations of the loop and liquid in the lower loop elevations. The vapor generated in the core flows through the hot legs and is condensed in the steam generators. This type of natural circulation is called either the reflux condensation or boiler condenser mode, depending on the type of steam generator. Reflux condensation refers to plants with UTSGs. The boiler condenser mode (or boiling condensation mode) applies to plants with OTSGs. Reflux/boiling condensation has been demonstrated as a viable means of decay heat removal in several integral test facilities.[20,24,28,40,55,56]

The general characteristics of the reflux/boiling condensation modes of natural circulation are discussed in Section 5.2. Sections 5.3 through 5.6 address analytical expressions used to describe reflux/boiling condensation, the influence of noncondensable gases, the effects due to conditions in the secondary sides of the steam generators, and non-uniform flow, respectively. The observations and conclusions concerning this mode of natural circulation in PWRs will be summarized in Section 5.7.

5.2 General Characteristics

Section 2 briefly described the general phenomena associated with the reflux condensation and the boiler condenser modes of natural circulation. This section will focus on the observed general characteristics exhibited by these natural circulation modes.

The flow phenomena associated with these two modes of natural circulation differ, so each will be addressed separately. However, the two modes do share similar characteristics. For example, during both reflux and boiling condensation, primary-to-secondary heat transfer is accomplished through vapor condensation in the steam generators. This heat transfer is very effective due to the high latent heat associated with condensation. Consequently, removal of decay heat from the core during reflux/boiling condensation does not require large mass flow rates or large primary-to-secondary temperature differences. Small mass flow rates and primary-to-secondary temperature differences are characteristic of both the reflux condensation and the boiler condenser modes of natural circulation.

5.2.1 Reflux Condensation, UTSG Plants

In plants with UTSGs, reflux condensation occurs when single-phase vapor generated in the core flows through the hot leg piping to the UTSGs, and is condensed in both the upflow and downflow sides of the steam generator U-tubes. Condensate in the upflow sides of the steam generator U-tubes drains back to the hot leg and eventually back to the vessel along the bottom of the hot leg. A counter-current flow of liquid and vapor exists in the upflow sides of the steam generator U-tubes and in the hot leg. Condensate in the downflow sides flows into the cold leg pump suction piping cocurrently with any uncondensed steam. The reflux condensation process (showing liquid distribution) is depicted in Figure 5-1.[63]

Figure 2-3 is a flow map of PKL natural circulation data.[23,70] This figure illustrates the characteristic small mass flow rates and primary-to-secondary temperature differences exhibited by reflux condensation, as compared with the single- and two-phase modes of natural circulation. Additionally, during normal reflux condensation, there is no temperature difference between the steam generator inlet and outlet plena.[33]

In the absence of noncondensable gases and for normal secondary side conditions, experiments have demonstrated an equal split of condensate in the upflow and downflow sides of

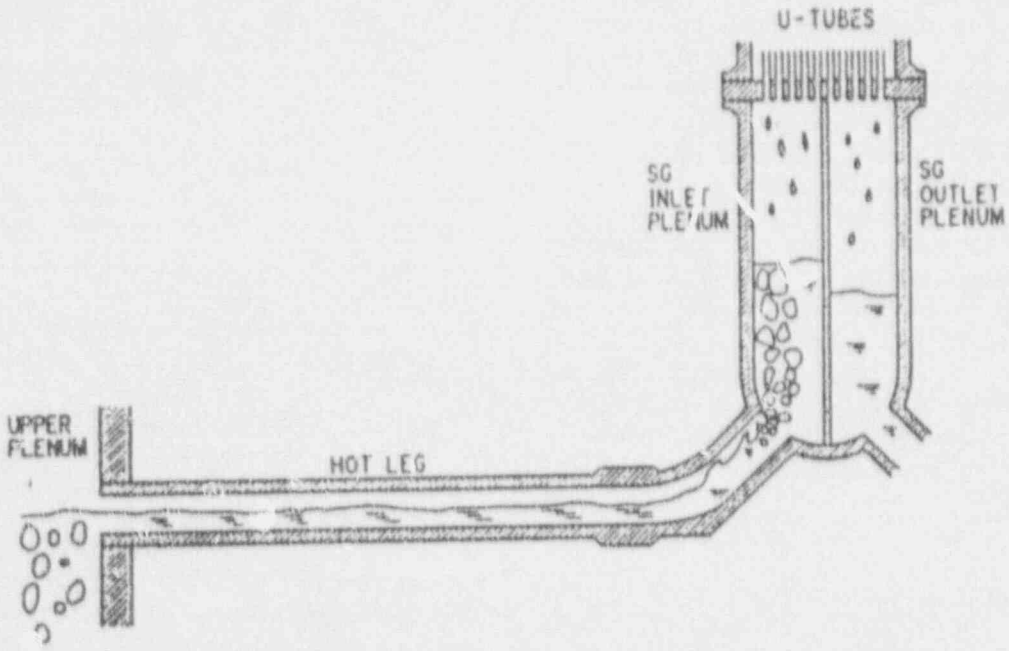

Figure 5-1. Schematic of liquid distribution during reflux condensation.[63]

the steam generator U-tubes.[20,24] This phenomena is depicted in Figure 2-4 for a single U-tube. Vapor condenses all along the inner surface of the steam generator U-tubes and then drains into the steam generator inlet and outlet plena. The equal condensation split appeared to be independent of core power, secondary inventory, and primary inventory in Semiscale experiments.[20] The independence from core power is especially interesting, considering that significantly different U-tube flow behavior occurs between low and high decay heats. At approximately 1.5% decay heat, the U-tubes were vapor filled with a film-wise condensation, while at approximately 3.0% decay heat, liquid holdup (due to flooding effects) occurred in some U-tubes.[20]

During reflux condensation natural circulation, the condensate draining back to the core provides little cooling compared with the boiling and subsequent condensation in the steam generators. The important contribution made by the liquid fall-back to the vessel is in providing circulation to maintain a two-phase froth level that covers the core.[20]

Following continuous two-phase natural circulation, liquid in the steam generator U-tubes will drain into the steam generator plena. In the upflow sides of the steam generator U-tubes, the liquid must drain against a steam counterflow. The rate of liquid drain from the upflow sides of the steam generator U-tubes may be limited by the interphase drag force. Such a restriction is termed counter current flow limitation (CCFL) or flooding. Flooding generally occurs at flow area restrictions or at locations where flow changes direction. Natural circulation experiments in tests modeling UTSGs have shown flooding at the hot leg bend[63,71,72] and at the U-tube inlet.[26,51,57,63,73,74] The results of these experiments are discussed in greater detail in Section 5.6.

Physically, flooding (also referred to as CCFL) is the limiting condition where the flow rates of both the vapor and the liquid cannot be increased further.[75] Thus, for a given upward flow of vapor, there is a maximum downward flow of liquid, above which the liquid cannot flow through the passage. Conversely, for a given downward flow of liquid, there exists a maximum upward flow of vapor, above which the vapor cannot flow through the passage.[75] The locus of these points forms an envelope of all the maximum flow rates of the two-phase flow system.[75] Numerous experimental and analytical studies have proposed correlations to predict this behavior for a wide range of fluid properties and test conditions.[74 - 95]

The Wallis correlation is a well known, commonly used flooding correlation expressed as[75,76]

$$(j_g^*)^{\frac{1}{2}} + m(j_f^*)^{\frac{1}{2}} = c_j, \qquad (5\text{-}1)$$

where

$$j_f^* = \left[\frac{j_f^2\,\rho_f}{g\,D\,(\rho_f - \rho_g)}\right]^{\frac{1}{2}} \qquad (5\text{-}2)$$

$$j_g^* = \left[\frac{j_g^2\,\rho_g}{g\,D\,(\rho_f - \rho_g)}\right]^{\frac{1}{2}} \qquad (5\text{-}3)$$

and

j_f = liquid superficial velocity $\left(j_f \equiv \frac{Q_f}{A}\right)$

j_g = vapor superficial velocity $\left(j_g \equiv \frac{Q_g}{A}\right)$

Q_f = liquid volumetric flow rate

Q_g = vapor volumetric flow rate

ρ_f = fluid density

ρ_g = steam density

D = U-tube pipe diameter

g = acceleration due to gravity

m = gas intercept ($j_f = 0$) divided by liquid intercept ($j_f = 0$). For turbulent flow, $m = 1.0$[76]

c_j = correlation parameter (c_j = 0.70 - 1.0)

h_{fg} = latent heat of vaporization.

Another widely accepted correlation is that proposed by Kutateladze[95] for total flooding (i.e., zero liquid downflow). This correlation assumes a constant value for the Kutateladze number, K_g, defined as

$$K_g = \left[\frac{j_g^2 \rho_g}{\sqrt{g\sigma}\sqrt{\rho_f - \rho_g}} \right]^{\frac{1}{2}} \qquad (5\text{-}4)$$

where σ is the surface tension. The constant value of K_g has been determined empirically to range between 1.8 and 3.2.[81] An additional correlation based on the Kutateladze number, in a form analogous to Equation 5-1, has been proposed by Tien[87]

$$(K_g)^{\frac{1}{2}} + m(K_g)^{\frac{1}{2}} = c_j \qquad (5\text{-}5)$$

where m and c_j are empirically determined correlation parameters. Equation 5-5 has been used to predict flooding with considerable success.[93]

Both the Wallis and Kutateladze correlations have general utility and wide acceptance.[75] Generally, use of the Wallis correlation is preferred when the value of the dimensionless diameter or Bond number (Bo), defined as

$$Bo = D\left(\frac{g(\rho_f - \rho_g)}{\sigma}\right)^{\frac{1}{2}}, \qquad (5\text{-}6)$$

is less than approximately 30. For larger values of the Bond number, the Kutateladze correlation should be used.[77,81]

5.2.2 Boiling Condensation, OTSG Plants

The boiler condenser (boiling condensation) mode of natural circulation occurs in OTSG plants. The discussion in Section 2 noted that during this mode of natural circulation, vapor generated in the core flows through the hot legs to the OTSGs and is condensed in the vertical steam generator tubes. Because of the plant geometry (see Section 2) there is no counterflow of steam and condensate in the hot leg. Steam and condensate flow cocurrently through the steam generator tubes into the cold leg suction piping. Boiling condensation is depicted in Figure 2-8.

There are two types of boiling condensation modes in plants with OTSGs. Pool boiling condensation occurs when the primary side vapor is adjacent to the secondary side liquid, or pool. Thus, pool boiling condensation requires a primary liquid level that is below the secondary liquid level. EFW boiling condensation occurs when the primary side steam is condensed by EFW sparger spray near the top of the OTSG. Experiments in the OTIS and MIST facilities confirmed that both types were effective in decay heat removal.[28,56] EFW boiling condensation for a single tube is depicted in Figure 2-9. Note that the radial, axial, and azimuthal penetration of EFW under vapor upflow conditions is much more complicated than Figure 2-9 depicts. The actual flow distribution is strongly dependent upon the EFW flow rate.[29,30] Flooding at the tube support plate in the secondary side of the OTSG also has a significant influence on the AFW fluid distribution.[29,30]

5.3 Analytical Expressions

5.3.1 Mass Flow Rate and Inventory Fraction

Duffey and Sursock[21] derived mass flow and inventory fraction expressions for all three modes of loop natural circulation, assuming that the transients under consideration were quasi-steady. The lower limit of the loop flow

rate occurs when the reflux condensation mode of natural circulation exists. This minimum theoretical mass flow rate is due to the heat input, and is given by the following expression[21]

$$W_{rc} = \eta \frac{P}{h_{fg}} \qquad (5\text{-}7)$$

where

W_{rc} = loop mass flow rate for reflux condensation

P = power

h_{fg} = latent heat of vaporization

η = efficiency (0.50) to account for heat losses.

As primary mass inventory is lowered until reflux condensation is just established, the net loop flow approaches zero. Because the static heads are nearly equal for the hot and cold sides and the temperatures equal to the saturation temperature, the inventory fraction, I_{rc}, at the start of reflux condensation can be given by[21]

$$I = I_{rc} = 1 - \alpha_1(V_1) - \alpha_2(V_2) \approx 1 - \alpha_1(V_1 + V_2) \qquad (5\text{-}8)$$

where

α_1 = void fraction for the core, steam generator hot side, upper plenum, and hot leg

α_2 = void fraction for the steam generator cold side (downside), pump, and downcomer. Note $\alpha_1 \approx \alpha_2$ for reflux condensation

V_1 = fractional volume for "hot" region

V_2 = fractional volume for "cold" region.

5.3.2 Overall Heat Transfer Coefficient (USTG)

The effective overall primary-to-secondary heat transfer coefficient, K_e, during reflux may be defined as[42]

$$Q = K_e F R \Delta T \qquad (5\text{-}9)$$

where

ΔT = steam generator primary-to-secondary temperature difference (saturation temperatures)

Q = total heat transfer rate

F = total heat transfer area of the steam generator U-tubes (based on the inner U-tube diameter)

R = ratio of the heat transfer area below the collapsed liquid level to the total heat transfer area.

Effective heat transfer coefficients were obtained from LSTF experiments for reflux condensation at 5% and 2% core powers. These results are plotted in Figure 3-5. The results imply that the effective heat transfer coefficients are nearly independent of the collapsed liquid level on the secondary side.[42]

5.3.3 Transitions Between Different U-tube Flow Modes

University of California at Santa Barbara (UCSB) studies have investigated different U-tube flow modes.[25,73,96,97,98] Three basic U-tube flow patterns have been identified by UCSB studies in an inverted U-tube heat exchanger.[25] The flow patterns observed were called classical reflux condensation, the oscillatory mode, and the carryover mode.[25] These flow patterns are illustrated in Figure 5-2. The characteristics of each flow mode are discussed in greater detail in Section 5.6. Criteria for the transition between

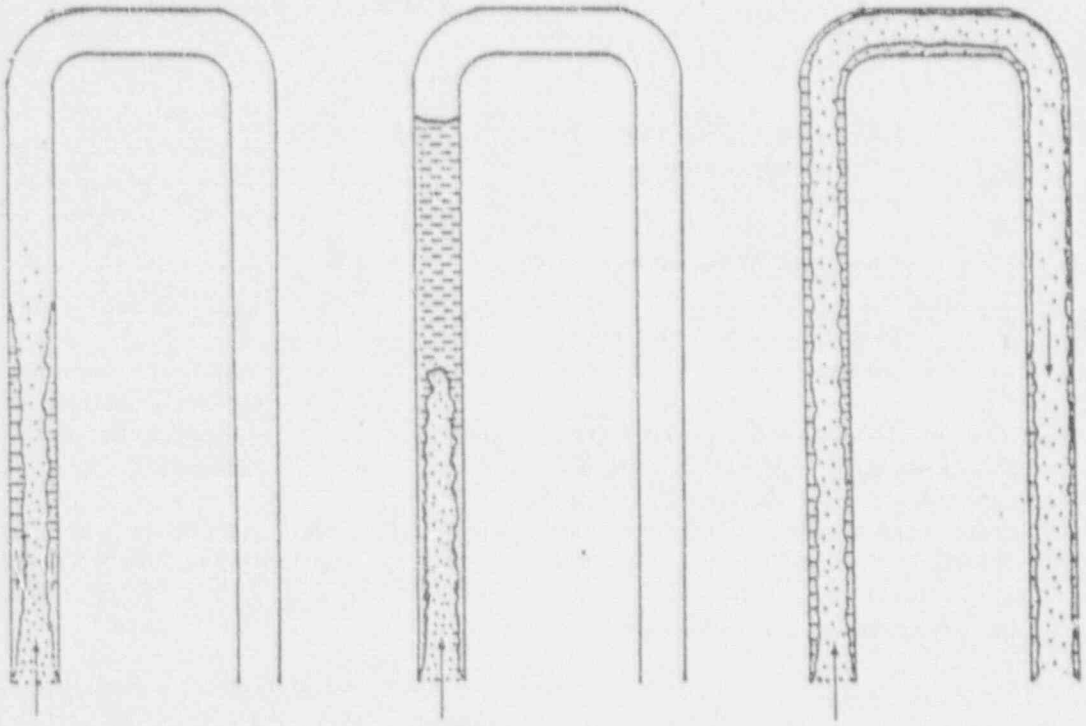

Reflux condensation Oscillatory Carryover

Figure 5-2. Different two-phase U-tube flow patterns.[73]

reflux condensation and the oscillatory flow pattern was quantified by a Wallis-type flooding correlation. The transition between the oscillatory and the carryover modes was shown to be in reasonable agreement with derived correlations using two different dimensionless vapor velocities.

5.3.3.1 Transition to the Oscillatory Mode. The transition from classical reflux condensation to an oscillatory flow pattern can be set at the U-tube flooding limit. The Bond number, Bo, in the University of California at Santa Barbara experiments was approximately 6. Because the Bond number was less than 30 (see Section 5.2.1), the use of a Wallis-type flooding correlation to predict the U-tube flooding limit was justified.[77,81] The general form of the Wallis flooding correlation is described in Section 5.2.1 (Equations 5-1 through 5-3). UCSB experimental data support the following flooding correlation to signal the transition from the reflux mode to the oscillatory mode in U-tubes,[25]

$$(j_g^*)^{\frac{1}{2}} + (j_f^*)^{\frac{1}{2}} = 0.8 \qquad (5\text{-}10)$$

Note that the tube diameters in the UCSB experiments [16 mm I.D. (0.629 in.)] are comparable to those of most steam generator U-tubes [18 mm I.D. (0.69 in.)], so that similar transitional flooding characteristics would be expected.[25]

Based on Equation 5-10, the transition to the oscillatory mode, with no liquid downflow, occurs when

$$j_g^* = 0.64. \qquad (5\text{-}11)$$

An expression for the core power in terms of j_g^* can then be used with Equation 5-11 to calculate the core power that initiates the transition to the oscillatory mode. Assuming all core power goes to vaporization (i.e., no subcooling), then

$$j_g = \frac{P_w}{\rho_g A h_{fg}}. \qquad (5\text{-}12)$$

Substituting Equation 5-12 into Equation 5-3 and solving for the core power gives

$$P_w = \rho_g A h_{fg} j_g^* \sqrt{\frac{gD(\rho_f - \rho_g)}{j_g^2 \rho_g}} \qquad (5\text{-}13)$$

Thus, assuming no liquid downflow, the substitution of 0.64 for j_g^* in Equation 5-13 yields the core power that initiates the transition from classical reflux condensation to the oscillatory mode.

Consider a sample 4-loop W-type PWR with a rated power of 3411 MW. Assume there are 5626 U-tubes per steam generator and each U-tube has an inner diameter of 0.0175 m (0.688 in.). Table 5-1 indicates the core power values necessary to initiate the transition to the oscillatory mode in the steam generator U-tubes under two different primary conditions. In Table 5-1, an active loop refers to one in which the steam generator is capable of removing decay heat. It is assumed that no flow passes through an inactive loop, and that there is no liquid down-flow in the upflow sides of the steam generator U-tubes.

The distinctive characteristic of the oscillatory mode is the liquid holdup and subsequent liquid column buildup.[25] The liquid column in the riser part of the U-tube exerts a back pressure on the core, reducing the amount of liquid available for core cooling. The UCSB research included the development of an analytical model for the U-tube liquid column buildup. It was noted in Reference 25 that additional validation of this model is needed, especially under conditions of high primary pressures.

A space and time averaged two-fluid model was also derived in Reference 25. This model calculated the wall and interfacial shear stresses, using the averaged measurements of the two-phase condensation region below the liquid column in the upflow side of the U-tube. An interfacial shear stress model, called the slug-churn model, was developed by UCSB by modifying the model in RELAP5. This model was based partially on experimental observation. The calculated shear stresses showed good agreement with the empirical results.[25]

Table 5-1. Calculated required core power for transition to the oscillatory mode in steam generator U-tubes in a sample PWR plant design (two primary conditions).

Pressure	Number of Active Loops	j_g^*	Power (MW)	Percent of rated plant power
7.0 MPa (1015 psia)	4	0.64	346	10.2
7.0 MPa (1015 psia)	1	0.64	86.4	2.56

5.3.3.2 Transition to the Carryover Mode. The transition between the oscillatory mode and the carryover mode occurs when the vapor velocity is sufficiently high to initiate and sustain a cocurrent flow of vapor and condensate over the U-tube U-bends.[25] Correlations used by UCSB to define the transition to the carryover mode include the nondimensional superficial vapor velocity and the Kutateladze number defined in Section 5.2.1. UCSB experiments discovered that the carryover mode is associated with relatively high vapor velocities. The carry-over mode is characterized by the following ranges for the dimensionless parameters j_g^* and K_g:

$$0.75 < j_g^* < 1.2 \text{ and } 1.9 < K_g < 3.1.$$

The transition to the carryover flow mode in all the steam generator U-tubes may signal a transition to the continuous two-phase mode of natural circulation.

Assuming all the core power goes to vaporization, Equation 5-4 and Equation 5-12 can be used to obtain the following expression for the core power in terms of K_g

$$P = \rho_g A h_{fg} K_g \left[\frac{g\sigma(\rho_f - \rho_g)}{\rho_g^2} \right]^{1/4} \qquad (5\text{-}14)$$

Tables 5-2 and 5-3 use Equations 5-13 and 5-14, respectively, to calculate (for the sample PWR, Section 5.3.3.1) core powers necessary to initiate the transition to the carryover mode in the steam generator U-tubes.

5.4 Effects of Noncondensable Gases

The effect of noncondensable gas on condensation heat transfer can be significant. A considerable amount of literature is devoted to this subject. Section 5.4.1 presents a very brief overview and discussion of issues associated with condensation in the presence of noncondensable gases. This information is intended to establish a foundation for subsequent discussions in Sections 5.4.2 and 5.4.3, concerning noncondensable gas effects on reflux condensation in plants with UTSGs and boiling condensation in plants with OTSGs, respectively.

The behavior of plants with UTSGs during reflux condensation is significantly different from the behavior of plants with OTSGs during the boiler condenser mode. The primary concern regarding noncondensable gases during reflux condensation in plants with UTSGs is that gases will accumulate in the steam generator U-tubes and disrupt the condensation of steam from the core. Noncondensable gas experiments have been conducted at Semiscale,[19,24] PKL,[23,99] and FLECHT-SEASET[49] facilities, and by EPRI/ SRI.[100] Important phenomena discovered in these experiments are discussed in Section 5.4.2.

In the case of a OTSG plant, the main question is whether steam generated in the core can reach a condensing surface in the steam generators. Experiments addressing this issue

Table 5-2. Calculated required core power for transition to the carryover mode in steam generator U-tubes in a sample PWR plant design (based on j_g^*).

Pressure	Number of Active Loops	j_g^*	Power (MW)	Percent of rated plant power
7MPa (1015 psia)	4	0.75 - 1.2	406 - 650	12 - 19
7MPa (1015 psia)	1	0.75 - 1.2	101 - 162	3.0 - 4.8

Table 5-3. Calculated required core power for transition to the carryover mode in steam generator U-tubes in a sample PWR plant design (based on K_g).

Pressure	Number of Active Loops	K_g	Power (MW)	Percent of rated plant power
7MPa (1015 psia)	4	1.9 - 3.1	439 - 716	13 - 21
7MPa (1015 psia)	1	1.9 - 3.1	110 - 179	3.2 - 5.2

have been performed at MIST[56] and by EPRI/SRI in a test facility modeled after TMI-2.[59] The influence of noncondensables on the boiler condenser mode is addressed in Section 5.4.3.

5.4.1 Condensation in the Presence of Noncondensable Gases

The effect of noncondensable gas in reducing heat flux during condensation is well known,[78,97,101-111] and the literature pertaining to this topic is quite large. This section does not provide an exhaustive review of this subject. Rather, its purpose is to introduce important issues and establish a link with the broader literature. A large proportion of the research investigating condensation in the presence of noncondensables has studied natural convection along vertical plates, or cylinders immersed in a vapor-gas mixture.[106-111] A limited amount of research has investigated condensation in tubes with noncondensables present. These studies include experimental and analytical investigations of gas-loaded heat pipes,[102-105] closed thermosyphons,[78] and U-tube type heat exchangers.[101] The phenomena exhibited in these simpler problems will likely occur in PWR natural circulation loops. Therefore, understanding these phenomena is an important step in successfully modeling the effects of noncondensable gases during natural circulation in PWR loops.

Researchers investigating condensation in the presence of small amounts of noncondensable gas (homogeneous vapor-gas

mixtures) have observed reductions in the heat transfer rate of 50% or more.[106,107,111] These investigations included natural convection along vertical plates and cylinders immersed in a vapor-gas mixture. Analytical studies of natural convection along a vertical plate in the presence of noncondensables have agreed well with experimental data.[108,109,110]

Physically, condensation heat transfer degradation is due to a buildup of noncondensable gas along the condensing surface. Non-condensables are swept along with the vapor to the condensing surface where the vapor is condensed from the vapor-gas mixture, leaving the noncondensables behind. The partial pressure of the vapor near the condensing surface is thereby reduced (according to Dalton's Law), due to the resulting high concentration of noncon-densable gas. This, in turn, lowers the saturation temperature of the vapor; and, hence, the thermal driving force for condensation is reduced. In this manner, the noncondensable gas concentration and the vapor partial pressure control the condensation heat transfer rate.[109]

Mori et al. observed that a homogeneous vapor-gas flow is difficult to maintain when large differences exist between the molecular weights of the vapor and the gas.[106] Noncondensables were separated from the vapor and deposited at a given location in the test apparatus.[106] Thus, the system geometry has a significant influence on the condensation process when noncondensable gases are present. Note that larger heat fluxes were found in the case of vapor and gas separation as opposed to the case of a homogeneous vapor-gas mixture.

Hein et al. investigated experimentally and analytically the condensation of steam in a U-tube type heat exchanger in the presence of noncondensable gas.[101] In this experiment, noncondensable gas was injected, in the form of a plug, into a steam filled system in four discrete steps.[101] The researchers observed that the region upstream of the gas plug was cut off from the steam supply. The temperature in this region cooled to the secondary temperature causing a pressure difference across the gas plug that pushed it towards the U-tube exit. This behavior eventually yielded a steady state where the U-tube was divided into what was called 'active' and 'passive' zones, separated by a transition region.[101] In the active zone, which extended from the U-tube inlet to the transition region, condensation was virtually unaffected by the noncondensable gas. In the passive zone, condensation did not occur because the steam and noncondensable gas mixture was at the secondary side saturation temperature, with the partial pressure of the steam equal to the pressure of the secondary side. This same behavior was observed with both nitrogen and helium as the noncondensable gas.[101] The noncondensable gases effectively reduced the available heat transfer area. Consequently, a higher primary-to-secondary temperature difference was necessary to condense the incoming steam. The developed analytical model agreed well with the experimental data.[101]

Hein et al. concluded that the nature of the gas (either nitrogen or helium) was only relevant in the transition region between the active and passive zones.[101] Significantly different behavior was exhibited in this region for the two different noncondensable gases used. A short, stable transition region with a step-wise change in temperature resulted when the buoyancy and shear forces exerted on the gas acted in the same direction. When these forces acted in opposite directions, an extensive transition zone with oscillating temperatures was observed.[101] For instance, assume the transition region is in the up-flow section of the U-tube and nitrogen is the noncondensable gas (heavier than steam); vapor flow is directed upward while the buoyancy force is directed downward, resulting in an unstable transition zone.

Similar behavior was observed by Tien et al. in a condensation experiment in a closed thermo-syphon with noncondensables.[78] In this experiment, noncondensable gases were swept along with the steam flow to the condenser end of the thermosyphon. This process resulted in a high concentration of noncondensable gases along part of the condenser, which effectively formed a diffusion barrier to condensation in that region. This analytical and experimental study demonstrated that concentration and temperature induced natural convection of noncondensable gases

can affect condensation efficiency by influencing the noncondensable gas distribution. It was deter-mined that radial diffusion of the noncondensable gas also strongly influences the noncondensable gas distribution.[78]

Some of the important issues that influenced the condensation processes in the preceding investigations are summarized as follows:

- Buoyancy forces, including those associated with both temperature and concentration gradients
- Variation in thermodynamic and transport properties of the vapor-gas mixture
- Interfacial resistance (However, Reference 109 concluded this parameter was a second order effect)
- System pressure level
- Amount of vapor superheat
- Diffusion
- System geometry
- Molecular weights of vapor and gas
- Amount of noncondensable gas and the manner in which it was introduced into the test apparatus.

5.4.2 UTSG Plants

The following general effects of noncondensable gases have been exhibited in experimental investigations conducted at the Semiscale facility,[19,24,60] the PKL facility,[23,99] the FLECHT-SEASET facility,[49] and by EPRI/SRI:[100]

- The condensation of vapor from the core is shifted to the upflow sides of the steam generator U-tubes
- Noncondensable gas is deposited in the downflow sides of the steam generator U-tubes, the steam generator exit plenum, and above the loop seal liquid vapor interface
- The steam generator is divided into active and passive zones, thereby reducing the total available heat transfer area
- When large amounts of noncondensable gases exist in the steam generator U-tubes, the active zone in the steam generator is confined to a short distance above the tube sheet along the upflow side of the steam generator U-tubes
- If steam is unable to reach a condensing surface in the steam generator U-tubes because of gas blockages, the system pressure will rise to compress the noncondensable gas volume until an adequate condensing surface is exposed in the lower portions of the upflow sides of the steam generator U-tubes
- Condensation effectiveness in a given region, is decreased by the presence of noncondensable gases. Therefore, a larger primary-to-secondary heat transfer area is needed to remove the core decay heat.

The Semiscale MOD-2A noncondensable gas experiments (S-NC-6a and 6b) were conducted at high temperature and pressure [6.1 to 11.1 MPa (884.5 psi to 1609.5 psi).[60] Nitrogen gas was injected in discrete amounts (up to 6.34% of the system volume at system temperature and pressure). The decay heat was 1.5% of core power and the primary mass inventory was 57%. Prior to the initial nitrogen gas injection, an equal condensation split existed between the upflow and downflow sides of the steam generator U-tubes. The first nitrogen injection resulted in a condensation shift to the U-tube upflow sides, and this condensation distribution was sustained for all subsequent gas injections. This phenomenon is demonstrated in Figure 5-3, which shows the reflux rate as a function of the nitrogen injection as a percent of the total system volume.[60] Though the area available for heat transfer in the steam generator U-tubes was reduced, the overall primary-to-secondary heat removal rate did not change and the steam generator continued to act as an effective heat sink.[60]

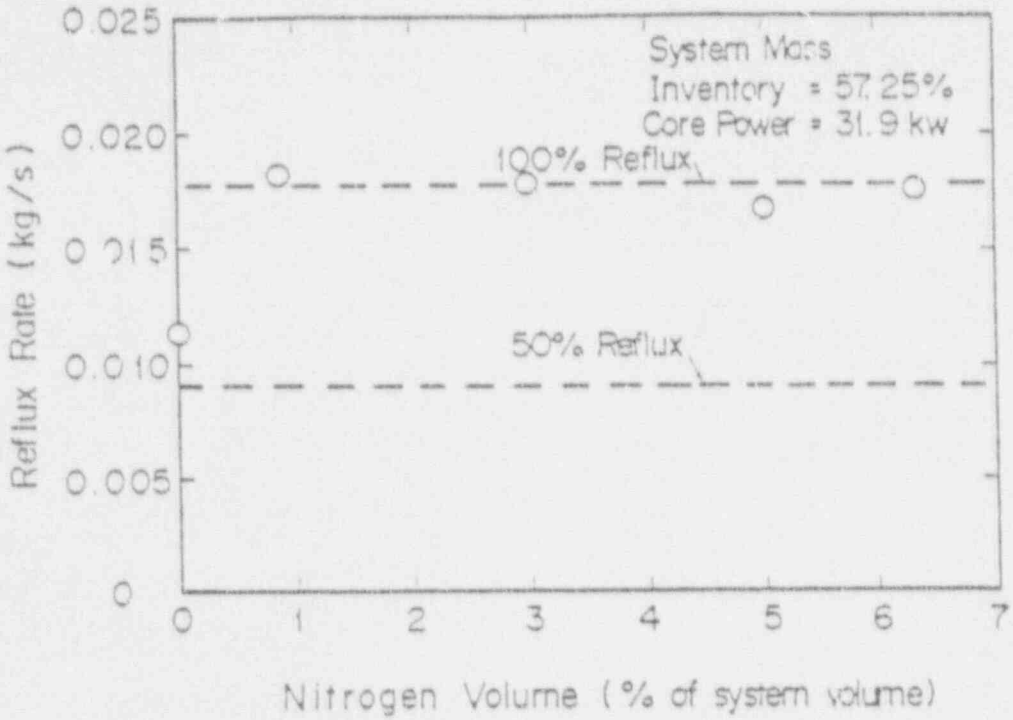

Reflux rate ∫ Amount of steam that is condensed in the SG U-tube upflow sides and flows back to the vessel.

100% reflux ∫ 100% of the steam generated in the vessel is condensed in the upflow sides of the SG U-tubes and flows back to the vessel.

50% reflux ∫ 50% of the steam generated in the vessel is condensed in the upflow sides of the SG U-tubes and flows back to the vessel (equal condensation split between U-tube upflow and downflow sides).

Figure 5-3. Hot Leg reflux rate as a function of nitrogen injection in the Semiscale MOD-2A facility.[60]

EPRI/SRI tests concluded that the amount of noncondensable gases that could be accommodated by the primary system is limited only by the design pressure of the system, provided secondary cooling is available.[100] This low pressure (< 0.52 MPa (75 psi)) experiment consisted of discrete helium gas injections (up to 60% system volume) into the primary system during the reflux condensation mode. The decay heat was approximately 1% and the primary mass inventory approximately 20%. The primary system was observed to be highly tolerant of noncondensable gases. Adequate core cooling was possible with reflux condensation even with significant amounts (up to 60 % of the system volume) of noncondensable gases.[100]

The low-pressure [0.965 MPa (140 psi)] PKL experiment demonstrated that at 2.4% decay heat, an increase in the primary-to-secondary temperature difference from 2K to 8K was necessary to remove the decay heat because of nitrogen gas in the steam generator U-tubes.[99] The nitrogen gas effectively reduced the available heat transfer area.

Experiments in the low pressure FLECHT-SEASET facility identified additional problems associated with noncondensable gases (helium) in the steam generator U-tubes.[49] At a mass inventory between 35% to 40% and a core power of approximately 2%, flooding and consequent liquid holdup was possible at the steam generator U-tube inlet. Hochreiter and Rupprecht determined that noncondensable gases in the steam generator U-tubes enhanced the liquid holdup effect because more condensation was forced to occur in the upflow sides of the steam generator U-tubes.[49] Thus, more condensate must drain from the U-tubes opposing the flow of steam from the core. It was also observed that helium gas aggravated loop seal depression effects on the core. The helium gas increased the back pressure on the core liquid level and extended the venting period of gas through the loop seal, prolonging core level depression. These phenomena are discussed in greater detail in Section 5.6.

5.4.3 OTSG Plants

There are few experimental investigations that studied the effects of noncondensable gases on the boiling condensation mode of natural circulation. High pressure, cold leg break tests were performed in the MIST facility[56] and low-pressure experiments were conducted by EPRI/SRI in a facility modeled after TMI-2.[59] The results of these experimental investigations are discussed in this section.

It was found by EPRI/SRI that noncondensable gases in the steam generators dictated the elevation of the condensation region in the OTSGs. High concentrations of noncondensable gas (nitrogen) accumulated above the primary side steam generator liquid level. Noncondensables were swept along (with the steam) to the steam generators where the steam was condensed from the steam-gas mixture leaving the noncondensable gas behind.[59] Noncondensable gas above the primary side liquid level impedes condensation, and may force the condensing region to a higher elevation in the steam generator. This behavior contrasts with the observations in a UTSG, where the condensing region is forced to lower elevations in the upflow sides of the steam generator U-tubes. If the condensing region in the OTSG is forced above the elevation of the secondary pool and EFW is not available, the heat removal ability of the steam generator may be temporarily lost.

However, pressure increases were observed to compress the noncondensable gas volume sufficiently to expose a new condensing surface. These observations led to the conclusion that the pressure limits of the facility determine the amount of noncondensable gas that may be accommodated by the system.[59]

Similar behavior was also observed in the high-pressure MIST facility.[56] Helium gas injection was immediately followed by primary pressure increases. At one point during a transient, the primary steam generator liquid level in one loop was 5 ft below the secondary liquid level with no primary-to-secondary heat transfer, indicating the severe impact that noncondensables can have upon condensation in the steam generator.[56]

MIST tests showed that the behavior using nitrogen gas was nearly the same as for helium

gas, implying that convective effects dominated buoyancy effects.[56]

Thermal stratification on the secondary side can further reduce the effectiveness of boiling condensation in the presence of noncondensables. During boiling condensation, primary-to-secondary heat transfer occurs in the upper elevations of the steam generator above the primary side liquid-steam interface. Because noncondensable gases can drive the condensing region to higher elevations in the steam generator, the secondary liquid is heated at the top and thermal stratification results. Thermal stratification on the secondary side effectively reduces the primary-to-secondary temperature difference, which in turn reduces the primary-to-secondary heat transfer. Increases in the primary temperature are necessary to compensate for the reduced primary-to-secondary heat transfer.

5.4.4 Summary of the Effects of Noncondensable Gases

The effects of noncondensable gases on condensation heat transfer can be profound. Section 5.4.1 presented an brief discussion of important issues and results from research in this subject area. A link with this broader range of literature is important because the use of this body of knowledge will assist efforts to analyze the effects of noncondensable gases during reflux/boiling condensation processes in PWRs.

Section 3.4 listed parameters that influence the effect of noncondensable gases on the single-phase mode of natural circulation. Uncertainties regarding the effects of these parameters are also relevant for the reflux condensation and boiler condenser modes of natural circulation. Until these uncertainties are resolved, a complete understanding of the effects of noncondensable gases will not be possible.

In both OTSG and UTSG plants, the primary system pressure acts as a correcting mechanism to compensate for the adverse effects of noncondensable gases. If noncondensable gas volumes prevent steam condensation, the primary system pressure rises to compress the gas volume and expose an adequate condensing surface. However, the reduced heat transfer area resulting from noncondensables in the steam generator requires larger primary-to-secondary temperature differences. General observations regarding the effects of noncondensable gases on reflux condensation in UTSG plants were listed in Section 5.4.2.

The effects of noncondensable gases are more severe in the case of OTSG plants. The heat sink behavior of the steam generator could be lost if the condensation elevation is driven above the secondary liquid pool elevation. Additionally, thermal stratification of the secondary side liquid may effectively reduce the primary-to-secondary temperature difference (the thermal driving force). In order to compensate for these adverse effects, higher pressure increases may be necessary to sufficiently compress the noncondensable gas volumes and expose an adequate heat transfer surface.

Buoyancy effects between different noncondensable gases and steam may also play a role in determining the effectiveness of reflux/boiling condensation cooling. In test facilities with OTSGs, different behaviors for nitrogen and helium gases were not observed, implying that convective effects dominated buoyancy effects. Hein et al., observed in a single U-tube experiment that the type of noncondensable gas was only significant in the transition region between the 'active' and 'passive' condensation zones of the U-tube. A short, stable transition region resulted when buoyancy and shear forces were in the same direction. Conversely, an unstable transition region resulted when buoyancy and shear forces opposed one another.[101] The significance of these effects is not well understood.

The effects of noncondensable gases on U-tube flooding, consequent liquid holdup, and loop seal depression phenomena are important issues related to UTSG plants. Flooding tendencies are enhanced when noncondensable gases force more condensation to occur in the upflow sides of the steam generator U-tubes. These phenomena are discussed further in Section 5.6.

5.5 Secondary Side Effects

5.5.1 UTSG Plants

Experiments performed in the low-pressure PKL facility investigated the effects of reduced steam generator secondary inventory on the effectiveness of reflux cooling.[23,99] The results indicated that the primary-to-secondary temperature difference doubled (from 2 K to 4 K) when the secondary inventory was reduced to uncover half of the steam generator U-tubes.

Results obtained from the LSTF experiments for an overall heat transfer coefficient, Ke, based upon the effective heat transfer area (see Section 5.3.2), found that Ke was nearly independent of the secondary collapsed liquid level for the reflux condensation mode. For the 5% core power test, Ke varied between 2.2 and 3.4 kW/(m^{2}K) (1256.1 and 1941.2 Btu/(hft^{2}F). During a 2% core power test, Ke varied between 1.5 and 2.5 kW/(m^{2}K) (856.4 and 1427.4 Btu/(hft^{2}F).

The effect of secondary level on the reflux condensation mode was also examined in the Semiscale facility.[19] These data indicate that low secondary levels had little influence on the effectiveness of reflux condensation cooling.

Low secondary inventories or noncondensable gases in the steam generator U-tubes, may promote steam condensation in the lower portion of the U-tubes, near the tube sheet. The secondary side water will be warmed at the bottom, and due to buoyancy, will be well mixed. Therefore, virtually all the secondary side liquid will be available as a reflux cooling heat sink.

5.5.2 OTSG Plants

Section 2 discussed the potential loss of heat sink behavior possible in OTSGs. In contrast to a UTSG, where the secondary liquid is normally available as a reflux cooling heat sink, only the secondary liquid above the steam generator primary level is available to condense steam during the boiler condenser mode, provided EFW sparger spray is not available. EFW sparger spray ensures the existence of a condensing surface high in the steam generators. If EFW is not operable, the secondary pool level must be high enough to provide a condensing surface in the steam generator or boiling condensation cooling will not occur. As a result, the secondary liquid level is an important parameter in maintaining boiling condensation in OTSGs.

As indicated in Section 5.4.3, thermal stratification on the secondary side, in which hotter water resides at the top of the secondary, is an important issue in OTSGs. When the condensing surface is near the elevation of the secondary liquid level, the primary-to-secondary temperature difference in this area will be reduced because of the hotter water at the top of the secondary. The effectiveness of boiling condensation may be diminished as a result of this thermal stratification phenomena.

5.5.3 Summary of Secondary Side Effects

Boiling condensation in plants with OTSGs is more sensitive to secondary side conditions than is reflux condensation in plants with UTSGs. This conclusion follows from the potential loss-of-heat-sink, characteristic of OTSG geometries. The UTSG geometry enables the secondary liquid to act as a reflux cooling heat sink even for low secondary inventories. The effectiveness of boiling condensation without EFW in a OTSG, however, depends on the relationship between the primary and secondary liquid levels.

5.6 Nonuniform Behavior in UTSG Plants

This section discusses phenomena associated with nonuniform behavior during reflux condensation in plants with UTSGs. Topics addressed include: flooding effects, different U-tube flow modes, and the potential for loop seal depression.

5.6.1 Flooding Effects

During reflux condensation, flooding is possible in the counter-current flow regions in the upflow sides of the steam generator U-tubes, and in the stratified counter-current flow regions in the hot legs. Generally, flooding occurs at

flow area restrictions or at locations where the flow changes direction.[63] The tendency for flooding is enhanced by low-system pressure and the presence of noncondensable gases. Low system pressure results in lower steam densities and higher steam velocities. Noncondensable gases in the steam generator U-tubes cause a greater fraction of the condensation to occur in the upflow sides of the U-tubes. As a result, more condensate must drain from the upflow sides of the tubes and the likelihood of liquid holdup is increased. Flooding has been observed in a number of reflux condensation experiments.[25,26,51,63,73,74,112]

5.6.1.1 Flooding at the Hot Leg Bend. The Upper Plenum Test Facility (UPTF)[71,72] and the LSTF[63] have investigated flooding in the hot leg of a PWR. The motivation for research in this area follows from the potential for liquid holdup in the vertical section of the hot leg bend leading to the steam generator inlet plenum, and the interruption of steam flow from the core to the steam generators during reflux condensation. Liquid holdup in the vertical section of the hot leg is a concern because a back pressure is exerted on the core liquid level, which can cause core liquid level depression. The maximum possible core level depression resulting from hot leg flooding, however, is less than that due to steam generator tube flooding because the hot leg elevation rise to the steam generator inlet plenum is small [approximately .91 m (3 ft)]. Interruption of steam flow from the core to the steam generators is a concern because core rod heatup may occur if reflux condensation cooling is lost.

The full-scale UPTF is designed to simulate three-dimensional, thermal hydraulic steam/water behavior in the upper plenum, reactor coolant loops, and downcomer of a four-loop Kraftwerk Union 3400 MW(t) PWR.[71] Hot leg CCFL tests in the UPTF were conducted at pressures of 3 bar and 15 bar. Reflux condensation processes were simulated using different steam flow rates from the core, while a constant reflux condensate flow rate was maintained. UPTF tests mapped out the CCFL curve at each of the above pressures. UPTF results demonstrated that there exists a significant margin between "typical" PWR operating conditions during reflux condensation and the flooding limits.[71] "Typical" PWR reflux conditions were based on calculated reflux condensation conditions for a four-loop W plant fifteen minutes after shutdown (2% decay heat), assuming one steam generator was lost. The difference between j_g^* for the typical PWR case and the flooding limit was approximately 0.27.[71] This important result indicates that steam flow through the hot legs will not inhibit the flow of condensed liquid back to the core from the steam generators during typical reflux conditions. The Richter et al. correlation was found to be consistent with the UPTF CCFL data.[71,113] This correlation is of the following form

$$\sqrt{j_g^*} + \sqrt{j_f^*} = 0.7. \qquad (5\text{-}15)$$

The linear approximation of the relationship between j_g^* and j_f^* at flooding conditions in the UPTF test is given by,[71]

$$\sqrt{j_f^*} = 0.7955 - 1.1564 \sqrt{j_g^*}. \qquad (5\text{-}16)$$

Comparisons with FLECHT-SEASET, Semiscale, PKL, and LSTF (ST-NC-01, ST-NC-02) data showed that each of these facilities simulated reflux conditions within the CCFL boundary defined by the UPTF tests. Because the UPTF is a full-scale facility, agreement with UPTF results[71] helps to validate the reflux condensation data of the small-scale tests.

The Variable-Power Test in the LSTF (ST-NC-04) demonstrated that flooding is possible in the stratified two-phase flow at the hot leg bend at 10% core power ($j_g^* \sim 0.30$).[63] LSTF flooding data were found to be better represented by the flooding correlation of Ohnuki[114] rather than that of Richter et al.,[71,72] the LSTF flooding limit being lower than that predicted by Richter et al. ($j_g^* \sim 0.47$).[71,113] Discrepancy with the Richter et al. correlation may be attributable to the fact that Richter used a shorter pipe [900 mm (2.95 ft.) versus 3,188 mm (10.46 ft.) in the LSTF].[63]

Although hot leg flooding was observed in the LSTF, test conditions were outside typical PWR reflux condensation operating conditions. In fact, they were more typical of the early

blowdown and reflood phases of a relatively-large break LOCA.[63] Table 5-4 presents hot leg flooding data for both the LSTF and UPTF test facilities, assuming $j_f^* = 0$. Equation 5-16 is used to predict j_g^* in the case of the UPTF facility. Additional information regarding each of these test facilities can be found in Appendix A.

The important conclusion to be drawn from this discussion is that the results of the UPTF hot leg CCFL tests indicate that hot leg flooding is not a concern during typical PWR reflux condensation operating conditions.[71] However, LSTF data demonstrate that hot leg flooding is possible under PWR operating conditions that yield high steam velocities.[63]

5.6.1.2 Flooding at the Steam Generator U-tube Inlet. The countercurrent flow of steam and condensate in the steam generator U-tubes during reflux condensation may lead to flooding at the U-tube inlet. In the upflow side of the U-tubes, steam flow opposes condensate draining and liquid holdup may result. Liquid holdup in the upflow sides of the steam generator U-tubes may provide a hydrostatic head that depresses the core level. Core uncovery is possible if sufficient core level depression occurs.

The U-tube flooding limit was defined by Nguyen and Banerjee (UCSB) to occur at $j_g^* \sim 0.50$. Complete liquid carryover to the downflow side was observed at $j_g^* \sim 0.90$.[73] Note that these tests were conducted on a single U-tube at atmospheric pressure. High-pressure reflux condensation data (at 55% primary mass inventory) obtained from the LSTF were in reasonable agreement with these results.[63] The LSTF data indicate liquid holdup was initiated in the steam generator U-tubes at $j_g^* \sim 0.40$ (5% core power) and became significant at $j_g^* \sim 0.56$ (7% core power).[26,63] These results are also consistent with Semiscale data where flooding started between $j_g^* \sim 0.1$ and $j_g^* 0.32$.[26,57] Liquid carryover to the U-tube downflow side was observed to occur in the LSTF at $j_g^* \sim 0.80$ (10% core power).[63] Countercurrent flow limitation (flooding) also occurred in the BETHSY facility.[51] There, it was observed that the Wallis correlation[76]

$$\sqrt{j_g^*} + \sqrt{j_f^*} = C \qquad (5\text{-}17)$$

correctly predicts flooding in the U-tubes with C between 0.77 and 0.88.[51] Calia and Griffith conducted separated effects experiments in a low-pressure, four-tube, inverted U-tube condenser. They observed flooding for j_g^* between 0.23 and 0.44.[74]

Table 5-5 summarizes the U-tube flooding data presented above. Recall that additional information on the integral test facilities may be found in Appendix A.

5.6.2 Different U-tube Flow Modes

Nguyen et al. identified three distinct U-tube flow modes associated with reflux condensation.[73] These three modes were referred to as classical reflux condensation, the oscillatory flow mode, and the carryover mode. At low vapor velocities, the classical reflux condensation phenomena was observed. At the onset of flooding at the steam generator inlet, there is a transition from the classical reflux mode to what Nguyen labeled the oscillatory mode.[25] This mode is characterized by the formation of liquid columns in the riser sections of the steam generator U-tubes. The transition to the oscillatory mode begins when portions of the liquid condensate are carried upwards by the vapor flow. This phenomenon can be quantified with a Wallis-type flooding correlation.[75] Liquid holdup was observed when the non-dimensional superficial vapor velocity, j_g^*, was 0.50. This result is supported by high-pressure LSTF data in which liquid holdup occurred for $j_g^* = 0.4$ and $j_g^* = 0.56$ corresponding to core powers of 5% and 7%, respectively.[26,63] Flooding also occurred in the FLECHT-SEASET facility for $j_g^* \sim 0.50$, which corresponds to core power levels of about 2.5% at a pressure of 140 psia.[45] In the FLECHT-SEASET facility, there were no stable reflux condensation modes for decay heat levels greater than 2.5% core power.[49] Calia and Griffith observed the oscillatory mode when $0.23 < j_g^* < 0.44$.[74]

Some researchers refer to the flow pattern described above as the 'fill and dump mode'.[74]

Table 5-4. Comparison of LSTF and UPTF hot leg flooding data.

Facility	Pressure	j_g^*
LSTF	6.5 MPa (943 psia)	0.30
UPTF	0.3 MPa (44 psia)	0.47
UPTF	1.5 MPa (218 psia)	0.47

Table 5-5. Comparison of U-tube flooding characteristics in BETHSY, MIT experiments, LSTF, Semiscale, and UCSB experiments.

Facility	Pressure	j_g^*
BETHSY	6.8 MPa (986 psia)	0.59-0.77
LSTF	Atmospheric	0.23-0.44
MIT	6.5 MPa (943 psia)	0.40-0.56
Semiscale	6.9 MPa (1000 psia)	0.16-0.32
UCSB	Atmospheric	0.50

Although similar, this flow behavior should not be confused with the cyclic fill and dump process described in Section 4.6.1. There, the inlet plena was filled with a two-phase mixture, and steam-water interphase drag was responsible for the high mixture levels in the steam generator U-tubes. In this case, steam fills the inlet plena and flooding initiates the oscillatory fill and dump behavior.

The carryover mode occurs when sufficiently high vapor velocities are able to carry the condensate over the upper U-bends of the U-tubes. In this situation, a cocurrent flow of liquid and vapor exists in both the upflow and downflow sides of the steam generator U-tubes and a transition to two-phase natural circulation may occur. Transition to the carryover mode in some U-tubes was observed by Nguyen et al. when $j_g^* = 0.9$,[73] while LSTF experiments observed this flow mode when $j_g^* = 0.8$ (10% core power).[63] Calia and Griffith observed complete liquid carryover in all four U-tubes of their test apparatus when $j_g^* = 1.56$.[74]

Similar flow modes have also been observed by Hein et. al.;[101] and in BETHSY;[51] LOBI-MOD2,[64] PKL,[99] and Semiscale[24,112] experiments. The three modes of U-tube behavior described in this section are illustrated in Figure 5-2.

The oscillating U-tube flow mode is important with regard to nuclear reactor safety analysis. A positive hydrostatic head in the steam generator U-tubes exerts a back pressure on the core liquid level; and while core cooling remains effective, core liquid level depression is possible.[25] This effect was first observed in Semiscale, where core coolant level depression during pump suction liquid seal formation can be aggravated by the existence of a positive hydrostatic head in the steam generator U-tubes.[112]

The oscillatory mode was so named due to the observed periodic fill and dump behavior in the U-tubes. As the liquid column in a U-tube reached the top of the U-tube bend, spillover would occur. After spillover, a siphoning effect

would pull the liquid column over the U-tube bend. Steam flow in this cleared tube would then increase significantly, allowing the remaining tubes to partially drain until the pressure drops in all tubes were equal. A liquid column would again form in the cleared tube and the pattern would repeat. The spillover event appeared to occur randomly in any one of the U-tubes. It is believed that the random nature of the fluctuations of the liquid columns is the cause of the randomness in the spillover event.[25] The oscillatory behavior in the LOBI-MOD2 facility during the initial stages of reflux condensation was attributed to a "syphon condensation" phenomena controlled by flooding in the upflow sides of the steam generator U-tubes.[64] This behavior closely resembles the oscillatory U-tube flow mode described above.

In the presence of noncondensable gases, spillover events may act to redistribute the noncondensables to other uncleared U-tubes or to other locations in the primary loop. The distribution of the noncondensables in the primary loop is very important in determining the thermal hydraulic behavior of the system. A redistribution of gases, due to U-tube spillover events, should be considered when determining the system thermal hydraulic response.

5.6.3 Loop Seal Formation/Clearing Phenomena

During reflux condensation, a liquid seal normally exists in the loop cold leg suction piping. This 'loop seal' impedes the flow of vapor through the loop piping. A Semiscale experiment demonstrated that the effect of the loop seal is more complicated than a simple manometric balance between the reactor vessel and downflow leg of the loop seals.[112] Several important parameters were identified: core vapor generation rate, the core coolant bypass flow, the U-tube condensation rate, and flooding tendencies.

If the core vapor generation rate is sufficiently high, a differential pressure may develop between the reactor vessel (hot leg) and the downcomer (cold leg).[24] Consequently, the vessel coolant level may be depressed relative to the downcomer. In addition, this core liquid level depression may be intensified by liquid holdup in the steam generator U-tubes resulting from flooding at the steam generator inlet.

In plants with UTSGs, there are often two sets of bypass paths capable of removing steam from the vessel upper plenum to the downcomer. One set is the downcomer inlet annulus-to-upper head flow path, and the second set is leakages through the gaps at each hot leg penetration by the slip fit between the core barrel assembly and the hot leg nozzles.[115] The flow behavior through these core bypass paths during the reflux condensation mode of natural circulation is not completely understood.

The Semiscale experiment demonstrated that core voiding was possible prior to the blowout of the pump suction liquid seals.[24,112] Figure 5-4 demonstrates the hydrostatic heads in the primary system that can lead to the core liquid level depression phenomena.[24] The figure illustrates the potential for core level depression below the bottom of the loop suction piping. Also, the figure shows hydrostatic heads in the upflow side of the steam generator U-tubes and the hot leg bends that aggravate the loop seal depression effects and result in a core collapsed liquid level that is 100 cm below the elevation of the bottom of the cold leg suction piping.[24]

Loop seal clearing during the high-pressure Semiscale SBLOCA experiments was observed to be a steady process. The downflow side of the loop seal was slowly depressed until loop seal clearing occurred. The loop seal did not reform because of loss of primary mass inventory through the break. However, in experiments conducted in the low-pressure FLECHT-SEASET facility (constant primary mass inventory), the clearing of the loop seal was periodic. Observations indicated that steady state reflux condensation was periodically interrupted by venting of steam through the intact loop seal.[41] The core vapor generation rate was greater than the steam generator condensation rate and consequently, uncondensed vapor flowed into the steam generator exit plenum and cold leg, displacing the liquid in those locations. The vapor depressed the liquid level in the downside of the cold leg suction piping and the vessel until steam eventually vented through the loop seal. The differential pressure between the loop

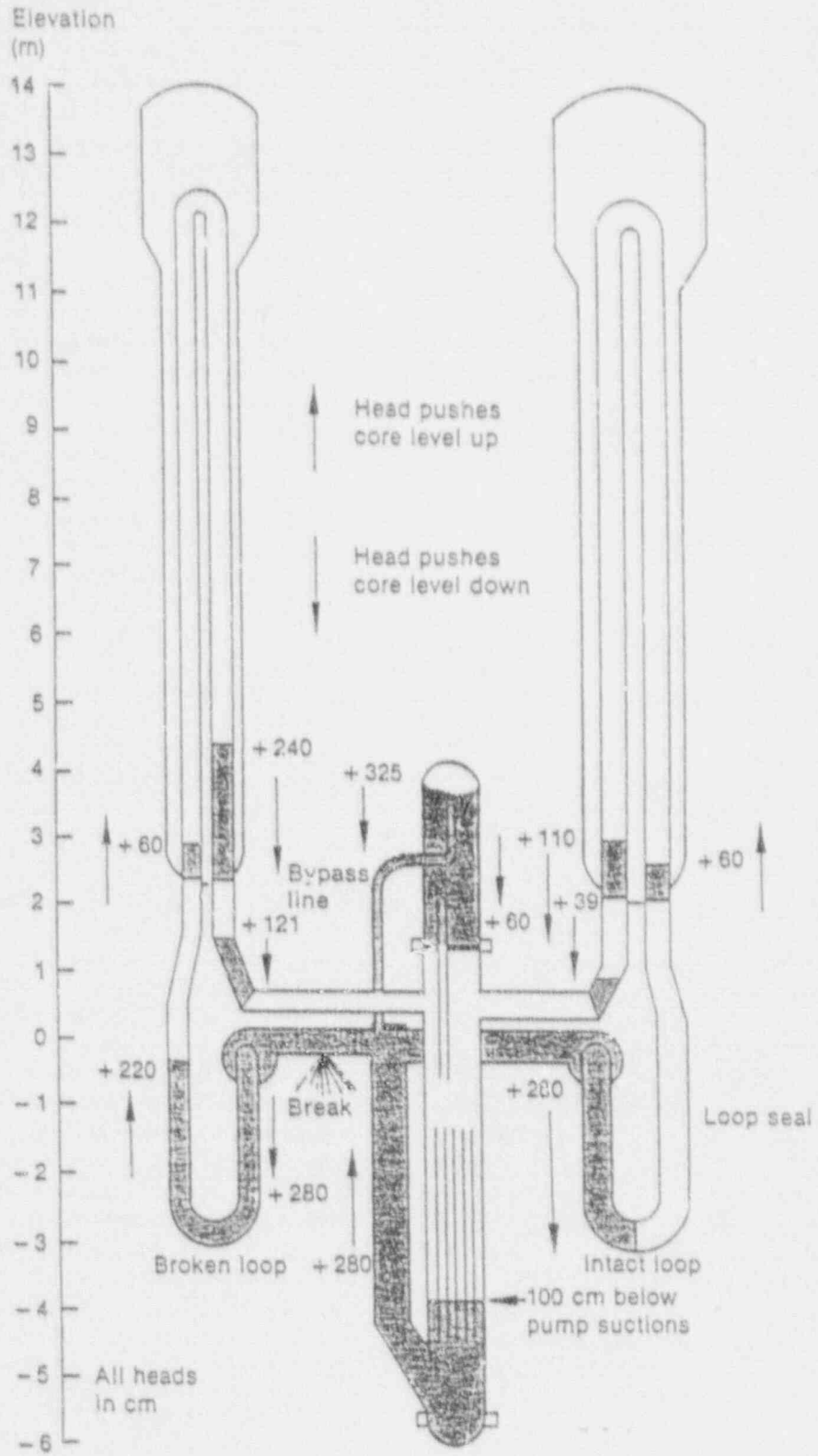

Figure 5-4. Hydrostatic heads in the primary system of the Semiscale facility which lead to core level depression.[24]

hot and cold leg nozzles was temporarily relieved, and the liquid seal reformed. This process is illustrated in Figure 5-5.

The following effects resulted from the venting of steam through the loop seal:[41,49]

- Fluid from the downcomer was forced into the rod bundle by the vented steam. This liquid replaced the two-phase mixture in the lower elevations of the vessel and temporarily stopped vapor generation in the lower vessel elevations. The liquid from the downcomer also forced the two-phase froth level well above the hot leg nozzle elevation.
- A two-phase mixture was forced into the steam generator inlet plenum.
- The flow in the steam generator U-tubes changed from reflux condensation to cocurrent two-phase flow.

It is believed that the periodic venting of steam through the loop seal during reflux conden-sation is a low-pressure effect. This phenomena has also been observed in the low-pressure PKL facility.[49]

5.6.4 Nonuniform Behavior Summary

The ability of steam to reach a condensing surface in the steam generator U-tubes is a primary concern during reflux condensation. In addition to the noncondensable gas effects discussed in Section 5.4, flooding at the steam generator U-tube inlet and/or the hot leg bend may also impede the flow of steam to a condensing surface. Experiments performed in the BETHSY,[51] LSTF,[26,63] and Semiscale[57] facilities, and by UCSB[73] indicate that flooding is possible at the steam generator inlet during reflux condensation. Flooding at the hot leg bend has been observed in the LSTF and the UPTF[71] facilities for high core power levels (>5% core power), but not for typical reflux condensation conditions (< 5% core power). Core level depression (loop level depression) is another reactor safety concern that may occur during the reflux mode of natural circulation. Loop seal depression effects can be aggravated by the formation of hydrostatic heads in the steam generator resulting from flooding and consequent liquid holdup. Important parameters in the loop seal depression process include the following: the core vapor generation rate, the core coolant by-pass flow, the U-tube condensation rate, and flooding tendencies.

Three modes of U-tube flow were identified in Section 5.6.2. These are classical reflux, the oscillatory mode, and the carryover mode. These flow modes have also been observed in LSTF experiments.[26] The occurrence of a given mode during reflux condensation depends on the core power and the U-tube length. It is possible to have different flow modes in different length tubes.[63]

The oscillatory flow mode is of primary interest with regard to reactor safety analysis. The transition to this U-tube flow mode is set at the flooding limit, and it is characterized by the growth of a liquid column in the upflow side of a steam generator U-tube that eventually spills over into the U-tube downflow side. Some of the effects of flooding and consequent liquid holdup have been stated. Additionally, when noncondensables are present, spillover incidents act to redistribute the gases to other stalled U-tubes or to other locations in the primary loop. This cause of noncondensable gas redistribution should be considered when determining the primary system thermal hydraulic response.

It is noted that the experimental results cited in this section are based on a limited number of U-tubes in the steam generators. In this situation, individual tube behavior has a greater effect on the system thermal hydraulic response than it would in an actual PWR steam generator with a much larger number of U-tubes (i.e., thousands of tubes).[19] In addition, the tube-to-tube interactions that may occur through the common steam generator inlet and exit plena are somewhat unpredictable.

5.7 Reflux/Boiling Condensation Summary

The reflux condensation and boiler condenser modes of natural circulation are very efficient heat removal mechanisms.

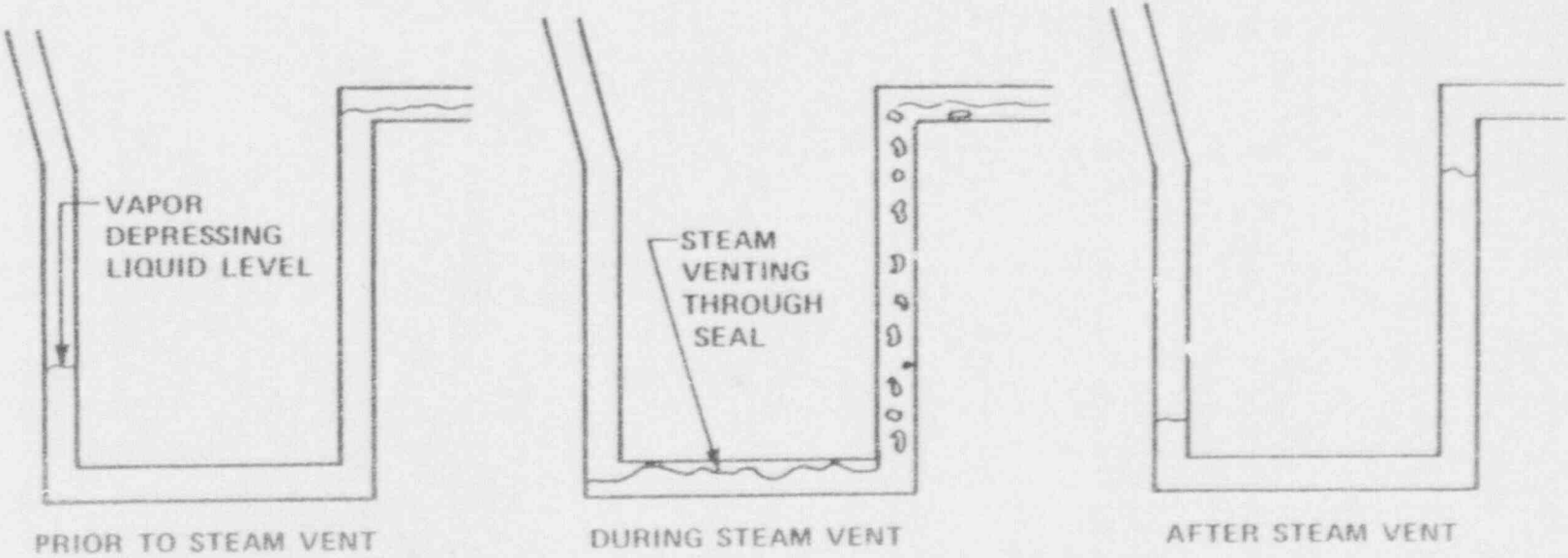

Figure 5-5. Loop seal liquid distributions.[49]

Consequently, both exhibit low mass flow rates and low primary-to-secondary temperature differences compared with the single- and two-phase modes of natural circulation.

There are two types of boiling condensation in plants with OTSGs. Pool boiling condensation occurs when a primary condensing surface exists below the secondary pool level. EFW boiling condensation occurs when a primary condensing surface exists below the EFW sparger spray elevation.

Noncondensable gas in the primary side of the steam generators during reflux/boiling condensation impedes the condensation process. Effective steam generator heat transfer areas are reduced, and increased primary-to-secondary temperature differences are required to remove the decay heat. System pressure acts as a correcting mechanism; when pressure increases (as a result of degraded primary-to-secondary heat transfer), the noncondensable gas volumes are compressed to expose an adequate condensing surface in the steam generators. The effects of noncondensable gases on the reflux/boiling condensation mode of natural circulation were discussed in Section 5.4.4.

The potential loss of heat sink behavior in OTSG plants has been demonstrated. The steam generator primary side condensing surface may be driven above the secondary pool level by changes in the steam generator primary/secondary liquid levels, and/or the presence of noncondensable gases in the steam generator tubes. If the condensing surface is driven above the secondary pool elevation and EFW is not available, the loss of the steam generator as a heat sink will result.

Flooding is possible in UTSG plants during reflux at both the hot leg bend and the steam generator U-tube inlet. Flooding at these locations will impede the flow of steam to condensing surfaces in the steam generator U-tubes. However, UPTF experiments found that for typical reflux conditions (approximately 2% core power), flooding at the hot leg bend will not impede the flow of condensed liquid back to the core.[71] Flooding at the steam generator U-tube inlet has been observed in a number of reflux condensation experiments.[26,51,57,63,73]

Three distinct U-tube flow modes were described in Section 5.6.2. These modes were referred to as classical reflux condensation, the oscillatory flow mode, and the carryover mode. Note that different flow modes have been observed to occur in different U-tubes at the same time. The oscillatory mode is important with regard to reactor safety analysis because it is characterized by flooding and consequent liquid holdup in the steam generator U-tubes. The oscillatory mode was so named because of the periodic spillover of liquid into the U down-flow sides. These spillover events may act to redistribute any noncondensable gases present in the primary system.

Liquid holdup caused by flooding may aggravate loop seal core level depression effects. Loop seal depression is not a simple manometric balance between the vessel and the downflow leg of the loop seal; but is influenced by the core vapor generation rate, the core coolant bypass flow, the U-tube condensation rate, and liquid holdup caused by flooding.[112]

6. APPLICATION OF THERMAL-HYDRAULIC SYSTEM CODES TO NATURAL CIRCULATION

Because natural circulation cooling may be an essential means of removing shutdown decay heat in PWRs, considerable effort has been made towards understanding its behavior and phenomena. As evidenced by the citations in previous sections of this report, a large amount of experimental data has been generated related to natural circulation. Because one of the objectives of PWR operation is to avoid abnormal conditions, natural circulation data from large-scale PWRs is limited to single-phase conditions. Therefore, the use of thermal-hydraulic system codes is necessary to apply information and data obtained from small-scale experimental facilities to large-scale operating reactors, especially regarding two-phase and reflux/boiling condensation modes of natural circulation. Thus, one of the main objectives of the experiments was to provide data for the development and assessment of thermal-hydraulic system codes.

Section 6.1 discusses the scalability and applicability of thermal hydraulic system codes; Section 6.2 discusses the assessment of thermal hydraulic codes against data from experimental test facilities; Section 6.3 describes calculations of operating plant natural circulation, and Section 6.4 addresses several potential problems associated with simulating transient natural circulation phenomena with thermal hydraulic system codes.

6.1 Thermal-Hydraulic System Codes

Reactor safety research has addressed scalability and applicability of best estimate thermal-hydraulic system codes. For example, the preservation of natural circulation similarity criteria by RELAP5/MOD2 was studied.[116] The following criteria were considered for assessing these codes:

- Establish similitude criteria for single- and two-phase natural circulation in a loop using the work of Ishii and Kataoka.[117]
- Generate two different scale size "paper models" of a hypothetical natural circulation loop.
- Construct RELAP5 models for each of these paper models.
- Conduct the same transient with each model.

The results of the study showed that for natural circulation in a single loop, the RELAP5/MOD2 code calculates similar physical phenomena at significantly different geometric scales. The kinematic and dynamic relationships between the phenomena in the two different geometric scale models were calculated to be consistent with expectations based on similarity criteria.

These results were considered generally applicable to other systems codes having a stage of development similar to RELAP5/MOD2. This is a significant conclusion, because these systems codes are intended for application to operating PWRs that are of a much larger geometric size than the scaled experimental facilities.

6.2 Calculation of Experimental Facility Data

Numerous thermal-hydraulic code calculations of experimental facility data have been made. As examples, the LOFT and Semiscale facility experiments were planned by utilizing system code predictive calculations, which were formally documented for the experiments conducted. Subsequently, several experiments from these facilities, as well as experiments from other facilities, were used for code assessment calculations. The material that follows describes some representative examples of assessment calculations.

TRAC-PF1/MOD2 is the most recent release of the TRAC-PF1 code. However, none of the

developmental assessments of this code, to date, have addressed natural circulation.[118]

The TRAC-PF1/MOD1 code was applied to Semiscale facility natural circulation experiments S-NC-2 and S-NC-6 in Reference 119. S-NC-2 was a natural circulation test investigating the effects of different core power levels and different primary mass inventory levels. All three modes of natural circulation were observed during experiment S-NC-2. Figure 6-1 shows the measured and calculated mass flow inventory for the 5.0% core power (100 kW) natural circulation test (S-NC-2).[119] TRAC-PF1/MOD1 mass flow rate calculations followed the measured data very closely.

Experiment S-NC-6 was a reflux condensation test that studied the effects of injecting various amounts of nitrogen gas into the system hot leg just below the steam generator inlet plenum.[119] With no nitrogen in the system, TRAC-PF1/MOD1 calculated the reflux rate from the upflow side of the steam generator U-tubes to be 10% lower than that observed in the experiment. With an amount of nitrogen amounting to 0.86% of the primary system volume at the primary temperature and pressure, the calculated reflux rate was only 3% higher than the measured value. The maximum measured and calculated reflux rate occurred when the amount of nitrogen injected amounted to 2.98% of the primary system volume. However, the TRAC-PF1/MOD1 calculated value was 20% higher than the measured value.[119] Reference 119 indicated that differences in the measured and calculated reflux rates could be attributed to the manner in which the reflux liquid was removed from the Semiscale system and then replaced by the makeup system during the reflux rate measurement. Other possible factors for the differences between the calculations and the data include uncertainties in the heat losses and measurement error.

The TRAC-PF1/MOD1 code was also applied to LOFT experiment L6-7/L9-2.[120] This was an anticipated transient experiment simulating a turbine trip from full power followed by a secondary side controlled rapid cooldown. In the L6-7 part of the experiment, the reactor coolant pumps were operating. In the L9-2 part of the experiment, the rapid cooldown continued, but the pumps were tripped and natural circulation became the heat removal mechanism.[35] Comparisons between calculation and data generally show good agreement, except for the loop flow during the L9-2 part of the experiment.[121,122] The difference was attributed to 3-D behavior in the downcomer, which was not modeled in the TRAC-PF1/MOD1 input model. This calculation and others illustrate the importance of input model development. Other assessment calculations of LOFT natural circulation experiment data show that TRAC code versions accurately predict the qualitative trends, and many of quantitative results.[a,123] Similar results were obtained in assessment calculations against the PKL experiments.[124]

The TRAC-PF1/MOD1 code was also applied to a LSTF 5% power natural circulation experiment (ST-NC-01).[125] The LSTF data showed flow in the forward direction in the shorter U-tubes and reverse flow in the longer U-tubes. As a consequence, two input models of the steam generator were constructed, one modeling the U-tubes with a single path and one modeling the U-tubes with three paths; representing the short, medium, and long U-tubes of the UTSG.[125] Analysis showed that the single U-tube path model was inadequate because it did not yield an accurate calculation of the experimental data.[125] The calculated single-phase mass flow rates using the single U-tube model were 14% to 20% higher than the measured values. The differences were attributed to the presence of the reversed flow in the longer U-tubes. The reversed flow is believed to reduce the overall loop mass flow rate by decreasing the net forward flow area and increasing the net loop frictional resistance.[125] The three U-tube path model yielded calculations that were much more representative of the experimental data, showing the effect of reverse flow in the long U-tubes. Calculated mass flow rates using the three U-tube model were only 2% to 8% higher than the measured values. This result demonstrates that reversed flow in the steam generator U-tubes is an important phenomenon and it should be

a. Safety Code Development Group, *TRAC-PF1 Independent Assessment*, Los Alamos National laboratory report (to be issued).

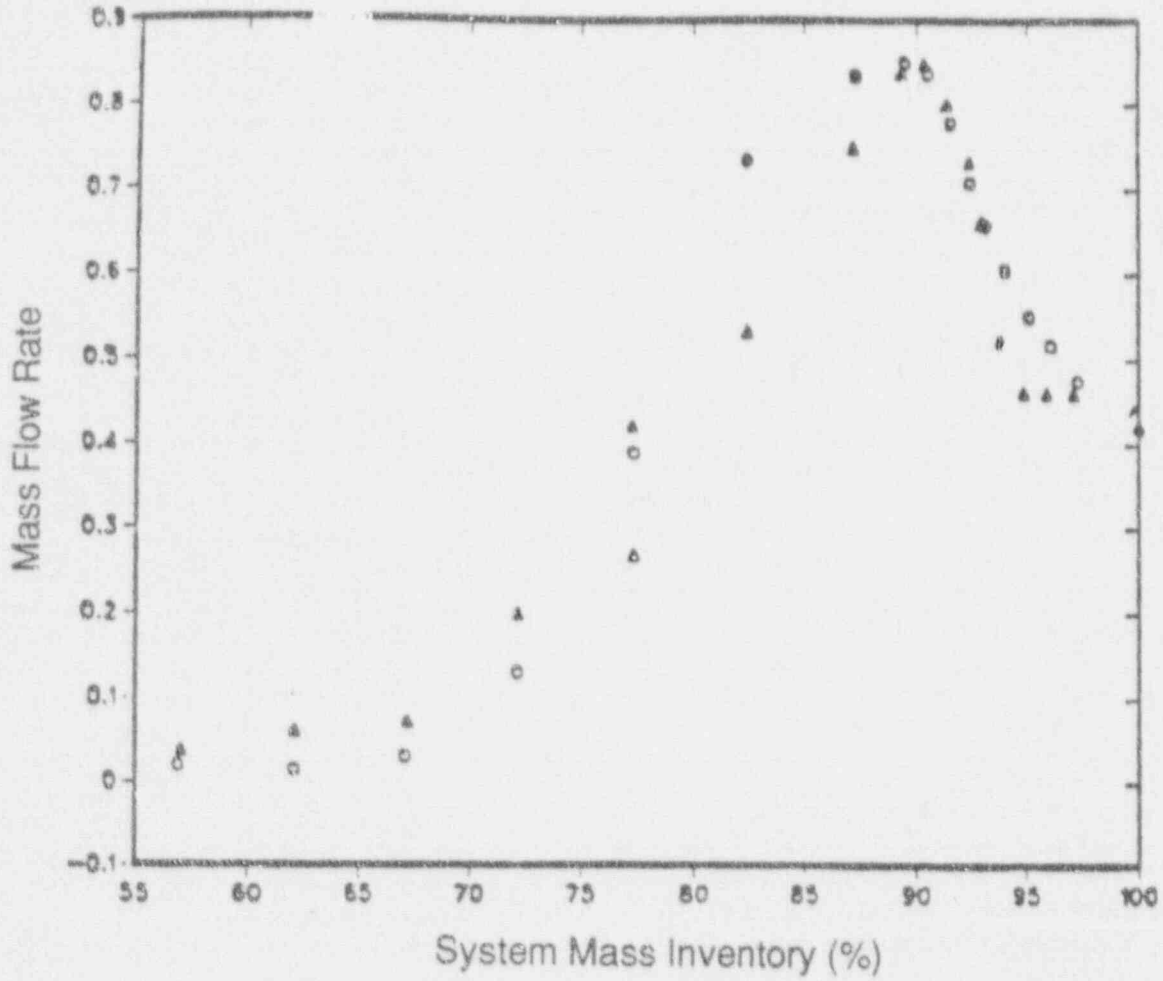

Figure 6-1. Comparison of calculated and measured mass flow rates for Semiscale experiment S-NC-2 (5% core power).

considered in analyzing natural circulation flow. TRAC-PF1 calculations are represented by circular symbols, while Semiscale data are represented by triangular symbols.[119] This is an important point, especially considering that the single U-tube model was created using standard modeling practices.[20]

The RELAP5/MOD3 code has been assessed against BETHSY natural circulation experiments.[126] Figure 6-2 shows the calculated and measured mass flow rates versus the primary system mass inventory fraction for BETHSY test 4.1a-TC (5% core power).[126] Initially, the calculated mass flow rates were approximately 14% higher than the measured values. Reference 2 suggested two explanations for this discrepancy: The first explanation cited differences in the primary density distribution in the experiment and the calculation. It was postulated that energy was removed from the primary system at a slower rate during the calculation than during the experiment, which reduced the net gravitational force driving the flow. However, insufficient instrumentation in the experiment made it impossible to prove or disprove this hypothesis.[126] The second explanation cited the presence of reversed flow in the steam generator U-tubes as a possible cause of the discrepancy. RELAP5/MOD3 could not simulate reversed flow because a single U-tube was used in the steam generator model. Recall that the single U-tube model used in the TRAC-PF1/MOD1 simulation of LSTF experiment ST-NC-01 was determined to be inadequate.[125] Flow reversal in the longest U-tubes was possible during the BETHSY experiment.[126] Although RELAP5/MOD3 predicted an earlier initiation of two-phase natural circulation than the data, the peak two-phase mass flow rates differed by only 9%. The minimum flow rate occurred at 52% mass inventory in both the experiment and the calculation. RELAP5/MOD3 predicted reflux condensation occurred in all three loops at a mass inventory of 37%, while in the experiment reflux, began in one loop at a mass inventory of 50%, in two loops at 46%, and in all three loops at 41%. Note that CCFL occurred in the experiment (37% mass inventory), but it was not predicted by RELAP5/MOD3.[126] The initiation of CCFL in the experiment led to the oscillatory flow phenomenon described in Section 5.6.2. Recall that this phenomenon was also observed in LSTF experiment ST-NC-01.

The RELAP5/MOD2 code has been assessed against Semiscale small break transient data[127,128] and LSTF natural circulation experiments.[63] The basic Semiscale system responses were adequately calculated by the code; however, the timing of certain events differed significantly from observed events.[127,128] Although the calculations agreed qualitatively with the measurements, quantitative differences were observed. These differences resulted from errors in modeling the experiment and deficiencies in the RELAP5/MOD2 computer code. Selected examples of these errors and deficiencies are listed as follows:

- Differences in the calculated and measured loop mass flow rates were attributed to the use of a lower system resistance in the model than that existing in the test facility[128]
- The failure of RELAP5/MOD2 to predict liquid holdup in the steam generator U-tubes was attributed to the lack of a CCFL model in this version of the code
- Deficiencies in the calculation of the interphase drag and sound velocity in the RELAP5/MOD2 choked flow model were identified after observing errors in the calculated void fractions and break flow[127,128]
- Geometric configurations must be accurate to ensure unbiased heat transfer calculation. A more quickly calculated depressurization during the recovery stage of the SBLOCA transient (as opposed to the observed depressurization) may have resulted from different stored energy relaxation of the metal in the steam generators.[127]

In spite of the above mentioned deficiencies, the code did correctly calculate two-phase natural circulation and reflux phenomena during the draining of the steam generator tubes (test S-LH-2).[127]

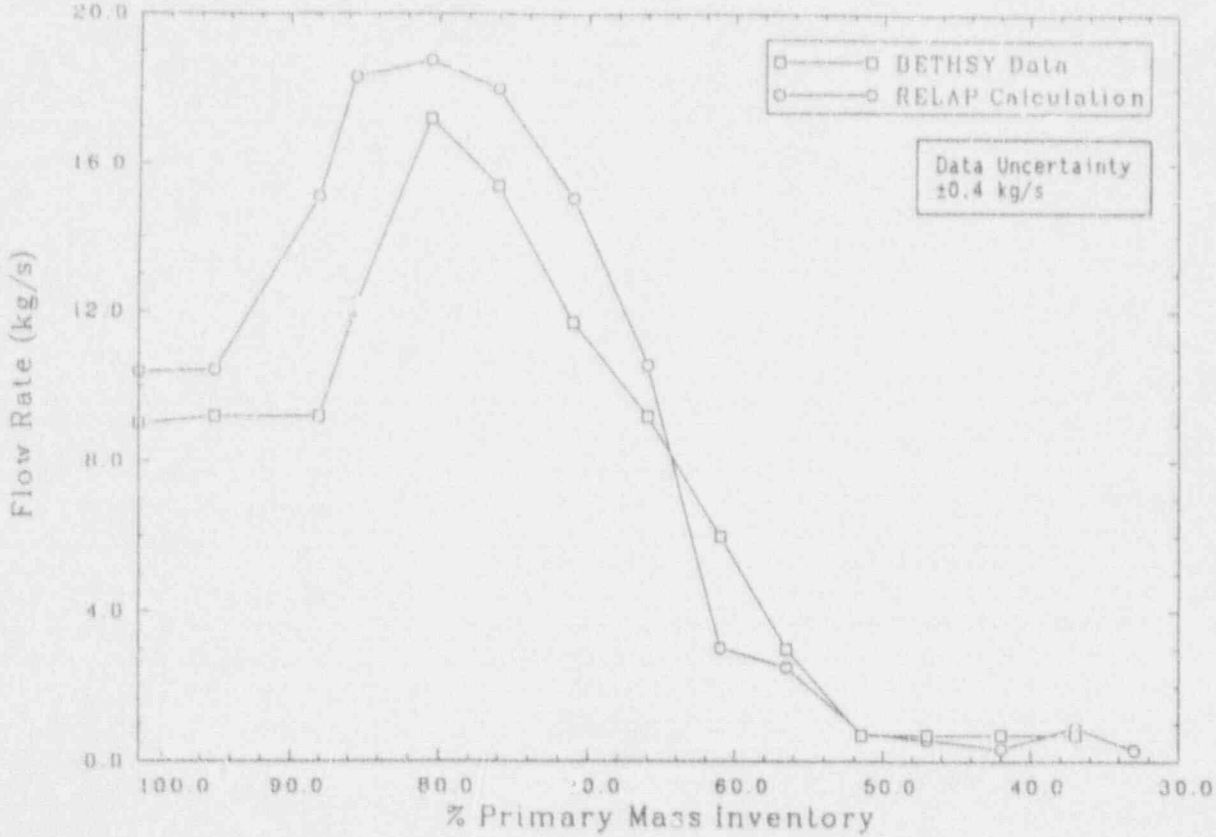

Figure 6-2. Comparison of calculated and measured mass flow rates for BETHSY experiment 4.1a-TC (5% core power).[126]

The LSTF experiments indicated the presence of flooding in the stratified two-phase flow at the hot leg bend located beneath the steam generator inlet, and showed that flooding controlled the coolant distribution in the primary system during both the two-phase and reflux condensation modes of natural circulation.[63] Initially, RELAP5/MOD2 significantly overpredicted the hot leg void fraction. Once again, this was primarily due to deficiencies in calculating the interphase drag. After a simple modification to the interphase drag calculation, the RELAP5/MOD2 code calculations agreed well with the experimentally observed flooding conditions. Calculations with the TRAC-PF1 code and the French code CATHARE[63] also agreed well with the LSTF data.

The RELAP5/MOD1 code was assessed against the Semiscale natural circulation experiments in References 129 and 130. The results showed the code qualitatively predicted all modes of natural circulation correctly for both single and two-loop Semiscale geometries. Quantitative disagreements with data were evident for two-phase natural circulation mass flow rates and for the system mass inventories at which mode transitions occur. The calculated two-phase mass flow rates were significantly higher than the measured values (10% to 40%). These results are consistent with comparative results from assessment calculations against PKL data.[131] The Semiscale assessment results also demonstrated that the code qualitatively describes the influence of steam generator secondary heat transfer degradation on two-phase and reflux condensation natural circulation.[130] However, discrepancies with the measured data occurred at low secondary inventories. Qualitative agreement with natural circulation phenomena was also obtained in the case of an ultra-small SBLOCA, and in assessment calculations against LOFT data[132,133,134] and LSTF SBLOCA data[135]

An example of RETRAN-02 code assessment is the comparison conducted against an OTIS natural circulation experiment[136]. Qualitative and near quantitative agreement with core inlet flow and temperature, and with OTIS secondary liquid level, were demonstrated for the two-phase natural circulation mode during a SBLOCA. However, differences in the magnitude of calculated and measured flow surges were observed during an intermittent type circulation pattern, similar to that described in Section 2 and in Section 4.6.2.2. These differences were attributed to piping heat losses that were not accounted for in the calculation.[136]

The preceding examples illustrate the capabilities and limitations of system thermal-hydraulic codes in simulating natural circulation phenomena. The data used in the assessment calculations were drawn from scaled facilities with a large range of geometric scales, therefore, it is anticipated that the system thermal-hydraulic codes are applicable to full-scale PWRs. This conclusion is supported by the study on the preservation of scaling criteria.[116]

6.3 Calculation of Operating Plant Natural Circulation

This section presents and discusses several examples of the use of thermal hydraulic system codes to calculate and/or predict operating plant behavior under natural circulation conditions. Code performance is discussed, and insights gained from code calculations are indicated.

The performance of a CE full-plant simulator for operator training was assessed by comparing it to the St. Lucie Unit 1 natural circulation cooldown transient.[137,138] A benchmark simulation of the Diablo Canyon Unit-1 natural circulation test was completed using the Westinghouse TREATcode.[139,140,141] This Diablo Canyon test consisted of four basic periods: hot standby with forced circulation, hot standby with natural circulation, cooldown and depressurization, and normal cooldown to cold shutdown using the Residual Heat Removal System (RHRS). TREAT calculations for the first three periods agreed well with the test data.

Small-break LOCA recovery has been studied for B&W plants.[142] For a 0.0012 m^2 (1.86 $in.^2$) break, single-phase natural circulation flow was interrupted by hot leg voiding in the "candy cane" region. The interrupted flow could not be restarted by the formation of a condensing surface in the steam

generators, by venting secondary steam, by venting primary steam, by injecting HPSI liquid into the candy canes, or by "bumping" the RCPs. Further effort was recommended to investigate recovery strategies.

A series of operational natural circulation events has been analyzed using the RELAP5 code.[b,143,144,145] The analyses were performed because conditions affecting natural circulation cooling are not always known for operational events, particularly operator actions taken during the events. Operator actions are often not recorded during operational events and must be inferred from the measured thermal-hydraulic parameters. The following 3 items were among insights obtained from the analytical studies:

1. Safety injection reduces the natural circulation flow rate and the reactor coolant temperature, but does not affect the achievement of adequate natural circulation.

2. Reactor coolant temperatures can be used as criteria for identifying the establishment of natural circulation flow.

3. When the RCPs are tripped sequentially, the initial reverse loop flows do not prevent the primary system from reaching a stable natural circulation state.[c]

Degraded-equipment scenarios have also been analyzed, such as the natural circulation cooldown of the Midland B&W plant using a single steam generator.[146] The calculations indicated that the Midland plant design is capable of achieving long-term cooldown using one steam generator.

Analytical methods have been used extensively by vendors to assist in understanding natural circulation phenomena in their plants and in the development of operator guidelines. The operator guidelines prepared by the vendors, and by owners groups, provide the current information regarding natural circulation procedures and the analyses used in preparing the procedures.

An analysis of a 0.0254 m (1.0 in.) diameter break in a W PWR has been published.[147] For this case, inadequate core cooling was reached 3 h after transient initiation when the core exit temperature exceeded 922 K. Studies were performed to determine the effectiveness of several recovery techniques and provide a basis for developing emergency procedure operating guidelines for recovery from this condition. All recovery techniques were begun when the predicted core exit temperatures reached 922 K (1200° F) at the time the core was uncovered.

Four techniques were examined:[147] (a) HPSI was restored; the core temperature increase was stopped in 2 minutes and the system recovered from the transient; (b) Operating the steam generator dump valves was considered. Over a 4-minute period, the steam generators were blown down from 7.41 MPa (1075 psia) to 2.07 MPa (300 psia), which was sufficient to start accumulator injection. The core was recovered within 2 minutes of accumulator injection. Continuation of the steam generator blowdown to atmospheric pressure would permit low-pressure safety injection (LPSI) and a long-term recovery from the transient; (c) Restarting the main RCPs was considered. With the RCPs restarted, the core was recovered. The system would continue to depressurize until the accumulators operated and then the LPSI was activated to provide long-term recovery; and (d) Opening the PORVs was considered. This action provided temporary once-through cooling but depleted the reactor coolant inventory at an increased rate. The inadequate core cooling condition returned 15 minutes after the operator opened the PORVs.

Several LOCA categories that depend on break size have been examined by CE for break sizes between 0.0254 and 0.0762 m (1.0 and 3.0 in.) in diameter.[148,149] Transitions from single-phase natural circulation to a two-phase/condensation mode and return to single-phase natural circulation have been described.

---

b. T. R. Charlton, *Transmittal of preliminary Results of Natural-Circulation Analyses for McGuire and North Anna*, Letter to P. E. Litteaker, TRC-90-83, EG&G Idaho, Inc., September 22, 1983.

c. Ibid

Two issues relating to the presence of noncondensable gases in the primary were discussed. First, noncondensable gas volumes equal to the sum of air dissolved in the refueling water, hydrogen dissolved in the primary coolant, and hydrogen contained in the pressurizer vapor space were considered. It was concluded that the degradation in the primary to secondary heat transfer coefficient would be approximately 3% and the primary-system pressure would increase approximately 2%.[148,149] Second, the potential impact noncondensables might have on the transition from the refluxing mode to the reestablishment of single-phase natural circulation was considered. It was concluded that the small amount of noncondensables present is not likely to prevent the return to single-phase natural circulation. However, the presence of more significant amounts of noncondensable gases in the steam generator tubes, extending below the U-tube bends, will prevent natural circulation.[148,149] In this case, increasing the system pressure and cooling down the steam generator secondary was sufficient to reduce the size of the gas bubble and allow spillover to occur. These operations are considered to be effective in operating plants as well.

Recovery studies for a CE plant (Calvert Cliffs-1), following 0.0505 m and 0.07140 m diameter (1.99 in. and 2.81 in. diameter) cold leg breaks with HPSI failure have also been performed.[150] The atmospheric steam dump system was calculated to be effective in depressurizing and cooling the primary system sufficiently to permit LPSI startup. Single-phase, two-phase, and reflux condensation modes of decay heat removal were predicted during these transients.

6.4 Problems Associated with Simulating Transient Natural Circulation Phenomena with Thermal-Hydraulic System Codes

Many comparisons of code calculations to experimental data for natural circulation have shown good agreement, and representative code calculations have been valuable for developing operating guidelines for nuclear plants. However, certain types of transients present unique modeling problems for the thermal hydraulic system codes. For example, the use of the thermal hydraulic system codes to simulate the complex phenomena associated with condensation in the presence of significant amounts of noncondensable gases requires that the calculated results be scrutinized. This area of application is beyond the assessment base of the codes. In these types of calculations, engineering judgement and/or hand calculations will be needed to support results or to determine likely biases in the results. Several specific improvements, modifications and deficiencies in RELAP5/ MOD2 and TRAC-PF1/MOD1 are discussed as follows.

One primary issue of concern is the noncondensable models in RELAP5/MOD2 and TRAC-PF1/MOD1. An improved model has been implemented in RELAP5/MOD3 that enables calculations with pure noncondensable gas as a working fluid.[151] However, this improvement does not solve problems associated with mixing and/or stratification of steam and noncondensable gas, or problems associated with vapor condensation in the presence of noncondensable gases. Both RELAP5/MOD3 and TRAC-PF1/MOD2 assume the steam and noncondensable gas are in thermal equilibrium and move with the same velocity.

Deficiencies in the RELAP5/MOD2 CCFL and interface drag models were identified in the assessment of the code. Developmental assessments of the modifications in the MOD3 version have shown good results, but further assessment is needed.[152,153] A special CCFL model was added to 3D VESSEL and 1D vertical components in TRAC-PF1/MOD2. Without use of the CCFL model, the code predicts the zero liquid downflow point, but overpredicts the amount of liquid downflow in the region of countercurrent flow.[118]

Additional concerns regarding the correlations used by RELAP5 and TRAC-PF1 in calculating the wall and interfacial shear stresses in the condensation region of a UTSG were identified by Nguyen.[25] Modifications were made to the existing RELAP5/MOD2

interfacial shear stress model by Nguyen to improve the accuracy of the RELAP5 prediction of the interfacial shear stress. These modifications included changes in the flow regime map and the corresponding drag coefficients in the condensation region. A need for improvements in the wall shear stress model in the condensation region was also identified, but it was noted that additional experimental data may be needed before these improvements can be made.[25] The modifications described above are not currently implemented in RELAP5/MOD2 or RELAP5/ MOD3. The ability of RELAP5/MOD3 to predict reflux condensation natural circulation, and the oscillatory mode, was tested against the experimental database of Nguyen et al.[d,96] The code had difficulty in properly simulating the data when noncondensable gases (air) were present in the system.[e]

These concerns can also be applied to other thermal-hydraulic system codes. It is emphasized that care must be taken when interpreting results from the system codes. However, the use of such codes—which provide full-plant simulation capability—is necessary to apply information and data obtained from small-scale experimental facilities to the large operating reactors. This is especially true for the two-phase and reflux/boiling condensation modes of natural circulation.

Another area of uncertainty with regard to the use of the common thermal hydraulic system codes is nodalization. Section 5 noted that during reflux/boiling condensation, noncondensables can force the condensing region to occur in relatively small regions in the steam generators. Consequently, finer nodalization in these regions may be necessary to simulate the condensation phenomena. In a TRAC-PF1 assessment of LSTF natural circulation data,[20] it was demonstrated that a single U-tube steam generator model was inadequate in simulating the transient, because it was not able to predict the nonuniform U-tube flow, which was observed in the experiment. Findings indicate that a three U-tube steam generator model was more accurate in simulating the transient phenomena.[20] These examples demonstrate the importance of nodalization in PWR natural circulation simulations.

Although some of the areas of code application described above may be beyond the assessment base of the common thermal hydraulic system codes, the codes are arguably still the best analysis tools available to improve understanding of complicated transient phenomena. Consequently, the use of thermal hydraulic system codes in these areas will continue and when more knowledge and data are available, code improvements may be required to obtain better results.

d. Carlson et al., RELAP5/MOD3 Code Manual Volume III: Development Assessment Problems (Draft), NUREG/CR-55345, EGG-2596, June 1990.

e. Ibid

7. DETECTION OF NATURAL CIRCULATION

Natural circulation is a backup means of decay heat removal in PWRs following the loss of forced circulation. Detection of natural circulation by plant operators is an important safety issue because operator action may be necessary to initiate natural circulation following the loss of forced circulation. In general, temperature measurements are more accurate than flow measurements in the reactor primary and secondary coolant systems. Natural circulation flow rates are much lower than full power flow rates, yet the flow rate measurements in natural circulation have error bounds similar to those at full power. Plant operators, therefore, cannot reliably depend on flow rate readings at natural circulation levels.[21] Thus, detecting the presence of natural circulation from temperature measurements is preferable to inferring natural circulation from flow measurements.

In general, if the core coolant exit temperature remains below saturation, and there is an absence of forced circulation, single-phase (subcooled) natural circulation has been established. If the core exit temperature reaches saturation and remains at saturation, two-phase or reflux/boiling condensation natural circulation has probably been established.

7.1 UTSG Plants

Generic emergency response guidelines for W plants have been developed.[154] Following loss of the RCPs, single-phase natural circulation is established and verified from trended values of the primary and secondary parameters. During natural circulation operations, the primary means available to the operator for verifying continued safe operation of the core (in the subcooled convective heat transfer regime) is the determination of an average core coolant exit temperature and the comparison of this temperature with the saturation temperature for the pressurizer pressure being maintained.

Natural circulation cooling is also covered in emergency procedure guidelines prepared by the CE owner's group.[31] Single-phase natural circulation cooling is the backup means of providing core cooling if the RCPs are not available.[62] Single-phase natural circulation should occur within 5 to 15 minutes after the RCPs are tripped. When single-phase natural circulation flow is established in at least one loop, the RCS will exhibit the following characteristics:

1. The hot-to-cold leg temperature difference is less than for normal full power
2. Cold leg temperatures are constantly decreasing, tracking the steam generator secondary saturation temperature
3. Hot leg temperatures are stable or decreasing slowly
4. There are no abnormal differences between the hot leg and the core exit thermocouple readings.

Item (4) provides the best single indication of the existence of loop natural circulation. Divergence between the hot leg and in-core thermocouple temperatures indicates a loss of single-phase natural circulation. When this occurs, the in-core thermocouple temperature will increase towards saturation. The hot leg temperature may increase at a slower rate, or it may decrease and begin to converge with the cold leg temperature. An additional indication of the loss of single-phase natural circulation is the cold leg temperature ceasing to follow the steam generator secondary saturation temperature.

Single-phase natural circulation phenomena were studied in the LOFT facility during an experiment investigating a severe core damage accident scenario and its subsequent recovery. This discussion is concerned only with natural circulation phenomena associated with system recovery. Following system refill, the primary coolant was stagnant because the steam generator was not in a heat sink mode. A slow cooldown of the steam generator secondary was initiated to regain the heat sink behavior of the steam generator.[35,155] The initiation of single-phase natural circulation is indicated by the temperature traces in Figures 7-1 and 7-2.[35,155] Figure 7-1 demonstrates the tracking of the steam generator secondary saturation

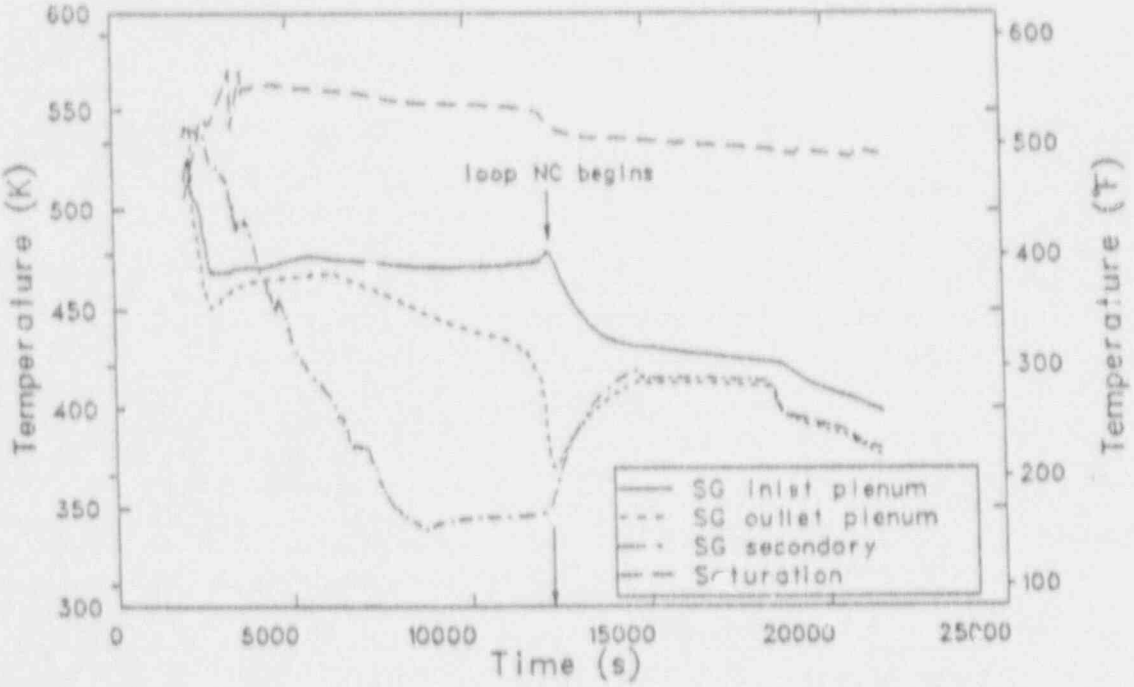

Figure 7-1. Initiation of single-phase natural circulation in the LOFT facility.[35,155]

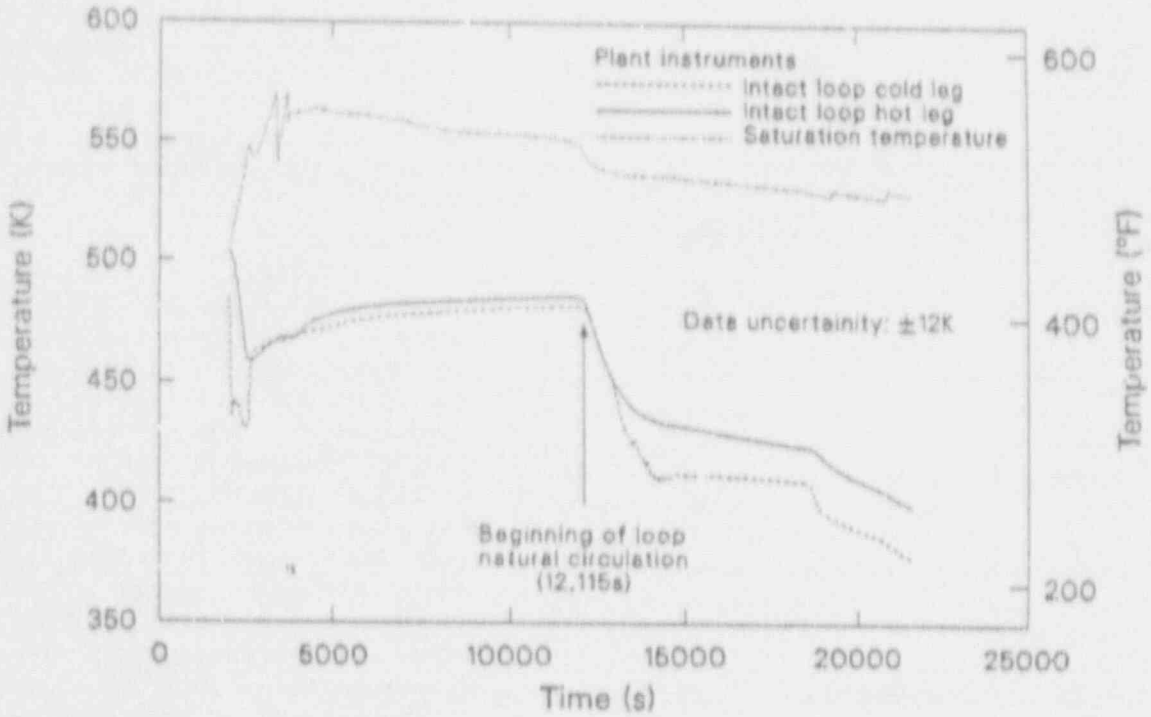

Figure 7-2. Hot and cold leg coolant temperatures before and after initiation of single-phase natural circulation in the LOFT facility.[35,155]

temperature by the cold leg temperature (steam generator outlet plenum) after the initiation of single-phase natural circulation. Notice also that the hot leg temperature (steam generator inlet plenum) is stable and slowly decreasing after the initiation of loop natural circulation. Figure 7-2 demonstrates the resulting temperature difference between the hot and cold legs following the initiation of single-phase natural circulation.

A subcooled (single-phase natural circulation) RCS is the desired state, but two-phase natural circulation can also be used to remove core heat. It may be necessary for the operator to take additional actions, however, to ensure the existence of a heat sink if enough primary inventory is lost such that two-phase natural circulation is disabled. Reflux condensation cooling can be ensured in a UTSG plant by raising the steam generator secondary level to 95% on the operating range.[156] The adequacy of the removal of core decay heat by any of the three modes of natural circulation is supported by the steam generator heat flux behavior determined for all modes in the case of UTSGs.[157] Primary-to-secondary heat transfer rates in typical steam generator tubes were found to be comparable for all three modes of natural circulation.

7.2 OTSG Plants

Abnormal transient operating guidelines for a B&W plant (Oconee-3) have been outlined in Reference 157. For conditions leading to single-phase natural circulation, the operator should assure natural circulation by keeping the RCS in a subcooled state and by raising the thermal center in both OTSGs. Normally this is accomplished when the RCPs trip; as automatic equipment transfers main feedwater injection to the upper nozzles, increasing the level to 50% on the operating range of each steam generator. When steady state has been attained, the cold leg temperatures will be nearly equal to the saturation temperatures in the secondary sides of the steam generators. The hot leg and in-core thermocouple temperatures will increase as necessary to develop the driving head required for flow.

The applicability of the Oconee operating guidelines to all B&W 177-FA plants is supported by the results of a RETRAN-02 comparison of natural circulation flow rates in those plants.[158] Flow rates and decay heat power levels were obtained from planned and unplanned natural circulation events that occurred at Arkansas Nuclear One, Crystal River, Davis-Besse, and Oconee nuclear power plants. The comparisons made indicate that the Oconee RETRAN model properly calculated natural circulation and that all 177-FA plants behave in a similar manner. The study also showed the ability of the raised loop design (Davis-Besse) to induce a greater natural circulation flow rate than in the lowered loop design.[158]

8. SUMMARY AND CONCLUSIONS

Natural circulation is a viable means for shutdown decay heat removal in current PWRs containing either UTSGs or OTSGs; provided either a liquid or two-phase mixture covers the core and the energy can be removed by the steam generators. Three modes of natural-circulation cooling have been identified: single-phase, two-phase, and reflux/boiling condensation. For UTSGs, the third mode is called reflux condensation and involves counter current flow of vapor and condensate in the upflow sides of the steam generator U-tubes. For OTSGs, the third mode is referred to as the boiler-condenser mode (BCM), or as boiling condensation. The BCM mode can be either EFW-BCM or pool-BCM depending on the primary/secondary water level relationship and the operational status of the emergency feedwater (EFW) system.

8.1 Single-Phase Natural Circulation

Single-phase natural circulation is the normal and preferred mechanism after a reactor trip when the RCPs are not available. The success of this mode of decay heat removal is amply verified by plant operational data, steady state and transient data from scaled experimental facilities, and from analysis with assessed computer codes that provide full-plant simulation capability. Results from the LOFT facility indicate that up to 18% of full power for removing decay heat can be removed by single-phase natural circulation.[35]

In single-phase natural circulation there exists a primary loop temperature hierarchy around the primary loop. The loop mass flow rate and the temperature difference between the primary and secondary are usually nearly constant during single-phase natural circulation. Analytical expressions for these parameters were given in Section 3.3.

Noncondensable gases in the primary coolant can affect primary conditions by causing flow interruption in either the candy cane region (OTSGs) or in some of the U-tubes in UTSGs. The effects are dependent on the amount, location, type, and rate of accumulation of the noncondensable gases. The longer U-tubes in single-phase natural circulation can exhibit flow stalling or reversal. Conditions in the steam generator secondary side can affect primary system temperature, pressure, and flow rate. As an example, low secondary liquid levels can produce oscillations in primary system conditions. An additional summary of the single-phase mode of natural circulation is presented in Section 3.7.

8.2 Two-Phase Natural Circulation

Ample evidence exists that two-phase natural circulation can successfully cool existing PWRs. The plant operational data base for this mode, however, is limited to the Gosgen test.[159] Nevertheless, data from scaled experimental facilities and analysis with assessed computer codes provide assurance that two-phase natural circulation is a viable mode of off-normal reactor cooling.

In two-phase natural circulation, as well as in single-phase, the loop mass flow rate is the most important parameter affecting heat removal from the primary system. The mass flow rate during two-phase natural circulation reaches its peak value as the void formation in the hot region adds its effect to the temperature induced density gradient that drives the loop flow. As voids are carried over into the cold region of the loop, the density gradient between the cold and hot regions decreases, acting to decrease the loop mass flow rate. An analytical model simulating the mass flow rate behavior is presented in Section 4.3.

Because condensation heat transfer is important during two-phase natural circulation, the primary to secondary temperature difference is smaller than for single-phase natural circulation. Noncondensable gases and secondary side conditions can affect conditions in the primary loop. Issues related to U-tube flow stalling and reversal, and flow interruption and intermittent flow for OTSG plants are important issues with regard to two-phase

natural circulation. Section 4.7 presents a more complete summary of the issues associated with the two-phase mode of natural circulation.

8.3 Reflux/Boiling Condensation Natural Circulation

There is no known operational data from a full-size plant for the reflux/boiling condensation mode of natural circulation cooling at typical operating conditions.[160] However, steady state and transient data from scaled experimental facilities such as Semiscale, FLECHT-SEASET, OTIS, MIST, the EPRI facilities, LSTF, and PKL demonstrate that reflux condensation is achievable, repeatable in each facility, and adequate for removing core decay energy. These data encompass UTSGs and OTSGs with scaled and full-height steam generator tubes. Confidence in this mode of heat transfer has been enhanced considerably by the results from the OTIS and MIST facilities, which include detailed OTSG secondary modeling. Also, the existence of reflux condensation cooling was inferred during at least one transient in LOFT, a scaled operational PWR with a UTSG.

The assessment of large-scale computer codes, such as TRAC-PF1 and RELAP5, under reflux condensation conditions is providing sufficient confidence to overcome the lack of plant operational data. As a result, long-term reflux condensation is an option for emergency cooling when other planned heat removal modes have failed.

In reflux/boiling condensation, loop mass flow rates approach zero. Liquid holdup in UTSGs can affect vessel pressure and the core mixture level. Countercurrent flow in the hot leg and the upflow side of the U-tubes is a characteristic of reflux condensation for plants with UTSGs. In plants with OTSGs, the condensate flows to the cold leg-loop seal and back to the vessel. In order to reduce the potential for the loss of the steam generators as heat sinks, some operator effort in OTSG plants is required to keep the secondary side liquid level high and the emergency feedwater spray operable.

Important issues regarding the reflux/boiling condensation mode of natural circulation are summarized in Section 5.7.

8.4 Thermal-Hydraulic Systems Codes

Most comparisons of code calculations to experimental data have shown good agreement, and representative code calculations have been valuable for developing operating guidelines for the nuclear plants. Though the thermal-hydraulic systems codes are very important and versatile, they do have some limitations. Below is a list of several important concerns with regard to the use of the thermal-hydraulic system codes:

- Condensation in the presence of noncondensable gases presents problems for the codes. If it is necessary to more accurately quantify detailed effects for reactor safety concerns, there may be a need for models that allow mixing or stratification of two gas phases, and account for the effects of noncondensable gas fraction on condensation efficiency.

- Modifications to the RELAP5 CCFL and interphase drag models have shown promising results in developmental assessment, but additional assessment is required.

- The correlations in the common thermal-hydraulic system codes, used to calculate the wall and interphase shear stresses in the condensation region, may need improvements.[25]

- Nodalization of the PWR system can significantly affect the accuracy of a natural circulation simulation. This is especially true of steam generator models. Insufficient nodalization may not allow the prediction of certain natural circulation phenomena. For instance, nonuniform U-tube flow in UTSGs cannot be simulated using a

single U-tube steam generator model. During reflux condensation in UTSGs, gases can force condensation to occur in a relatively small region in the steam generators. Thus, insufficiently fine nodalization in this region will cause inaccuracies in the numerical simulation.

The use of such codes will continue as they are improved to better simulate the complex phenomena of the different natural circulation modes.

8.5 Application to Operating Plants

The loss of natural-circulation cooling at TMI-2 highlighted the need to examine off-normal operating modes, system trips, and operator actions for their impact on natural circulation. Because plant data for off-normal natural circulation cooling are limited, and experimental data often cannot be applied directly to nuclear plants, computer codes such as TRAC-PF1 and RELAP5 had to be assessed for their use in the investigation of two-phase and reflux/boiling condensation natural circulation cooling. The acquisition of an appropriate experimental data base and the development of the thermal-hydraulic systems codes and plant simulators are now sufficiently complete to allow the design of valid plant recovery procedures incorporating the three natural circulation modes.

Operator guidelines prepared by the vendors and owners groups, provide some information regarding natural circulation procedures and the analyses used in preparing the procedures.

Natural circulation cooling is covered in emergency procedure guidelines prepared by the CE owner's group.[31] Single-phase natural circulation cooling is the secondary means of providing core cooling if the RCPs are not available.[62] Single-phase natural circulation should occur within 5 to 15 minutes after the RCPs are tripped. Several LOCA categories that depend on break size were examined by CE for break sizes between 0.0254 and 0.0762 m (1.0 and 3.0 in.) in diameter.[148,149] Transitions from single-phase natural circulation to a two-phase/condensation mode and return to single-phase natural circulation were described. Issues related to the presence of noncondensable gases in the primary were discussed.

Abnormal transient operating guidelines for a B&W plant (Oconee-3) have been outlined.[157] For conditions leading to single-phase natural circulation, the operator assures natural circulation by keeping the RCS in a subcooled state and by raising the thermal center in both OTSGs. Normally, automatic equipment will transfer main feedwater injection to the upper nozzles and increase the level to 50% on the operating range of each steam generator when the RCPs trip. When steady state is attained, the cold-leg temperatures will be nearly equal to the saturation temperatures in the steam generators. The hot leg and in-core thermocouple temperatures will increase as necessary to develop the driving head required for flow. The applicability of the Oconee operating guidelines to all B&W 177-FA plants is supported by the results of a RETRAN-02 comparison of natural circulation flow rates in those plants.[158]

Generic emergency response guidelines for W plants have been developed.[154] Following loss of the RCPs, single-phase natural circulation is established and verified from trended values of the primary and secondary parameters. Several LOCA categories dependant on break size were examined.[154]

8.6 Conclusions

Single-phase natural circulation is generally an effective and dependable means for removing decay heat in PWRs. Although conditions may produce flow stall/reversals in longer tubes of a UTSG, this does not interrupt the single-phase natural circulation process. Nonuniform flow, noncondensable gases, and secondary side conditions can significantly influence the single-phase mode of natural circulation.

Although it can be much more complex than single-phase natural circulation, the two-phase natural circulation can provide an adequate method for removing decay heat from the core. Two-phase natural circulation is more tolerant

of noncondensable gases than is single-phase natural circulation, but the effects of noncondensables can still significantly influence two-phase natural circulation cooling effectiveness.

It is concluded that the reflux/boiling condensation modes of natural circulation are very efficient heat removal mechanisms. However, system behavior can vary significantly under different operating conditions (i.e., with noncondensable gases present). In plants with UTSGs, core level depression, flooding, and consequent liquid holdup are also important issues regarding reflux condensation.

In all modes of natural circulation, the heat sink must remain active. A potential loss of heat sink in OTSG plants was demonstrated in Sections 2, 4.5.2, 5.4.3, and 5.5.2. This can occur from changes in the steam generator primary/secondary liquid levels or the presence of sufficient noncondensable gases, particularly if EFW is not available. Results indicate that all the the modes of natural circulation were dependant, to a certain degree, on the effects of noncondensable gases, secondary side conditions, and nonuniform flow behavior.

Information from integral test facilities, separate effects experiments, operating plant data, and analysis have made significant contributions to the knowledge base concerning natural circulation cooling in PWRs. Many important natural circulation phenomena have been identified through these studies. It is extremely important that the common thermal hydraulic system codes are able to simulate this phenomena because they will be relied upon to predict full-scale plant behavior. Considerable progress has been made by the codes in predicting most of the important phenomena associated with natural circulation phenomena. However, additional code and model development is necessary so that simulation of the more complex phenomena can be performed.

9. REFERENCES

1. United States Nuclear Regulatory Commission, *Unresolved Safety Issues Summary*, NUREG-0606, Vol. 4, No. 2, August 20, 1982.

2. United States Nuclear Regulatory Commission, Long Range Research Plan, NUREG-0961, April 1983.

3. *NRC Action Plan Developed as a Result of the TMI 2 Accident*, NUREG-0660, Vol. 1-2, May 1980.

4. G. Kocamustafaogullari and M. Ishii, *Scaling Criteria for Two-Phase Flow Natural and Forced Convection Loop and Their Application to Conceptual 2X4 Simulation Loop Model*, NUREG/CR-3420, ANL-83-61, Argonne National Laboratory, Argonne, Illinois, May 1983.

5. Y. Zvirin and Y. Rabinoviz, *Modeling of Natural Circulation Phenomena in Nuclear Reactor Cooling Loops*, Palo Alto, CA, Electric Power Research Institute, NP-2951, March 1983.

6. M. Ishii and I. Kataoka, "Scaling Laws for Thermal-Hydraulic System Under Single-Phase and Two-Phase Natural Circulation," *Nuclear Engineering and Design* 81,1984, pp. 411-425.

7. G. Kocamustafaogullari and M. Ishii, *Reduced Pressure and Fluid-to-Fluid Scaling Laws for Two-Phase Flow Loop*, NUREG/CR-4584, ANL-86-19, Argonne National Laboratory, Argonne, IL, April 1986.

8. Y. Zvirin, *Dimensional Analysis of Natural Circulation Experiments*, EPRI/NP-5428, October 1987.

9. C. J. Crowley, P. H. Rothe, G. B. Wallis, and B. J. Hutchings, *Scaling of Two-Phase Flow during Natural Circulation in a PWR Hot Leg*, EPRI/NP-4854, November 1986.

10. A. Carbiener and R. A. Cudnik, *Trans. Am. Nucl. Soc.* 12, 361, 1969.

11. M. Ishii and O. Jones, Jr., "Derivation and Application of Scaling Criteria for Two-Phase Flows," *Proc. Conf. Two-Phase Flows and Heat Transfer, Istanbul, Turkey, August 16-27, 1976, Vol. 1*, p. 163, NATO Advanced Study Institute,1976.

12. F. Mayinger, "Scaling and Modelling Laws in Two-Phase Flow and Boiling Heat Transfer," *Two-Phase Flow and Heat Transfer in the Power and Processing Industries*, Hemisphere Publishing Corp., Washington, D.C., 1981.

13. R. L. Kiang, "Scaling Criteria for Nuclear Reactor Thermal Hydraulics," *Nuclear Science and Engineering* 89, 1985, pp. 207-216.

14. Y. Zvirin, "Natural Circulation Loops with Parallel Channels-Transient Behavior," *Nuclear Engineering and Design* 84, 1985, pp. 73-81.

15. K. G. Condie et al., *Evaluation of Integral Continuing Experimental Capability (CEC) Concepts for Light Water Reactor Research - PWR Scaling Concepts*, NUREG/CR-4824, EGG-2494, February 1987.

16. A. T. Wassel et al., "Modeling of Natural Circulation in Reactor Coolant Systems," EPI R88-05-04, June 1988.

17. W. D. Lanning and R. R. Wunderlick, "Natural Circulation Response of Pressurized Water Reactors," *Proceedings of the Meeting on Anticipated and Abnormal Plant Transients in Light Water Reactors, Jackson, Wyoming, Sept. 26-29, 1983*, New York: Plenum Press, 1984, p. 239.

18. Y. Zvirin, "A Review of Natural Circulation Loops in Pressurized Water Reactors and Other Systems," *Nuclear Engineering and Design* 67, 1981, pp. 203-225.

19. D. J. Shimeck and G. W. Johnsen, *Nuclear Science Engineering* 88, 1984, pg. 311.

20. R. R. Schultz et al., "Single and Two-Phase Natural Circulation in Westinghouse Pressurized Water Reactor Simulators: Phenomena, Analysis, and Scaling," *ASME Winter Meeting, Boston, MA, December 13-18, 1987*, FED-Vol. 61, HTD-Vol. 92, 1987.

21. R. B. Duffey and J. P. Sursock, "Natural Circulation Phenomena Relevent to Small Breaks and Transients," *Nuclear Eng. and Design Vol. 102, No. 2*, June 1987, pp. 115-128.

22. R. L. Kiang and P. R. Jeuck, III, "Natural Circulation in a Scale PWR Integral Test Facility," *ASME Winter Meeting December 13-18, 1987*, FED-Vol. 61, HTD-Vol. 92, 1987.

23. H. Weisshauph and B. Brand, "PKL Small Break Tests and Energy Transport Mechanisms," *Proceedings of the ANS Specialists' Meeting on Small Break Loss-Of-Coolant Accident Analyses in LWRs, Monterey, California, August 25-27, 1981*, EPRI-WS-81-201, Electric Power Research Institute, 1981.

24. G. G. Loomis, *Summary of the Semiscale Program (1965-1986)*, NUREG/CR-4945, EGG-2509, July 1987.

25. Quan Trung Nguyen, *Condensation in Inverted U Tube Heat Exchangers*, Ph. D. Thesis, University of California Santa Barbara, August 1988.

26. Y. Kukita et al., "Nonuniform Steam Generator U-tube Flow distribution During Natural circulation Tests in ROSA-IV Large Scale Test Facility," *24th ASME/AIChE National Heat Transfer Conference, Pittsburgh, PA, August 9-12, 1987.*

27. J. A. Valenzuela et al., *Survey of the Literature Applicable to Two-Phase Natural Circulation Flows in the Hot Leg of a PWR*, EPRI-4855, October 1986.

28. J. R. Gloudemans, *Once-Through Integral System (OTIS): Final Report*, NUREG/CR-4567, EPRI/NP-4572, BAW-1905, September 1986.

29. G. E. McCreery et al., "Once Through Steam Generator AFW Flow Distribution and Heat Transfer," *Proceedings, 1989 ASME Winter Annual Meeting*, Chicago, IL, November 1988.

30. G. B. Wallis et al., "Modeling Babcock & Wilcox Steam Generators During Auxiliary Feedwater Injection," EPRI-NP-5812, 1988.

31. *Combustion Engineering Emergency Procedure Guidelines*, CEN-152, Rev. 01, Combustion Engineering, November 1982.

32. R. L. Kiang, P. R. Jeuck III, and J. P. Sursock, "Natural-Circulation Experiments in Two SRI-EPRI Test Facilities," *Proceedings of the Second International Topical Meeting on Thermal Hydraulics of Nuclear Reactors, Santa Barbara, California, Jan. 11-14, 1983*, Vol. II, American Nuclear Society, 1983, pg. 833.

33. G. G. Loomis, T. K. Larson, and J. E. Streit, "Natural Circulation Cooling During a Small-Break Loss-of-Coolant Accident in a Simulated Pressurized Water Reactor," *ASME Winter Meeting, December 13-18, 1987*, FED-Vol. 61, HTF-Vol. 92, 1987.

34. Y. Zvirin et al., *Experimental and Analytical Investigation of a PWR Natural Circulation Loop*, EPRI/NP-1364-SR, March 1980.

35. C. L. Nalezny, *Summary of Nuclear Regulatory Commission's LOFT Program Research Findings*, NUREG/CR-3005, EGG-2231, April 1985.

36. Zvirin et al., "Experimental and Analytical Investigation of a Natural Circulation System with Parallel Loops," *Journal of Heat Transfer 103*, pp. 645-652.

37. Babcock and Wilcox, *Abnormal Transient Operator Guidelines, Bellefonts Plant 1 and 2, Part 1, Procedural Guidelines*, 74-1135402-00, June 1976.

38. Y. Y. Hsu et al., *Final Design Report for the UMCP 2X4 B&W Simulation Loop*, Department of Chemical and Nuclear Engineering, University of Maryland.

39. J. R. Larson, *System Analysis Handbook, Rev. 1*, NUREG/CR-4041-Rev-1, November 1985.

40. B. E. Boyack, "Survey of Natural-Circulation Cooling in U.S. Pressurized Water Reactors," *Nuclear Science and Engineering*, 91, 1985, pp. 248-261.

41. S. D. Rupprecht et al., "Results of the FLECHT-SEASET Natural Circulation Experiments," *Transamerican Nuclear Society* 45, 1983, pg. 460.

42. Y. Koizumi et al., "Investigation of Natural Circulation Heat Transfer in Primary and Secondary Sides of Pressurized Water reactor Steam Generator," *ASME Winter Meeting December 13-18, 1987*, FED-Vol. 61, HTD-Vol. 92.

43. J. Sanders, "Stability of Single Phase Natural Circulation with Inverted U-Tube Steam Generators," *ASME Wirter Meeting December 13-18, 1987*, FED-Vol. 61, HTD-Vol. 92.

44. M. Massoud, *An Analytical and Experimental Investigation of Natural Circulation Transients in a Model Pressurized Water Reactor*, NUREG/CR-4788, January, 1987.

45. Jo g Hee Cha and Yong Suk Jin, "The Effects of Coolant Inventory and Noncondensible Gas on the Natural Circulation in a PWR Loop," *Fourth International Meeting on Nuclear Reactor Thermal-Hydraulics*, NURETH-4, Karlsruhe Federal Republic of Germany, October 10-13, 1989, pg. 504.

46. P. R. Jeuck, III, L. Lennert, and R. L. Kiang, *Single-Phase Natural Circulation Experiments on Small-Break Accident Heat Removal*, EPRI/NP-2006, Electric Power Research Institute, August 1981.

47. B. Brand, R. Mandl, and K. Umminger, "Influence of Non-Condensible Gas on Natural Circulation in PWR," *European Two Phase Flow Group Meeting*, Varese, Italy, May 1990.

48. P. R. Jeuck, III, and R. L. Kiang, *Natural-Circulation Experiments in a UTSG Four-Loop Test Facility*, EPRI/NP-2615, Electric Power Research Institute, September 1982.

49. L. E. Hochreiter and L. E. Rupprecht, *PWR FLECHT-SEASET Systems Effects Natural Circulation and Reflux Condensation*, NUREG/CR-3654, August 1984.

50. K. Umminger et al., "PKL-III Transients and Small-Break Programme," *Fourth International Meeting on Nuclear Reactor Thermal-Hydraulics*, NURETH-4, Karlsruhe Federal Republic of Germany, October 10-13, 1989, pg. 455.

51. P. Bazin et al , "Natural Circulation Under Variable Primary Mass Inventories at BETHSY Facility," *Fourth International Meeting on Nuclear Reactor Thermal-Hydraulics*, NURETH-4, Karlsruhe Federal Republic of Germany, October 10-13, 1989, pg. 484.

52. E. Ohlmer et al., "The LOBI-MOD2 Integral System Test Facility," *Proceedings of the Specialists Meeting on Small Break LOCA Analyses in LWRs, Vol. 1, Pisa, Italy, June 1985*, 1985 pp. 455-469.

53. W. L. Riebold, "LOBI-MOD2 Program, Status and Plans," *Proceedings of the Specialists Meeting on Small Break LOCA Analyses in LWRs, Vol. 1, Pisa, Italy, June 1985*, pp. 685-699.

54. G. F. De Santi, L. Piplies, and T. Sanders, "Mass Flow Instabilities in LOBI Steam Generator U-tubes Array Under Natural Circulation Conditions," *Proceedings of the Second International Topical Meeting on Nuclear Power plant Thermal Hydraulics and Operations, Tokyo, April 15-17, 1986*, pp. 158-165.

55. J. H. Kim, "Heat Removal By Natural Circulation in Light Water Reactors," *Fourth International Meeting on Nuclear Reactor Thermal-Hydraulics*, NURETH-4, Karlsruhe Federal Republic of Germany, October 10-13, 1989, pg. 430.

56. J. R. Gloudemans, *Multiloop Integral System Test (MIST): Final Report, Test Group 35, Noncondensables and Venting*, NUREG/CR-5395, EPRI/NP-6480, BAW-2066, Vol. 7, July 1989.

57. G. G. Loomis and K. Soda, *Results of the Semiscale Mod-2A Natural-Circulation Experiments*, NUREG/CR-2335, September 1982.

58. J. P. Adams, G. E. McCreery, and V. T. Berta, "Natural-Circulation Cooling Characteristics During PWR Accident Simulations," *Proceedings of the Second International Topical Meeting on Thermal Hydraulics of Nuclear Reactors, Santa Barbara, California, January 11-14, 1983, Vol. II*, American Nuclear Society, 1983, pg. 825.

59. R. L. Kiang, *Two-Phase Natural-Circulation Experiments in a Test Facility Modeled After Three-Mile Island Unit-2*, EPRI/NP-2069, Electric Power Research Institute, October 1981.

60. K. Soda and G. G. Loomis, "Effects of Noncondensable Gas on Natural Circulation in the Semiscale Mod-2A Facility," *Proceedings of the International Meeting on Thermal Nuclear Reactor Safety, Chicago, Illinois, August 29-September 2, 1982*, NUREG/CR-0027, U.S. Nuclear Regulatory Agency, February 1983.

61. E. R. Rosal et al., *PWR FLECHT-SEASET System-Effects Natural-Circulation and Reflux Condensation Task Plan Report*, EPRI/NP-2015, Electric Power Research Institute, March 1983.

62. *Response of Combustion Engineering Nuclear Steam Supply System to Transients and Accidents*, CTN-128, Vol. 1, nonproprietary, Combustion Engineering, April 1980.

63. Y. Kukita et al., "Flooding at Steam Generator Inlet and Its Impacts on Simulated PWR Natural Circulation," *ASME Winter Meeting December 13-18, 1987*, HED-Vol. 61, HTD-Vol. 92.

64. F. D'Auria and G. M. Galassi, "Characterization of Instabilities During Two-Phase Natural Circulation in PWR Typical Conditions," *Fourth International Meeting on Nuclear Reactor Thermal-Hydraulics*, NURETH-4, Karlsruhe Federal Republic of Germany, October 10-13, 1989, pg. 455.

65. K. Almenas et al., "Two-Phase Flow Instabilities in a Scaled Integral Test Facility," *Fourth International Meeting on Nuclear Reactor Thermal-Hydraulics*, NURETH-4, Karlsruhe Federal Republic of Germany, October 10-13, 1989, pg. 455.

66. M. Ishii, S. Y. Lee, and S Abou El-Seoud, "Results of Two-Phase Natural Circulation in Hot-Leg U-Bend Simulation Experiments," *Proc. 15th Water Reactor Safety Information Meeting*, NUREG/CP-0091 1988.

67. S. Y. Lee and M. Ishii, "Simulation Experiments on Two-Phase Natural Circulation in a Freon-113 Flow Visualization loop," NUREG/CR-5082, ANL-88-1, January. 1988.

68. S. B. Kim and M. Ishii, "Flow Visualization Experiment on Hot-Leg U-Bend Two-Phase Natural Circulation Phenomena," NUREG/CR-4621, ANL-86-27, May 1986.

69. J. T. Hsu and M. Ishii, "Experimental Study on Two-Phase Natural Circulation and Flow Termination in a Loop," NUREG/CR-4682, ANL-86-32, June 1986.

70. R. M. Mandl and P. A. Weiss, "PKL Tests on Energy Transfer Mechanisms During Small break LOCAs," *Nuclear Safety 23*, No. 2, March-April 1982.

71. *Summary of Results from the UPTF Hot Leg Separate Effects Test, Comparison to Scaled Tests and Application to U.S. Pressurized Water Reactors*, MPR-1024 Revision 1, December 1987.

72. *Quick Look Report for UPTF 2D/3D Program, Test No. 11, Countercurrent Flow in PWR Hot Leg Test*, R 515/87/08, March 1987.

73. Q. T. Nguyen and S. Banerjee, "Flow Regimes and Heat Removal Mechanisms in a Single Inverted U-Tube Steam condenser," *Trans. Am. Nucl. Soc. 43*, 1982, pp. 788-789.

74. C. Calia and P. Griffith, "Modes of Circulation in an Inverted U-Tube Array with Condensation," NUREG/CR-1699, October 1980.

75. C. L. Tien et al., "Flooding in Two-Phase Countercurrent Flows," EPRI-NP-1283, December 1979.

76. G. B. Wallis, *One-Dimensional Two-Phase Flow*, McGraw-Hill, 1969.

77. C. K. Fan and V. E. Schrock, "Steam-Water Interactions in a Vertical Tube," *Nuc. Eng. and Design, 95*, 1986, pp. 129-141.

78. C. L. Tien et al., "Condensation Inside Tubes," EPRI-NP-5700, January 1988.

79. S. G. Bankoff et al., "Countercurrent Flow of Air/Water and Steam/Water Through a Horizontal Perforated Plate," *Int. J. Heat Mass Transfer, 24*, 1981, pp. 1381-1395.

80. D. Bharathan, "Air-Water Countercurrent Annular Flow," EPRI-NP-1165, September 1979.

81. G. B. Wallis and J. T. Kuo, "The Behavior of Gas-Liquid Interfaces in Vertical Tubes," *Int. J. Multiphase Flow, 2*, 1976, pp. 521-536.

82. G. B. Wallis et al., "Countercurrent Gas-Liquid Flow in Parallel Vertical Tubes," *Int. J. Multiphase Flow, 7*, 1981, pp. 1-19.

83. J. G. Reed and C. L. Tien, "Modeling of Reflux Condensation and Countercurrent Annular Flow in a Two-Phase Closed Thermosyphon," EPRI-NP-4307, December 1985.

84. V. Marcolong et al., "Experimental Study on Reflux Condensation Inside a Tube Simulating a U-tube of a PWR Steam Generator," CISE-4191, Milan (Italy) 1987.

85. Y. Sudo and A. Ohnuki, "Mechanism of Falling Water Limitation Under Countercurrent Flow," *Bulletin of JSME, 27*, 1984, pp. 708-715.

86. G. B. Wallis, "Countercurrent Annular Flow Regimes for Steam and Subcooled Water in a Vertical Tube," EPRI-NP-1336, January 1980.

87. C. L. Tien, "A Simple Analytical Model for Countercurrent Flow Limiting Phenomena with Vapor Condensation," *Letters in Heat and Mass Transfer, 4*, 1977, pp. 231-238.

88. C. L. Tien and K. S. Chung, "Entrainment Limits in Heat Pipes," *AIAA J., 17*, 1979, pp. 643-646.

89. T. Fukano et al., "Operating Limits of the Closed Two-Phase Thermosyphon," *ASME/JSME Thermal Eng. Joint Conf.*, *1*, pp. 95-101 (1983).

90. H. Imura et al., "Flooding Velocity in a Countercurrent Annular Two-Phase Flow," *Chemical Eng. Science*, *32*, 1977, pp. 79-87.

91. C. L. Tien and C. P. Lin, "Survey on Vertical Two-Phase Countercurrent Flooding," EPRI-NP-984, February 1979.

92. H. Nguyen-Chi and M. Groll, "Entrainment of Flooding Limit in A Closed Two-Phase Thermosyphon," *Advances in Heat Pipe Technology*, D. A. Reay (ed.), Pergamon Press, N.Y., 1981, pp. 147-162.

93. K. H. Sun, "Flooding Correlation for BWR Bundle Upper Tie Plates and Bottom Side-Entry Orifices," *2nd Multi-Phase Flow and Heat Transfer Symposium*, Miami, 1979.

94. C. J. Crowley et al., "Steam/Water Interaction in a Scaled Pressurized Water Reactor Downcomer Annulus," Report No. COO-2294-4, Thayer School of Engineering, Dartmouth College, Hanover, NH, 1974.

95. S. S. Kutateladze, "Elements of Hydrodynamics of Gas-Liquid Systems," *Fluid Mechanics - Soviet Research*, *1*, 1972, pp. 29-50.

96. Q. Nguyen and S. Banerjee, *Experimental Data Report on Condensation in a Single Inverted U-tube*, EPRI/NP-3471, May 1984.

97. S. Banerjee, J. S. Chang, R. Girard, and V. S. Krishnan, "Reflux condensation and Transition to Natural Circulation in a Vertical U-Tube," *Journal of Heat Transfer, ASME, Vol. 105*, 1983, pp. 719-727.

98. Q. Nguyen and S. Banerjee, "Analysis of Experimental Data on Condensation in an Inverted U-Tube," EPRI/NP-4091, July 1985.

99. R. M. Mandl and P. A. Weiss, "PKL Tests on Energy TransferMechanisms During Small-Break LOCAs," *Nuclear Safety* 23, March-April 1982, pg. 146.

100. R. L. Kiang, P. R. Jeuck, III, and J. C. Eid, *Decay Heat Removal Experiments in a UTSG Two-Loop Test Facility*, EPRI/NP-2621, Electric Power Research Institute, September 1982.

101. D. Hein et al., "The Distribution of Gas in a U-tube Heat Exchanger and Its Influence on the Condensation Process," *Proceedings of the 17th International Heat Transfer Conference*, Munchen, Fed. Rep. of Germany, 1983.

102. K. Hijikata et al., "Noncondensible Gas Effect on Condensation in a Two-Phase Closed Thermosyphon," *Int. J. Heat Mass Transfer*, *27*, 1984, pp. 1319-1325.

103. D. K. Edwards, et al., "Heat and Mass Transfer in the Vicinity of the Vapor-Gas Front in a Gas-Loaded Heat Pipe," *J. Heat Transfer*, *94*, 1972, pp. 155-162.

104. A. R. Rohani and C. L. Tien, "Steady Two-Dimensional Heat and Mass Transfer in the Vapor-Gas Region of a Gas Loaded Heat Pipe," *J. Heat Transfer*, *95*, 1973, pp. 377-382.

105. V. V. Galaktionov and L. P. Trukhanova, "Study of the Process of Heat and Mass Trunsfer in the Region of the Vapor-Gas Front in a Gas Regulable Heat Pipe," *J. Eng. Phys.*, *48*, 1985, pg. 276.

106. Y. Mori et al., " The Effect of Noncondensable Gas on Film Condensation Along a Vertical Plate in an Enclosed Chamber," *J. Heat Transfer*, *99*, 1977, pp. 257-262.

107. H. K. Al-Diwany and J. W. Rose, "Free Convection film Condensation of Steam in the Presence of Non-condensing Gases," *Int. J. Heat Mass Transfer*, *16*, 1973, pp. 1359-1369.

108. J. W. Rose, "Condensation of a Vapour in the Presence of a Non-Condensing Gas," *Int. J. Heat Mass Transfer*, *12*, 1969, pp. 233-237.

109. W. J. Minkowycz and E. M. Sparrow, "Condensation Heat Transfer in the Presence of Noncondensables, Interfacial Resistance, Superheating, Variable Properties, and Diffusion," *Int. J. Heat Mass Transfer*, 9, 1966, pp. 1125-1144.

110. E. M. Sparrow and S. H. Lin, "Condensation Heat Transfer in the Presence of a Noncondensable Gas," *J. Heat Transfer*, *86*, 1964, pp. 430-436.

111. D. F. Othmer, "The Condensation of Steam," *Industrial and Engineering Chemistry*, *21*, 1929, pp. 577-583.

112. M. T. Leonard, *Vessel Coolant Mass Depletion During a Small Break LOCA*, EGG-SEMI-6010, September 1982.

113. H. J. Richter et al., "De-Entrainment and Countercurrent Air-Water Flow in a Model PWR Hot-Leg," U. S. Nuclear Regulatory Commission Report NRC-0193-9, 1978.

114. A. Ohnuki, "Experimental Study of Counter-Current Two-Phase Flow in Horizontal Tube Connected to Inclined Riser," *J. Nucl. Sci. and Technol.*, Vol. 23, 1982, pp. 219-232.

115. C. D. Fletcher and R. A. Callow, "Long-Term Recovery of Pressurized Water Reactors Following a Large Break Loss-Of-Coolant Accident," *Nuclear Engineering and Design* 110, 1989, pp. 313-328.

116. T. K. Larson and R. A. Dimenna, "Preservation of Natural Circulation Similarity Criteria in Mathematical Models," *Nuclear Science & Engineering*, September 1988.

117. M. Ishii and I. Kataoka, *Similarity Analysis and Scaling Criteria for LWRs Under Single-Phase and Two-Phase Natural Circulation*, NUREG/CR-3267, ANL-82-32, Argonne National Laboratory, Argonne, Illinois, March 1983.

118. N. M. Schnurr, Letter to P. R. McHugh, Los Alamos National Laboratory, N-6-91-245, 1990.

119. C. P. Booker, *TRAC-PF1 Posttest Predictions for the Semiscale Natural-Circulation Tests S-NC-2 and S-NC-6*, LA-UR-83-2806, Los Alamos National Laboratory, September 1983.

120. B. D. Stitt and J. M. Divine, *Experiment Data Report for LOFT Anticipated Transient Experiment L6-7 and Anticipated Transient with Multiple Failures Experiment L9-2*, NUREG/CR-2277, EGG-2121, September 1981.

121. J. K. Meir, *TRAC-PF1 Analysis of Loss-of-Fluid Test L6-7/L9-2*, LA-UR-83-3658, 1984.

122. J. K. Meier, "A TRAC-PF1 Analysis of Loss-of-Fluid Test L6-7/L9-2," *Trans. Am. Nucl. Soc. 46:1*, 1984, pg. 140-141.

123. Safety Code Development Group, *TRAC-PD2 Independent Assessment*, LA-10166-MS, NUREG/CR-3866, Los Alamos National Laboratory, December 1984.

124. G. Svikantiah, "Methods for PWR Transient Analysis," Presented in "Nuclear Power Plant Transients: Where Are We?" DOE/ID-10119, May 1984.

125. H. Stumpf et al., "Reverse Primary-Side Flow in Steam Generators During Natural Circulation Cooling," *International Symposium on Natural Circulation, ASME Winter Annual Meeting, Boston, MA, December 13-18, 1987*.

126. P. A. Roth and R. R. Schultz, "Analysis of Reduced Primary and Secondary Coolant Level Experiments in the BETHSY Facility Using RELAP5/MOD3," EGG-EAST-9251, EG&G Idaho, Inc., September 1990.

127. R. Y. Yuann et al., *RELAP/MOD2 Assessment Using Semiscale Experiments S-NH-1 and S-LH-2*, NUREG/CR-5010, EGG-2520, October 1987.

128. M. M. Megahed, *RELAP5/MOD2 Assessment Simulation of Semiscale MOD-2C Test S-NH-3*, NUREG/CR-4799, EGG-2519, October 1987.

129. J. M. McGlaun and L. N. Kmetyk, *RELAP5 Assessment: Semiscale Natural Circulation Tests S-NC-2 and S-NC-7*, NUREG/CR-3258, SAND83-0833, May 1983.

130. C. N. C. Wong and L. N. Kmetyk, *RELAP Assessment: Semiscale Natural Circulation Tests S-NC-3, S-NC-4, and S-NC-8*, NUREG/CR-3690, SAND84-0402, May 1984.

131. D. L. Reeder, *LOFT System and Test Description (5.5-ft. Nuclear Core 1 LOCEs)*, NUREG/CR-0247, TREE-1208, Change 1, September 1980.

132. D. J. Varacalle, A. H. Giri, Y. Koizumi, and J. E. Koske, "Analysis of Results from a Loss-of Offsite-Power-Initiated ATWS Experiment in the LOFT Facility," ASME paper 83-HT-14.

133. W. H. Grush and G. E. McCreery, *Posttest Analysis of Loss-of-Fluid Tests L3-2 and L3-7*, EGG-LOFT-5632, EG&G Idaho, Inc., October 1981.

134. K. G. Condie et al., "RELAP5 Calculations of LOFT Small-Break Experiments L3-1 and L3-7," *Proceedings of the ANS Specialists' meeting Small-Break Loss-of-Coolant Accident Analyses in LWRs, Monterey, California, Aug. 25-27, 1981*, EPRI-WS-81-201, Electric Power Research Institute, 1981.

135. Y. Koizumi et al., "Blind-Blind Prediction by RELAP5/MOD1 for a 0.1% Very Small Cold-Leg Break Experiment at ROSA-IV Large-Scale Test Facility," *Nuclear Technology* 73, June 1986.

136. M. A. Langerman et al., "Numerical Simulation of Transient Two-Phase Natural Circulation in a Reactor With Once-Through Steam Generators," *Trans. Am. Nucl. Soc. 47* , 1984.

137. P. K. Doherty et al., "Natural-Circulation Cooldown Using the Combustion Engineering Simulator," *Proceedings of the First Nuclear Thermal Hydraulics, San Francisco, California, Oct. 31 - Nov. 3, 1983*, American nuclear Society, 1983, pg. 177.

138. *Analysis and Evaluation of St. Lucie Unit 1 Natural-Circulation Cooldown*, NSAC-16, Nuclear Safety Analysis Center, December 1980.

139. *Diablo Canyon Unit 1 Natural Circulation, Boron Mixing, Cooldown Test Final Post Test Report*, WCAP-11095, 1986 (non-proprietary).

140. A. C. Cheung et al., "The Westinghouse Transient Real-Time Engineering Analysis Tool," *Proceedings of the Specialists Meeting on Small Break LOCA Analysis in LWRs, Pisa, Italy, June 23-27, 1985*.

141 A. E. Tajbakhsh et al., "A Benchmark Simulation of the Diablo Canyon Unit-1 Natural Circulation Test with a Plant Analyzer," FED-Vol. 61, HTD-Vol. 92.

142. R. J. Henninger, J. R. Ireland, and N. S. DeMuth, *Small-Break LOCA Recovery in B&W Plants*, LA-UR-83-2786, Los Alamos National Laboratory, 1983.

143. C. B. Davis, *Analysis of April 7, 1980, Loss-of-Offsite Power Transient at Arkansas Nuclear One, Unit 1*, EGG-SAAM-6381, EG&G Idaho, Inc., August 1983.

144. P. D. Bayless, *Analysis of the January 29, 1980, Turbine Trip at Arkansas Nuclear One, Unit 2*, EGG-NTAP-6309, EG&G Idaho, Inc., September 1983.

145. P. D. Bayless, *Analyis of the January 29, 1980, Turbine Trip at Arkansas Nuclear One, Unit 2*, EGG-SAAM-6415, EG&G, Idaho, Inc., September 1983.

146. T. A. McDonald, "Post-LOOP Single-Loop Natural Circulation Cooldown of a B&W Plant," *Trans. Am. Nucl. Soc. 45*, October 1983.

147. C. M. Thompson and R. H. Mark, "Small-Break Inadequate Core Cooling Studies in Westinghouse Pressurized Water Reactors," *Proceedings of the ANS Specialists' Meeting on Small-Break Loss-of-Coolant Accident Analyses in LWRs, Monterey, California, August 25-27, 1981*, EPRI-WS-81-201, Electric Power Research Institute, 1981.

148. R. L. Kiang and J. S. Marks, *Two-Phase Natural-Circulation Experiments on Small-Break Accident Heat Removal*, EPRI/NP-2007, Electric Power Research Institute, August 1981.

149. Review of Small-Break Transients in Combustion Engineering Nuclear Steam Supply Systems, CEN-114-NP, *Combustion Engineering*, July 1979.

150. B. E. Boyack, *Use of an Atmospheric Steam Dump Procedure to Cool and Depressurize Calvert Cliffs-1, Following a Small-Break Loss-of-Coolant Accident with Failure of the High-Pressure Injection System*, LA-UR-84-3860, Los Alamos National Laboratory, December 1984.

151. K. E.Carlson, "Improvements to the RELAP5/MOD3 Noncondensable Model," EGG-EAST-8879, January 1990.

152. R. A. Riemke, "Junction Based Interphase Drag And Vertical Stratification Modifications for RELAP5/MOD3," EGG-EAST-8580, June 1989.

153. R. A. Riemke, "Report on CCFL and Interphase Drag Models for RELAP5/MOD3," EGG-TFM-8012, February 1988.

154. *Emergency Response Guideline Information Package, Low-Pressure Version, Vol. II, Optional Recovery Guidelines and Emergency Contingencies*, Westinghouse Electric Corporation, July 1982; *Vol. III, Critical Safety Fuction Status Trees and Function Restoration Guidelines*, Westinghouse Electric Corporation, September 1982.

155. C. L. Nalezny, *Summary of Nuclear Regulatory Commission's LOFT Program Experiments*, NUREG/CR-3241, EG&G Idaho, Inc., July 1983.

156. J. T. Dederer and L. E. Hochreiter, "Steam Generator Heat Flux Behavior for Different Natural-Circulation Cooling Modes," *Trans. Am. Nucl. Soc. 45*, October 1983.

157. "Fundamentals of Reactor Control for Abnormal Transients," *Abnormal Transient Operating Guidelines, Vol. 1, Part II*, BWNP-20007, Babcock & Wilcox, June 1976.

158. H. T. Simms, "RETRAN-02 Comparison of Natural Circulation Flow Rates at Babcock & Wilcox 177-FA Plants," *Nuclear Technology 70*, July 1985.

159. J. Landold, Jr., G. Frei, R. Gille, and W. Schwarz, *Nuclear Safety 22*, 1981 pg. 175.

160. J. L. Crews et al., "Loss of Residual Heat Removal System, Diablo Canyon, Unit 2, April 10, 1987 (Augmented Inspection Team Report April 15 [illegible], 29 and 1 May 87)," Nuclear Regulatory Commission, NUREG-1269, June1987.

161. R. Deruaz et al., "Investigation of PWR Accident Transients with the BETHSY Facility," *Seventeenth Water Reactor Safety Information Meeting, Rockville, Maryland Oct. 23-25*, 1989, NUREG/CP--0105-Vol. 3, 1989.

162. J. P. Sursock and R. L. Kisong, "Two-Phase Natural Circulation Using Once-Through Steam Generator: Analysis and Experiment," *Proceedings of the ANS specialists' Meeting on Small Break Loss-of-Coolant Accident Analysis in LWRs, Monterey, California, August 25-27, 1981*, EPRI-WS-81-201, Electric Power Research Institute, 1981.

163. C. Addabbo et al., "Adequacy of LOBI-MOD2 U-Tube Steam Generators for Simulating NPP-SG Transient Behaviour," *NEA CSNI-UNIPEDE Specialist Meeting on Steam Generator Problems, Stockholm, October 1984*.

164. G. F. De Santi, "Analysis of Steam Generator U-Tube Rupture and Recovery Scenarios in LOBI-MOD2 Facility," *Fourth International Meeting on Nuclear Reactor Thermal-Hydraulics*, NURETH-4, Karlsruhe Federal Republic of Germany, October 10-13, 1989, pg. 455.

165. L. J. Ybarrondo et al., "Examination of LOFT Scaling," 74-WA/HT-53, *ASME Winter Annual Meeting*, November 1974.

166. A. N. Nahavandi, F. S. Castellana, and E. N. Moradkhanian, *Nucl. Sci. Eng.*, 72, p. 75, 1979.

167. P. D. Bayless, J. B. Marlow, and R. H. Averill, *Experiment Data Report for LOFT Nuclear Small-Break Experiment L3-1*, NUREG/CR-1145, EG&G Idaho, Inc., January 1980.

168. D. L. Gillas and J. M. Carpenter, *Experiment Data Report for LOFT Nuclear Small-Break Experiment L3-7*, NUREG/CR-1570, EG&G Idaho, Inc., August 1980.

169. L. T. L. Dao and J. M. Carpenter, *Experiment Data Report for LOFT Nuclear Small-Break Experiment L3-1/L3-5A*, NUREG/CR-1695, EG&G Idaho, Inc., November 1980.

170. J. P. Adams, *Quick-Look Report on LOFT Nuclear Experiment L6-7/L9-2*, EGG-LOFT-5526, EG&G Idaho, Inc., August 1981.

171. M. L. McCormick-Barger and J. M. Devine, *Experiment Data Report for LOFT Anticipated Transient with Multiple Failure Experiment L9-1 and Small-Break Experiment L3-1*, EGG-LOFT-5526, EG&G Idaho, Inc., August 1981.

172. D. L. Batt, J. M. Divine, and K. J. McKenna, *Experiment Data Report for LOFT Anticipated Transient Without Scram Experiment L9-4*, NUREG/CR-2978, EGG-2227, November 1982.

173. M. L. Carboneau, V. T. Berta, and S. M. Modro, *Experiment Analysis and Summary Report for OECD LOFT Project Fission Product Experiment LP-FP-2*, OECD LOFT-T-3806, 1988.

174. *ROSA-IV Large Scale Test Facility (LSTF) System description*, JAERI-M84-237, January 1985.

175. K. Tasaka et al., "The Results of 5% Small-Break LOCA Tests and Natural Circulation Tests of the ROSA-IV LSTF," NUREG/CP-0082, Vol. 4, February 1987.

176. J. C. Chapman and R. R. Schultz, *The ST-NC-01 Experiment: A Data Review and Summary of the First Natural circulation Test conducted in the LSTF*, EGG-RTH-7716, February 1988.

177. G. G. Geissler, *Group Report, MIST Test Group 20 Mapping Tests*, BAW-1950, June 1987.

178. G. G. Loomis, K. Soda, C. M. Kullberg, and J. L. Steiner, *Quick-Look Report for Semiscale Mod-2A Test S-NC-1*, EGG-SEMI-5492, EG&G Idaho Inc., July 1981.

179. T. M. O'Connell, *Experiment Data Report for Semiscale Mod-2A Natural Circulation Test Series (Test S-NC-1)*, NUREG/CR-2379, EG&G Idaho Inc., November 1981.

180. G. G. Loomis and K. Soda, *Quick Look Report for Semiscale Mod-2A Test S-NC-2*, EGG-SEMI-5507, EG&G Idaho Inc., July 1981.

181. T. M. O'Connell, *Experiment Data Report for Semiscale Mod-2A Natural-Circulation Tests S-NC-2B, S-NC-3 and S-NC-4B*, NUREG/CR/2454, EG&G Idaho Inc., August 1981.

182. G. G. Loomis and K. Soda, *Quick Look Report for Semiscale Mod-2A Test S-NC-3*, EGG-SEMI-5522, EG&G Idaho Inc., July 1981.

183. K. Soda and D. J. Shimeck, *Quick Look Report for Semiscale Mod-2A Test S-NC-4*, EGG-SEMI-5549, EG&G Idaho Inc., July 1981.

184. K. Soda and G. G. Loomis, *Quick Look Report for Semiscale Mod-2A Test S-NC-6*, EGG-SEMI-5591, EG&G Idaho Inc., September 1981.

185. T. M. O'Connell, *Experiment Data Report for Semiscale Mod-2A Natural-Circulation Tests S-NC-5 and S-NC-6*, NUREG/CR-2501, EG&G Idaho Inc., January 1982.

186. R. A. Larsen, *Experiment Data Report for Semiscale Mod-2A Natural Circulation Test S-NC-7C*, NUREG/CR-2618, EG&G Idaho, Inc., March 1982.

187. G. G. Loomis and C. M. Kullberg, *Quick Look Report for Semiscale Mod-2A Tests S-NC-8A and 8B*, EGG-SEMI-5678, EG&G Idaho, Inc., December 1981.

188. K. L. Sackett and L. B. Clegg, *Experiment Data Report for Semiscale Mod-2A Natural Circulation Test Series (Tests S-NC-8B and S-NC-9)*, NUREG/CR-2648, EG&G Idaho Inc., April 1982.

189. D. J. Shimeck, and J. L. Steiner, *Quick-Look Report for Semiscale Mod-2A Test S-NC-9*, EGG-SEMI-5679, November 1981.

190. T. M. O'Connell, *Experimental Data Report for Semiscale Mod-2A Natural Circulation Test S-NC-10*, NUREG/CR-2554, EG&G Idaho, Inc., February 1982.

191. J. E. Streit, *Results of Semiscale Mod-2C Small Break Loss-of-Coolant Accident without HPI (S-NH) Experiment Series*, NUREG/CR-4793, EGG-2482, January 1987.

192. J. E. Streit, "Semiscale Recovery Investigations: A Comparison of Results from Semiscale Mod-2C small Break LOCA Without HPI Tests," *14th Water Reactor Safety Information Meeting, Gaithersburg, Maryland*, October 27-31, 1986.

193. K. Almenas et al., "Small Break Loss-of-Coolant Test Results for UMCP 2X4 Loop One and Two-Phase natural Circulation in Multi-Loop System, " NUREG/CP-0082, Vol. 4, February 1987.

194. M. Popp, *The Simulation of Thermohydraulic Phenomena in a Pressurized Water Reactor Primary Loop*, NUREG/CR-4789, January1987.

ADDITIONAL SOURCES OF INFORMATION

J. T. Adams, *Experiment Analysis and Summary Report for LOFT ATWS Experiments L9-3 and L9-4*, NUREG/CR-3417, EGG-2267, September 1983.

C. P. Booker, "TRAC-PF1 Posttest Predictions for the Semiscale Natural-Circulation Tests S-NC-2 and S-NC-6," *Anticipated and Abnormal Plant Transients in Light Water Reactors, Vol. 2 Jackson WY., USA, Sept. 26, 1983.*

W. E. Burchill, *Nuclear Safety 23*, 1982, pg. 525.

D. J. Denver, J. D. Harrison, Jr., and N. G. Trikouros, "RETRAN Natural-Circulation Analyses During the Three Mile Island Unit 2 Accident," *Proceedings of the Thermal Reactor Safety Meeting Knoxville, Tennessee, April 6-9, 1980*, CONF-800403, Vol. 2, available from National Technical Information Service, 1980, pg. 908.

C. D. Fletcher et al., *Thermal -Hydraulic Processes Involved in Loss of Residual Heat Removal During Mid-Loop Operation*, EGG-EAST-9337, EG&G Idaho, Inc., October 1990.

C. D. Fletcher, "The Use of RELAP4/MOD7 Computer Code for Simulating Small-Break Sequences in Pressurized Water Reactors," *Proceedings of the ANS Specialists' Meeting on Small Break Loss-of-Coolant Accident Analyses in LWRs, Monterey, California, August 25-27, 1981*, EPRI-WS-81-201, Electric Power Research Institute, 1981.

N. Fujita, R. E. Helrich, and P. A. Bergeron, "RETRAN-02 Analysis of Upper-Head Cooling During Controlled Natural-Circulation Cooldown of Yankee Nuclear Power Station," *Proceedings of the Second International RETRAN Conference, San Diego, California, April 26-28, 1982*, EPRI/NP-2494-SR, Electric Power Research Institute, July 1982.

S. S. Kutateladze, "Heat Transfer in Condensation and Boiling," AEC Translation 3770, U. S. AEC Tech. Info. Service, 1952.

W. D. Lanning, *Natural Circulation in Pressurized Water Reactors*, AEOD/E413, U. S. Nuclear Regulatory Commission, Office for the Analysis and Evaluation of Operational Data, May 1984.

W. C. Phoenix and K. L. Johnson, "Core-Heat-Driven Natural Circulation Testing at SONGS2," Trans. Am. Nucl. Soc. Vol. 45, October 1983, pp. 686-687.

R. Ripple, *The Influence of Noncondensible Gases on the Heat Transfer in Steam Generators of Pressurized Water reactors Duiring a Loss-of-Coolant Accident*, PhD thesis, Technical University of Munich, March 1981.

Safety Code Development Group, *TRAC-PF1 Developmental Assessment* , LA-9704-M, NUREG/CR-3280, Los Alamos National laboratory report, July 1983.

B. W. Sheron, *Generic Assessment of Delayed Reactor Coolant Pump Trip During Small-Break Loss of Coolant Accidents in Pressurized Water Reactors*, NUREG-0623, U.S. Nuclear Regulatory Commission, November 1979.

S. L. Thompson and J. N. Kmetyk, *RELAP5 Assessment: PKL Natural Circulation Tests*, NUREG/CR 4100, SAND82-2902, January 1983.

U. S. Nuclear Regulatory Commission, *Evaluation of Long-Term Post-Accident Core Cooling of Three Mile Island Unit 2*, NUREG-0557, May 1979.

M. R. Yeung, A. H. Meadows, and K. W. Turner, "Reactor coolant System Coastdown and Natural Circulation," *Proceedings of the Thermal Reactor Safety Meeting, Knoxville, Tennessee, April 6-9, 1980*, CONF-800403, Vol. 1, (available from national Technical Information Service), 1980, pg. 145.

APPENDIX A

INTEGRAL TEST FACILITY REFERENCE INFORMATION

APPENDIX A

INTEGRAL TEST FACILITY REFERENCE INFORMATION

This appendix provides a quick reference source for common design information pertinent to the integral test facilities cited in this report. Table A-1 presents this information along with references. Note that the pressure and temperature data represent values at which the facilities were designed to operate, unless otherwise indicated.

Table A-1. Integral Test Facility Information

FACILITY	REF. PWR	PRESS. (MPa)	TEMP. (K)	POWER (MW) (max.)	# LOOPS	STEAM GENERATORS		SCALING	VOL. (m^3)	CORE	COMPONENT INFORMATION	REFERENCES
						TYPE	# TUBES					
BETHSY	3-loop 900MWe Framatom PWR	17.2	600	3	3 identical loops	UTSG	34	power-to-vol.- 1/100	—	428 electrical heater rods	All components of reference PWR	51,161
EPRI #1	W 4-Loop	.1013	345	1	4 equal loops	UTSG	12	—	1.0	Electric heater	Partially transparent Pressurizer	32,38,46
EPRI #2	CE's 2-Loop Design	0.8	444	.045	2	UTSG	12	—	.04	Electric heater	Cylindrical vessel, Pressurizer	32,100,148
EPRI #3	TMI Unit-2	0.8	444	0.09	2	OTSG	116 (78 active)	power-to-vol.- 1/18	.057	3 immersion heaters	Cold leg to vessel bypass, no pressurizer	59,162
EPRI #4	2X4 lowered loop B&W PWR	approx. 0.7	approx. 400	.068	2 •each loop with 1 hot leg and 2 cold legs	OTSG	48	length=1/4 flow area = 1/324	—	15 active electrical heater rods	HPI, EFW simulation, pump simulation, pressurizer	22
FLECHT-SEASET	W 4-Loop	1.03	450	1.2	2 •broken=1[a] •intact=3[b]	UTSG	intact loop=33 broken loop=11	power-to-vol.- 1/307	—	161 electrical heater rods	Accumulators and containment used as pressurizer	41,49,61

Table A-1. (continued)

FACILITY	REF. PWR	PRESS. (MPa)	TEMP. (K)	POWER (MW) (max.)	# LOOPS	STEAM GENERATORS		SCALING	VOL. (m^3)	CORE	COMPONENT INFORMATION	REFERENCES
KAERI	---	0.5 (max.)	424.15 (max.)	0.015	2	UTSG	8	Ishii & Kataoka	---	6-element immersion type electric heater	-expansion tank - no pressurizer	45
LOBI	KWU 4-loop 1300MWe PWR	15.8	567.15 - 599.15	5.3	2 -broken :1 a -intact=3[b]	UTSG	intact loop=24 broken loop=8	power-to-vol. - 1/712	---	64 electrical heater rods	Pumps, upper/lower plena, upper head	43,52,53,54, 64,74,163, 164
LOFT	W 4-Loop (ZION)	15.51	538	50	2 -broken=1[a] - broken loop only has SG simulation -intact=3[b]	UTSG	1845	power-to-vol.- 1/50	7.896	Nuclear core	Pumps, pressurizer, ECCS, one complete intact loop	35,58,131, 132,155,165-173
LSTF	W 4-Loop (TROJAN)	15.6	600	10	2 equal loops	UTSG	141	power-to-vol.- 1/48	8.2	1064 electrical heater rods	All components of reference PWR	18,20,21,26, 42,174-176
MIST	2X4 lowered loop B&W PWR	Full Pressure	---	0.33	2 -each loop with 1 hot leg and 2 cold legs	OTSG	19	power-to-vol.- 1/817	---	45 electrical heater rods (full length)	Pumps, RVVVs, HPI, leak simulation,guard heaters, Pressurizer	56,177
OTIS	1X1 raised loop B&W PWR	Full Pressure	---	0.18	1	OTSG	19	power-to-vol.- 1/1686	---	Electrical heaters in reactor vessel	Pressurizer, no pump	28

Table A-1. (continued)

FACILITY	REF. PWR	PRESS. (MPa)	TEMP. (K)	POWER (MW) (max.)	# LOOPS	STEAM GENERATORS		SCALING	VOL. (m^3)	CORE	COMPONENT INFORMATION	REFERENCES
PKL	KWU 4-loop 1300MWe PWR	3.5 (max.)	400	.4	3 •intact=1[c] •broken=1[a] •double=2[d]	UTSG	intact loop=30 broken loop=30 double loop=60	power-to-vol.-1/134	2.4	304 electrical heater rods	•Pressurizer •Pump simulator.	23,47,50,70, 99
Semiscale	W 4-Loop	15.2	600	2	•broken=1[a] •intact=3[b]	UTSG	broken loop= 2 intact loop=6	power-to-vol.-1/1705	.21	5X5 array of electrical heater rods	•no pressurizer during stdy st.	19,24,33, 57,60,112, 178-192
UMCP	2X4 lowered loop B&W PWR	2.0685 (max.)	505.4 (max.)	0.2	2 •each loop with 1 hot leg and 2 cold legs	OTSG	56	Ishii, Linear - 1/500	.596	Electrical heater rods	RVVVs, HPI, EFW, Pressurizer	38,44,65 193,194
UPTF	KWU 4-loop 3400MWt PWR	1.8	480.15	---	4 equal loops	Steam/ water separators simulate SGs	---	Full scale, j_g^* is preserved in pressure scaling		None, controlled steam flow from vessel.	Vessel, accumulators, SG simulators	71,72

a. Broken loop equivalent to a single loop of the reference PWR.
b. Intact loop equivalent to three loops of the reference PWR.
c. Intact loop equivalent to one loop of the reference PWR.
d. Third loop simulate two loops of reference PWR.

APPENDIX B

THERMAL-HYDRAULIC SYSTEMS CODES REFERENCE INFORMATION

APPENDIX B

THERMAL-HYDRAULIC SYSTEMS CODES REFERENCE INFORMATION

This appendix provides a quick reference source for information regarding the common thermal hydraulic systems codes. The following table presents information concerning TRAC-PF1, RELAP5/MOD2, ATHLET, and RETRAN-02 thermal hydraulic systems codes.

Table B-1. Description of the common thermal hydraulic system codes

CODE FEATURES	CODES			
	TRAC-PF1	RELAP5/MOD3	ATHLET	RETRAN-02
Dimensions	•3-D Vessel •Rest of system - 1-D	• 1-D	• 1-D	• 1-D with vector momentum equation.
Computer	•Mainframe	•Mainframe •Workstation	Mainframe	Mainframe
Equations	• 6 equation, 2 fluid model	• 6 equation, 2 fluid model	•4 equation	•4 equation
Numerical Method	•Two-step, semi-implicit	•Semi-implicit •Nearly-implicit	•Semi-implicit	•Semi-implicit iterative implicit
Neutronics	•Point model	•Point model	•Point model	•Point model and 1-D models
Control System	•Available	•Available (extensively used)	•Available	•Available (extensively used)
BOP Modeling	•Generic	•Generic	•Specific models	•Generic (includes turbine model)
Additional Models	—	—	•Mixture level tracking	•Separator •nonequilibrium pressurizer •subcooled boiling
Validation	•LOFT, Semiscale, PKL, and LSTF tests (and continuing)	•LOFT, Semiscale, PKL, and LSTF tests (and continuing)	•integral and separate effects tests (continuing)	•OTIS, Semiscale, LOFT, and full-scale plant tests (and continuing)
User-Orientated Features	•Planned	•User-oriented I/O features	—	•User-oriented I/O features
Applications	•PWR, best for LBLOCA, also SBLOCA, and operational transients	•PWR, LBLOCA, SBLOCA, and operational transients	•PWR, LBLOCA, SBLOCA, and operational transients	•PWR, LBLOCA, SBLOCA (limited), ATWS, and operational transients •BWR models

APPENDIX C

INDEX

APPENDIX C

INDEX

NRC FORM 335 (2-89) NRCM 1102, 3201, 3202

U.S. NUCLEAR REGULATORY COMMISSION

BIBLIOGRAPHIC DATA SHEET

(See Instruction on the reverse)

1. REPORT NUMBER (Assigned by NRC, Add Vol., Supp., Rev., and Addendum Numbers, if any.)
NUREG/CR-5769
EGG-2653

2. TITLE AND SUBTITLE
Natural Circulation Cooling in U.S. Pressurized Water Reactors

3. DATE REPORT PUBLISHED
MONTH: January
YEAR: 1992

4. FIN OR GRANT NUMBER
A6328

5. AUTHOR(S)
P. R. McHugh, R. D. Hentzen

6. TYPE OF REPORT
Technical

7. PERIOD COVERED (Inclusive Dates)

8. PERFORMING ORGANIZATION – NAME AND ADDRESS (If NRC provide Division, Office or Region, U.S. Nuclear Regulatory Commission, and mailing address. If contractor, provide name and mailing address.)
Idaho National Engineering Laboratory
EG&G Idaho, Inc.
Idaho Falls, ID 83415

9. SPONSORING ORGANIZATION – NAME AND ADDRESS (If NRC, type "Same as above"; If contractor, provide NRC Division, Office or Region, U.S. Nuclear Regulatory Commission, and mailing address.)
Division of Systems Research
Office of Nuclear Regulatory Research
U. S. Nuclear Regulatory Commission
Washington, D C 20555

10. SUPPLEMENTARY NOTES

11. ABSTRACT (200 words or less)

This document is a synthesis of data and analysis concerning natural circulation cooling in U.S. Pressurized Water Reactors during off-normal operation and accident transients. Its objective is the integration of important research findings concerning PWR natural circulation phenomena into a single reference document. Sources of information include the Nuclear Regulatory Commission, reactor vendors, utility sponsored research groups, utilities, national laboratories, research reports, meeting papers, archival literature, and foreign sources.

Three modes of natural circulation are discussed: single-phase, two-phase, and reflux/boiling condensation. General characteristics, analytical expressions, noncondensible gas effects, secondary effects, and nonuniform flow are described with regard to each of the natural circulation modes. Plant operational data, tests in scaled experimental facilities, and analysis with thermal hydraulic system codes have demonstrated the effectiveness of single-phase natural circulation as a cooling mechanism. Evidence suggests that two-phase natural circulation and reflux/boiling condensation can also be effective methods of alternate core cooling. Experimental test facility data and analysis are the primary components of the two-phase and reflux/boiling condensation natural circulation knowledge base.

12. KEY WORDS/DESCRIPTORS (List words or phrases that will assist researchers in locating the report.)
Alternate Core Cooling
Large-Scale Test Facility
Once Through Steam Generator
Thermal Hydraulic System Codes
U-tube Steam Generator

13. AVAILABILITY STATEMENT
Unlimited

14. SECURITY CLASSIFICATION
(This Page)
Unclassified
(This Report)
Unclassified

15. NUMBER OF PAGES

16. PRICE

UNITED STATES
NUCLEAR REGULATORY COMMISSION
WASHINGTON, D.C. 20555